Sanitized Copy Approved for Release 2010/06/30 : CIA-RDP81-01043R000200070007-1

#1

[redacted]

STAT

SOME PROPERTIES OF LUMPED-FILTER CIRCUITS FOR TRAVELING-WAVE TUBES

Technical Report No. 4

July 20, 1956

NAVY Review Completed

Prepared under Office of Naval Research Contract
Nonr 225(24), NR 373 360
Jointly supported by the U.S. Army Signal Corps,
the U.S. Air Force, and the U.S. Navy
(Office of Naval Research)

STAT

Sanitized Copy Approved for Release 2010/06/30 : CIA-RDP81-01043R000200070007-1

Sanitized Copy Approved for Release 2010/06/30 : CIA-RDP81-01043R000200070007-1

TABLE OF CONTENTS

I. Introduction 1

II. General Equations 2

III. Characteristics of the low-pass circuits 5

IV. Characteristics of the high-pass circuits. 19

V. Characteristics of the three-element inductively coupled band-pass circuit. 33

VI. Characteristics of the three-element capacitively coupled band-pass circuit. 51

VII. Characteristics of the four-element band-pass circuits 66

STAT

Sanitized Copy Approved for Release 2010/06/30 : CIA-RDP81-01043R000200070007-1

Sanitized Copy Approved for Release 2010/06/30 : CIA-RDP81-01043R000200070007-1

LIST OF ILLUSTRATIONS

Figure		Page
2.1	Tee and Pi filter sections	3
3.1	M-derived low-pass circuits	6
3.2	Phase angle per section of low-pass circuits	8
3.3	Phase velocity of low-pass circuits	9
3.4	Group velocity of low-pass circuits	10
3.5	Circuit impedance of low-pass circuits of Pi section	11
3.6	Circuit impedance of low-pass circuits of Tee section	12
3.7	Transverse interaction impedance K_{TO} of a series m-derived low-pass circuit	13
3.8	Transverse interaction impedance K_{T-1} of a series m-derived low-pass circuit	14
3.9	Transverse interaction impedance K_{TO} of a shunt m-derived low-pass circuit	15
3.10	Transverse interaction impedance K_{T-1} of a shunt m-derived low-pass circuit	16
3.11	Longitudinal interaction impedance K_{LO} of a shunt m-derived low-pass circuit	17
3.12	Longitudinal interaction impedance K_{L-1} of a shunt m-derived low-pass circuit	18
4.1	High-pass circuits	20
4.2	Phase angle per section of high-pass circuits	22
4.3	Phase velocity of high-pass circuits	23
4.4	Group velocity of high-pass circuits	24
4.5	Circuit impedance of high-pass circuits of Pi section	25
4.6	Circuit impedance of high-pass circuits of Tee section	26
4.7	Longitudinal interaction impedance K_{LO} of a series m-derived high-pass circuit	27
4.8	Longitudinal interaction impedance K_{L+1} of a series m-derived high-pass circuit	28
4.9	Longitudinal interaction impedance K_{LO} of a shunt m-derived high-pass circuit	29
4.10	Longitudinal interaction impedance K_{L+1} of a shunt m-derived high-pass circuit	30
4.11	Transverse interaction impedance K_{TO} of a series m-derived high-pass circuit	31
4.12	Transverse interaction impedance K_{T+1} of a series m-derived high-pass circuit	32
5.1	Three-element inductively coupled band-pass circuit	34
5.2	Phase angle per section of the positive mutual coupled three-element band-pass circuit	36

LIST OF ILLUSTRATIONS (Cont'd)

Figure		Page
5.3	Phase velocity y_{pn} of the positive-mutual-coupled three-element band-pass circuit	37
5.4	Group velocity y_g of the positive-mutual-coupled three-element band-pass circuit	38
5.5	Circuit impedance Z_{OT} of the positive-mutual-coupled three-element band-pass circuit.	39
5.6	Circuit impedance Z_{OT} of the positive-mutual coupled three-element band-pass circuit of Tee section	40
5.7	Transverse interaction impedance K_{TO} of the positive-mutual-coupled three-element band-pass circuit	41
5.8	Transverse interaction impedance K_{T-1} of the positive-mutual-coupled three-element band-pass circuit	42
5.9	Phase angle per section of the negative-mutual-coupled three-element band-pass circuit.	43
5.10	Phase velocity y_{pn} of the negative-mutual coupled three-element band-pass circuit	44
5.11	Phase velocity of the negative-mutual-coupled three-element band-pass circuit	45
5.12	Group velocity y_g of the negative-mutual-coupled three-element band-pass circuit	46
5.13	Circuit impedance Z_{OT} of the negative-mutual-coupled three-element band-pass circuit of Pi section.	47
5.14	Circuit impedance Z_{OT} of the negative-mutual-coupled three-element band-pass circuit of Tee section	48
5.15	Transverse interaction impedance K_{TO} of the negative-mutual-coupled three-element band-pass circuit.	49
5.16	Transverse interaction impedance K_{T+1} of the negative-mutual-coupled three-element band-pass circuit.	50
6.1	Three-element capacitively coupled band-pass circuits.	52
6.2	Phase angle per section of the three-element capacitively coupled band-pass circuit.	54
6.3	Phase velocity y_{pO} of the three-element capacitively coupled band-pass circuit.	55
6.4	Phase velocity of the three-element capacitively coupled band-pass circuit y_{p+1}	56
6.5	Phase velocity y_{p+1} of the three-element capacitively coupled band-pass circuit.	57
6.6	Group velocity y_g of the three-element capacitively coupled band-pass circuit.	58

Sanitized Copy Approved for Release 2010/06/30 : CIA-RDP81-01043R000200070007-1

Sanitized Copy Approved for Release 2010/06/30 : CIA-RDP81-01043R000200070007-1

LIST OF ILLUSTRATIONS (Cont'd)

Figure		Page
6.7	Circuit impedance $Z_{O\pi}$ of the three element capacitively coupled band-pass circuit of Pi section	59
6.8	Circuit impedance Z_{OT} of the three-element capacitively coupled band-pass circuit of Tee section	60
6.9	Transverse interaction impedance K_{TO} of the three-element capacitively-coupled band-pass circuit	61
6.10	Transverse interaction impedance $K_{T\pm1}$ of the three-element capacitively-coupled band-pass circuit	62
6.11	Transverse interaction impedance $K_{T\pm1}$ of the three-element capacitively-coupled band-pass circuit	63
6.12	Longitudinal interaction impedance K_{LO} of the three-element capacitively-coupled band-pass circuit	64
6.13	Longitudinal interaction impedance $K_{L\pm1}$ of the three-element capacitively-coupled band-pass circuit	65
7.1	Four-element band-pass circuits	67

TABLE OF FIGURES OF THE
4-ELEMENT BAND PASS CIRCUIT

x_1	θ	y_{pn}	y_g	$\frac{Z_{O\pi}}{\frac{L_2}{C_1}}$	$\frac{Z_{OT}}{\frac{L_2}{C_1}}$	$\frac{K_{TO}}{\frac{L_2}{C_1}}$	$\frac{K_{T\pm1}}{\frac{L_2}{C_1}}$	$\frac{K_{LO}}{\frac{L_2}{C_1}}$	$\frac{K_{L\pm1}}{\frac{L_2}{C_1}}$
10	7.2 -69-	7.3 -70-	7.4 -71-	7.5 -72-	7.6 -73-	7.7 -74-	7.8 -75-	7.9 -76-	7.10 -77-
5	7.11 -78-	7.12 -79-	7.13 -80-	7.14 -81-	7.15 -82-	7.16 -83-	7.17 -84-	7.18 -85-	7.19 -86-
2	7.20 -87-	7.21 -88-	7.22 -89-	7.23 -90-	7.24 -91-	7.25 -92-	7.26 -93-	7.27 -94-	7.28 -95-
1.70	7.29 -96-	7.30 -97-	7.31 -98-	7.32 -99-	7.33 -100-	7.34 -101-	7.35 -102-	7.36 -103-	7.37 -104-
1.6	7.38 -105-	7.39 -106-	7.40 -107-	7.41 -108-	7.42 -109-	7.43 -110-	7.44 -111-	7.45 -112-	7.46 -113-
1.5	7.47 -114-	7.48 -115-	7.49 -116-	7.50 -117-	7.51 -118-	7.52 -119-	7.53 -120-	7.54 -121-	7.55 -122-
0.5	7.56 -123-	7.57 -124-	7.58 -125-	7.59 -126-	7.60 -127-	7.61 -128-	7.62 -129-	7.63 -130-	7.64 -131-
0.3	7.65 -132-	7.66 -133-	7.67 -134-	7.68 -135-	7.69 -136-	7.70 -137-	7.71 -138-	7.72 -139-	7.73 -140
0.16	7.74 -141-	7.75 -142-	7.76 -143-	7.77 -144-	7.78 -145-	7.79 -146-	7.80 -147-	7.81 -148-	7.82 -149-
0.100	7.83 -150-	7.84 -151-	7.85 -152-	7.86 -153-	7.87 -154-	7.88 -155-	7.89 -156-	7.90 -157-	7.91 -158-

Sanitized Copy Approved for Release 2010/06/30 : CIA-RDP81-01043R000200070007-1

Sanitized Copy Approved for Release 2010/06/30 : CIA-RDP81-01043R000200070007-1

LIST OF SYMBOLS

b	Pierce's velocity parameter $b = \frac{u_0 - v_{pn}}{v_{pn}}$
c	velocity of light
C_n	Pierce's circuit-beam coupling parameter $C_n^3 = I_0/4V_0\ K_n$
d	length of the gap
f	frequency
f_c	cut-off frequency
g	subscript for group velocity
m_r	$= 1/\sqrt{1 + 4C_1/C_2}$
m_s	$= 1/\sqrt{1 + 4L_2/L_1}$
n	index for the nth space-harmonic component
r	capacitance ratio $r = 4C_1/C_2$
s	inductance ratio $s = 4L_2/L_1$
u_0	d-c velocity of the electron beam
v_{pn}	phase velocity of the nth space harmonic
v_g	group velocity
x	normalized frequency $x = f/f_c$
x_1	one of the normalized cut-off frequencies
y_{pn}	normalized phase velocity $y_{pn} = 2x/\beta_n D$
y_g	normalized group velocity $y_g = 2dx/d\theta$
C_1	capacitance in the X_1 arm
C_2	capacitance in the X_2 arm
D	length of one space-harmonic period
E_n	magnitude of the electric field of the nth space-harmonic component
K_{Tn}	interaction impedance of the nth space-harmonic component of the transverse interaction structure
K_{Ln}	interaction impedance of the nth space-harmonic component of the longitudinal interaction structure
L_1	inductance in the X_1 arm

LIST OF SYMBOLS (Cont'd)

L_2	inductance in the X_2 arm
M_n	amplitude of the nth space-harmonic field component
P	total power carried by the circuit
V	peak voltage between line and ground
V_0	d-c beam voltage
V_n	synchronism voltage of the nth space harmonic component

$$V_0 = V_n\ (1 + bC_n)^2$$

$$V_n = 2800 \left[y_{pn}\ f_c\ (\text{Mc/sec})\ D\ (\text{cm}) \right]^2 \quad \text{volts}$$

$$= 18100 \left[y_{pn}\ f_c\ (\text{kMc/sec})\ D\ (\text{inch}) \right]^2 \quad \text{volts}$$

X_1	reactance in arm 1 or the series arm
X_2	reactance in arm 2 or the shunt arm
Z_{0T}	characteristic circuit impedance of a T filter section
$Z_{0\pi}$	characteristic circuit impedance of a Pi filter section
β_n	wave number of the nth space harmonic component $\beta_n D = \theta + 2n\pi$
θ	circuit phase constant
ω	angular frequency $\omega = 2\pi f$

Sanitized Copy Approved for Release 2010/06/30 : CIA-RDP81-01043R000200070007-1

Sanitized Copy Approved for Release 2010/06/30 : CIA-RDP81-01043R000200070007-1

I. INTRODUCTION

Since the development of the external-circuit traveling-wave tube, many different types of slow-wave circuits can be used with a traveling-wave tube structure with a single basic interaction geometry containing the electron beam and the interaction electrodes. To use such a versatile device it becomes necessary to investigate theoretically the properties of the various possible external circuits. Some sample calculations were obtained for the various types of circuits, either lumped or distributed-lumped, which can be used as slow-wave structures.[1]

In this report, results of more detailed calculations for several lumped-filter circuits are presented in normalized graphic form. The circuits include the low-pass, the high-pass,* the three-element inductive band-pass,* the three-element capacitive band-pass and the four-element band-pass circuits.

The characteristics presented include the phase-frequency characteristics, the phase velocity characteristics, the group velocity characteristics, the circuit impedance characteristics and the interaction impedance characteristics.

The interaction geometry considered here is uniformly periodic, i.e. all cylinders have equal lengths and all gaps have equal lengths. The quantities investigated are all normalized and plotted as a function of the normalized frequency.

---

* These circuits can never be obtained physically in their exact forms due to distributed coil capacitance and lead inductance.

Sanitized Copy Approved for Release 2010/06/30 : CIA-RDP81-01043R000200070007-1

Sanitized Copy Approved for Release 2010/06/30 : CIA-RDP81-01043R000200070007-1

II. GENERAL EQUATIONS

In this section a list of formulae for Tee and Pi filter circuits shown in Fig. 2.1 is given in terms of the reactances X_1 and X_2 and of the normalized frequency x. The circuit properties are

phase constant

$$\theta = \pm 2 \sin^{-1} \sqrt{-\frac{X_1}{4X_2}} \qquad (2.1)$$

phase velocity

$$y_{pn} = \frac{2x}{\theta + 2n\pi} \qquad (2.2)$$

group velocity

$$y_g = 2 \frac{dx}{d\theta} \qquad (2.3)$$

circuit impedances

$$Z_{O\pi} = \frac{\sqrt{-X_1 X_2}}{\sqrt{1 + \frac{X_1}{4X_2}}} \qquad (2.4)$$

$$Z_{OT} = \sqrt{-X_1 X_2} \sqrt{1 + \frac{X_1}{4X_2}} \qquad (2.5)$$

The interaction impedance is defined by

$$K_n = \frac{M_n^2 V^2}{\beta_n^2 D^2 2P} \qquad (2.6)$$

where the amplitude factor of the nth space harmonics is[1]

$$M_n^2 = 4 \sin^2 \frac{\beta_n D}{4} \qquad \text{transversely loaded} \qquad (2.7)$$

$$M_n^2 = 4 \sin^2 \frac{\beta_n D}{2} \qquad \text{longitudinally loaded} \qquad (2.8)$$

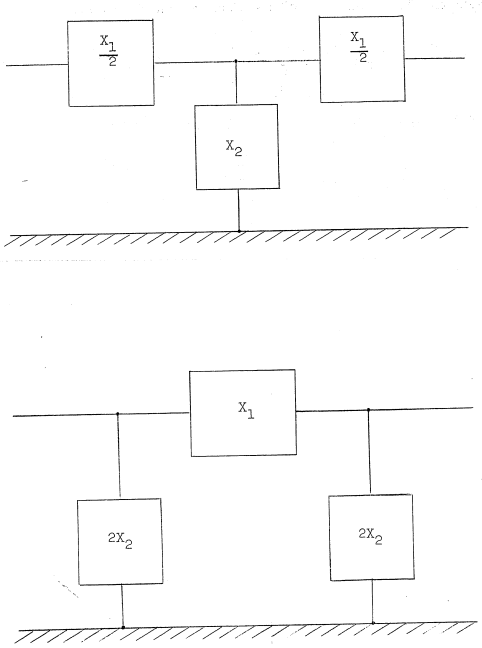

FIG. 2.1.--Tee and Pi filter sections.

Sanitized Copy Approved for Release 2010/06/30 : CIA-RDP81-01043R000200070007-1

Sanitized Copy Approved for Release 2010/06/30 : CIA-RDP81-01043R000200070007-1

Thus the longitudinal interaction impedance becomes

$$K_{Ln} = Z_{O\pi} \left(\frac{\sin \frac{\beta_n D}{2}}{\frac{\beta_n D}{2}} \right)^2 \tag{2.9}$$

and the transverse interaction impedance becomes

$$K_{Tn} = Z_{O\pi} \frac{1}{4} \left(\frac{\sin \frac{\beta_n D}{4}}{\frac{\beta_n D}{4}} \right)^2 \tag{2.10}$$

III. CHARACTERISTICS OF THE LOW-PASS CIRCUITS

The low-pass circuits are shown in Fig. 3.1. The first two have transverse interaction gaps and the third one has longitudinal interaction gaps.

The equations for the characteristics are

$$\theta = 2\sin^{-1} \frac{mx}{\sqrt{1-(1-m^2)x^2}} \tag{3.1}$$

$$y_{pn} = \frac{2x}{\theta+2n\pi} \tag{3.2}$$

$$y_g = \frac{\sqrt{1-x^2}}{m} \left[1-(1-m^2)x^2\right] \tag{3.3}$$

$$\left.\begin{aligned} Z_{O\pi} &= \sqrt{\frac{L_1}{C_2}} \; \frac{1-x^2(1-m^2)}{\sqrt{1-x^2}} \qquad (3.4) \\ Z_{OT} &= \sqrt{\frac{L_1}{C_2}} \; \sqrt{1-x^2} \qquad (3.5) \end{aligned}\right\} \text{Fig. 2(a)}$$

$$\left.\begin{aligned} Z_{OT} &= \sqrt{\frac{L_1}{C_2}} \; \frac{\sqrt{1-x^2}}{1-x^2(1-m^2)} \qquad (3.6) \\ Z_{O\pi} &= \sqrt{\frac{L_1}{C_2}} \; \frac{1}{\sqrt{1-x^2}} \qquad (3.7) \end{aligned}\right\} \text{Figs. 2(b) and 2(c)}$$

$$K_{Tn} = \sqrt{\frac{L_1}{C_2}} \; \frac{1}{4} \left(\frac{\sin \frac{\beta_n D}{4}}{\frac{\beta_n D}{4}} \right)^2 \frac{1}{\sqrt{1-x^2}\left[1-x^2(1-m^2)\right]} \tag{3.8}$$

Fig. 2(a)

Sanitized Copy Approved for Release 2010/06/30 : CIA-RDP81-01043R000200070007-1

Sanitized Copy Approved for Release 2010/06/30 : CIA-RDP81-01043R000200070007-1

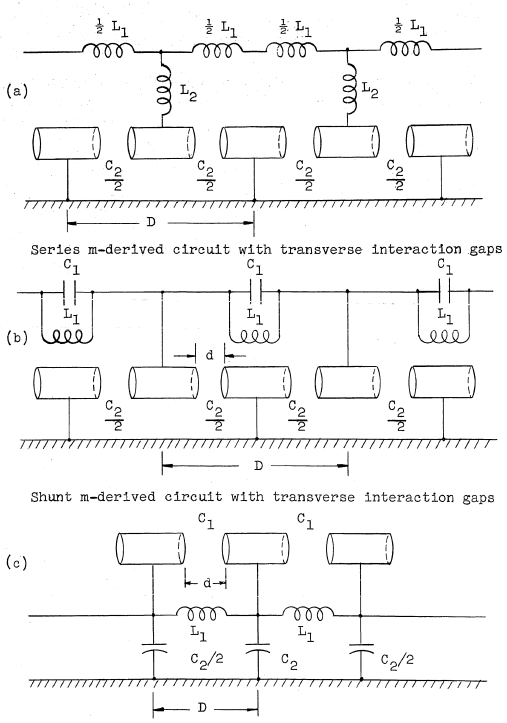

Series m-derived circuit with transverse interaction gaps

Shunt m-derived circuit with transverse interaction gaps

Series m-derived circuit with longitudinal interaction gaps

FIG. 3.1.--M-derived low-pass circuits.

$$K_{Tn} = \sqrt{\frac{L_1}{C_2}}\ \frac{1}{4}\left(\frac{\sin\frac{\beta_n D}{4}}{\frac{\beta_n D}{4}}\right)^2 \frac{1}{\sqrt{1-x^2}} \qquad \text{Fig. 2(b)} \qquad (3.9)$$

$$K_{Ln} = \sqrt{\frac{L_1}{C_2}}\left(\frac{\sin\frac{\beta_n D}{2}}{\frac{\beta_n D}{2}}\right)^2 \frac{1}{\sqrt{1-x^2}} \qquad \text{Fig. 2(c)} \qquad (3.10)$$

These equations are plotted as curves in Figs. 3.2 to 3.12.

Sanitized Copy Approved for Release 2010/06/30 : CIA-RDP81-01043R000200070007-1

Sanitized Copy Approved for Release 2010/06/30 : CIA-RDP81-01043R000200070007-1

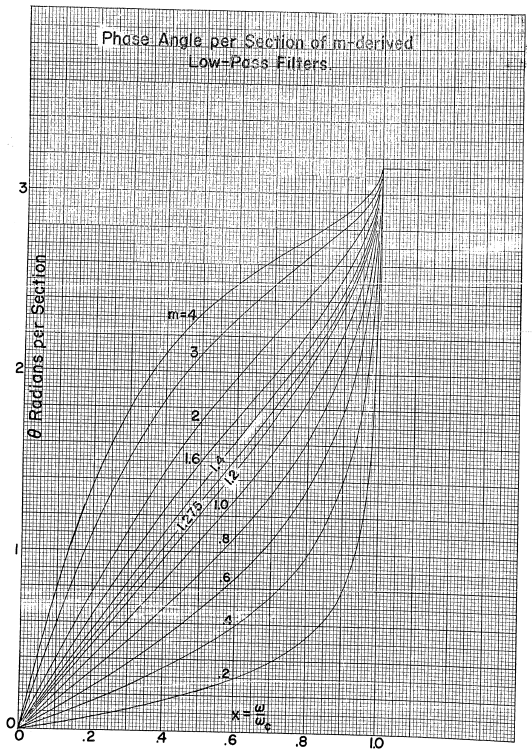

FIG. 3.2.--Phase angle per section of low-pass circuits.

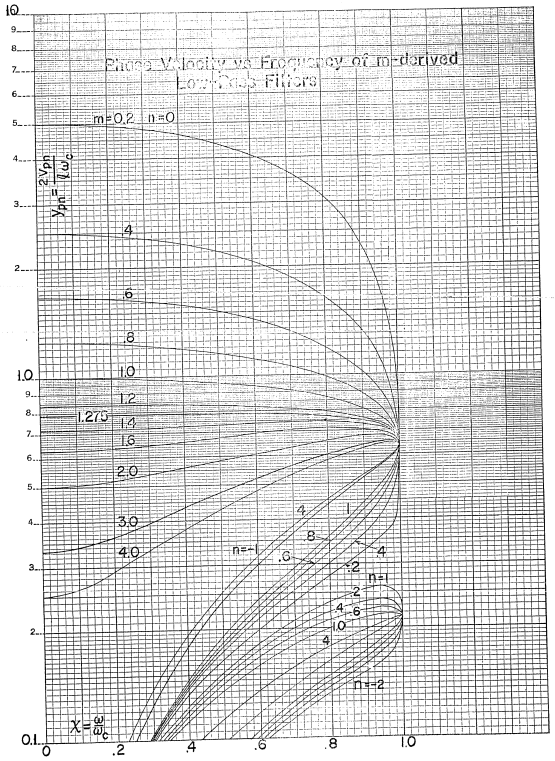

FIG. 3.3.--Phase velocity of low-pass circuits.

Sanitized Copy Approved for Release 2010/06/30 : CIA-RDP81-01043R000200070007-1

Sanitized Copy Approved for Release 2010/06/30 : CIA-RDP81-01043R000200070007-1

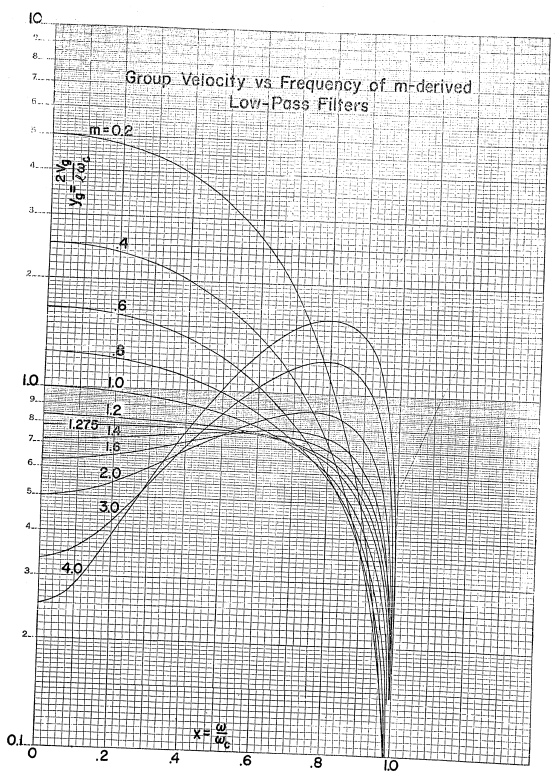

FIG. 3.4.--Group velocity of low-pass circuits.

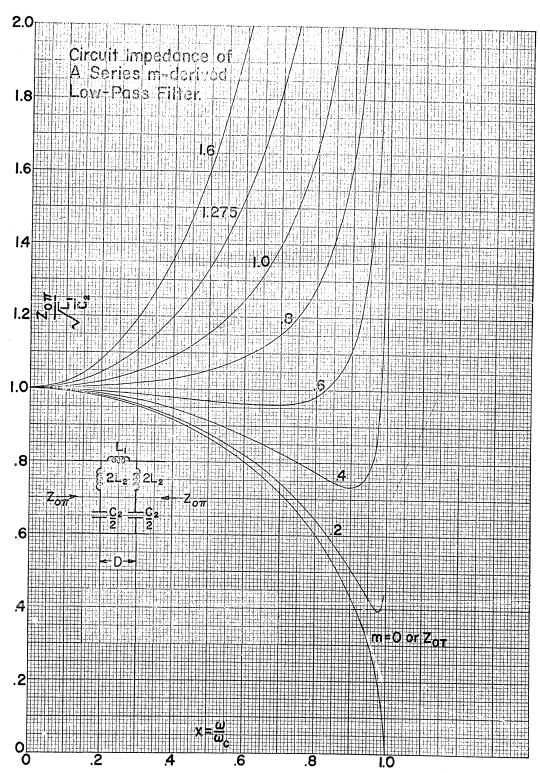

FIG. 3.5.--Circuit impedance of low-pass circuits of Pi section.

Sanitized Copy Approved for Release 2010/06/30 : CIA-RDP81-01043R000200070007-1

Sanitized Copy Approved for Release 2010/06/30 : CIA-RDP81-01043R000200070007-1

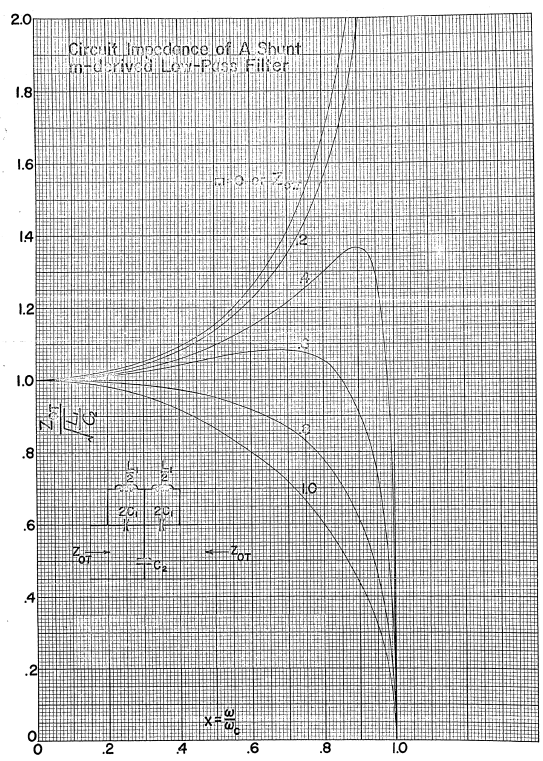

FIG. 3.6.--Circuit impedance of low-pass circuits of Tee section.

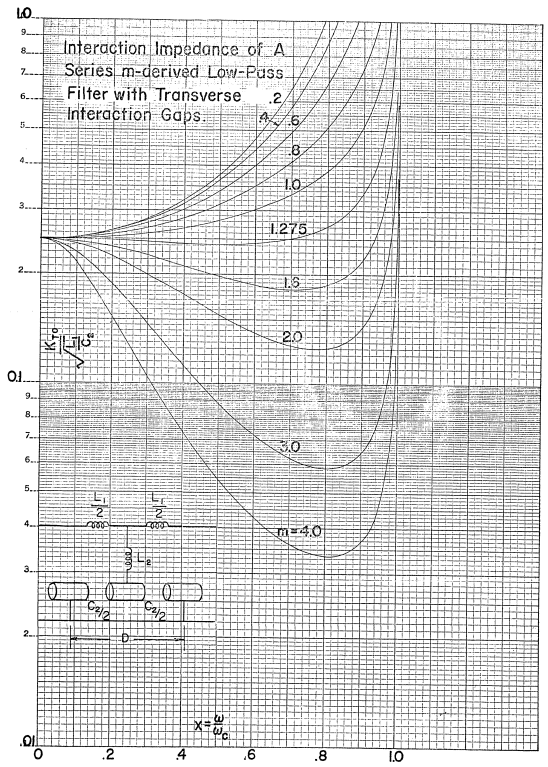

FIG. 3.7.--Transverse interaction impedance K_{TO} of a series m-derived low-pass circuit.

Sanitized Copy Approved for Release 2010/06/30 : CIA-RDP81-01043R000200070007-1

Sanitized Copy Approved for Release 2010/06/30 : CIA-RDP81-01043R000200070007-1

POOR COPY

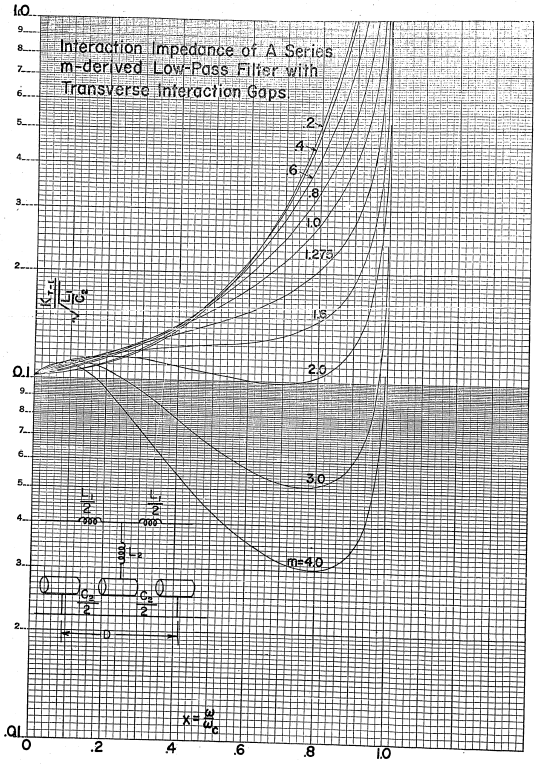

FIG. 3.8.--Transverse interaction impedance K_{T-1} of a series m-derived low-pass circuit.

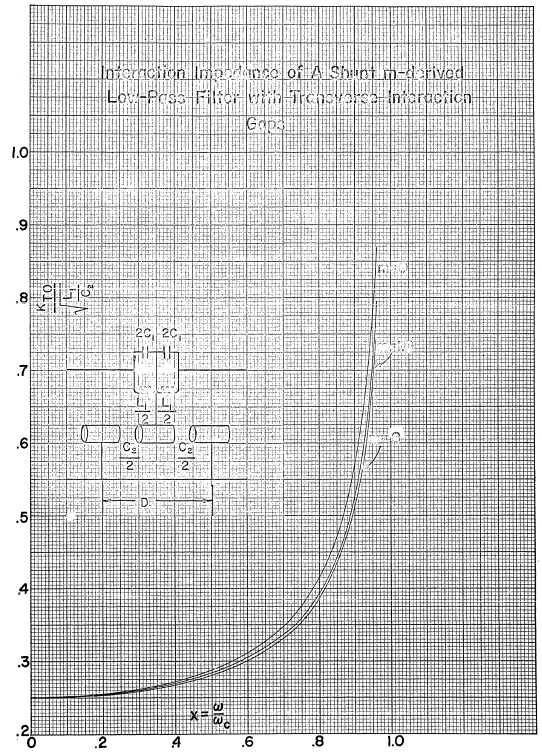

FIG. 3.9.--Transverse interaction impedance K_{TO} of a shunt m-derived low-pass circuit.

Sanitized Copy Approved for Release 2010/06/30 : CIA-RDP81-01043R000200070007-1

Sanitized Copy Approved for Release 2010/06/30 : CIA-RDP81-01043R000200070007-1

POOR COPY

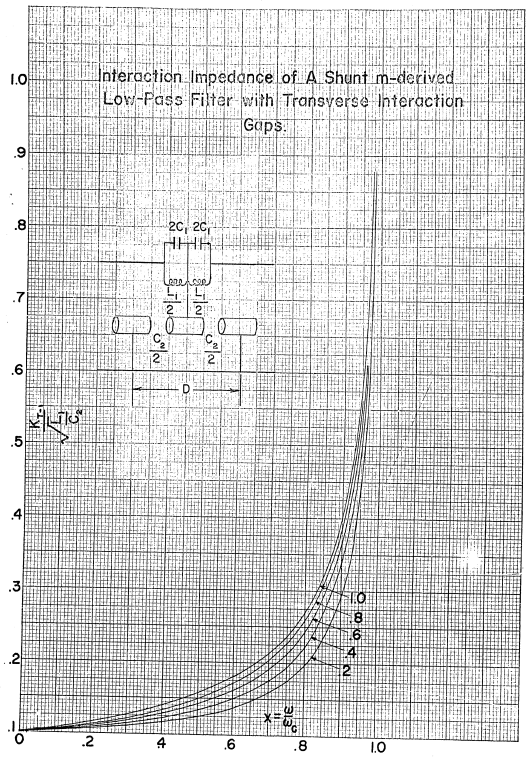

FIG. 3.10.--Transverse interaction impedance K_{T-lo} of a shunt m-derived low-pass circuit.

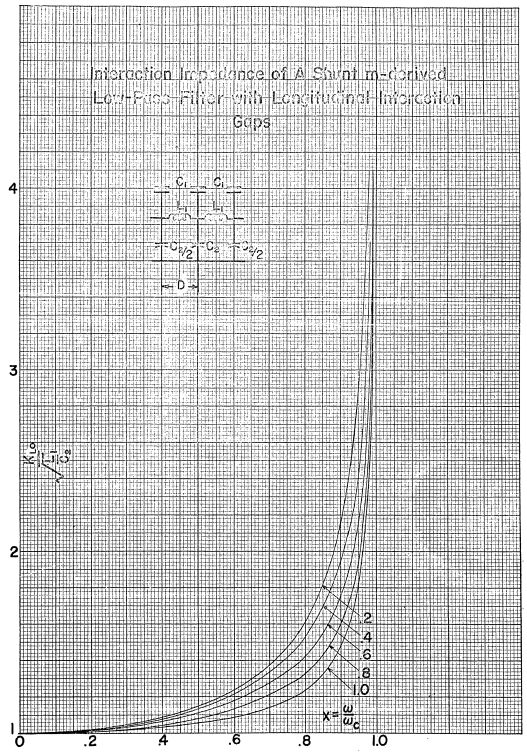

FIG. 3.11.--Longitudinal interaction impedance K_{LO} of a shunt m-derived low-pass circuit.

Sanitized Copy Approved for Release 2010/06/30 : CIA-RDP81-01043R000200070007-1

Sanitized Copy Approved for Release 2010/06/30 : CIA-RDP81-01043R000200070007-1

POOR COPY

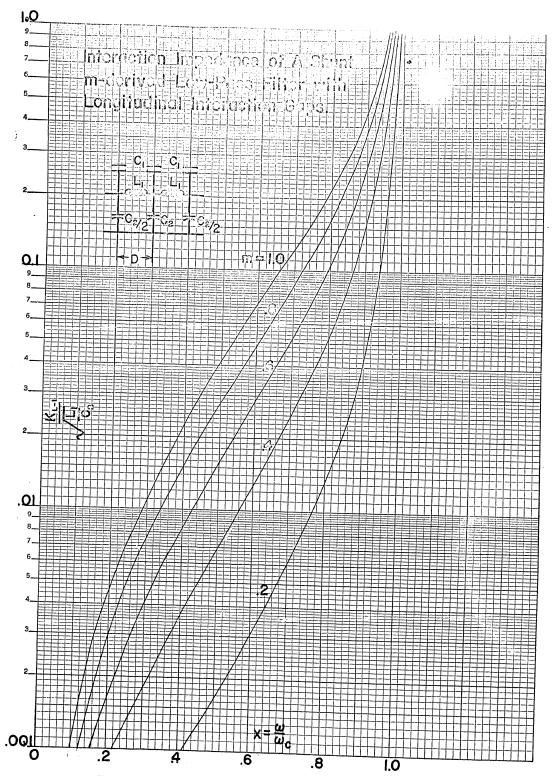

FIG. 3.12.--Longitudinal interaction impedance K_{L-1} of a shunt m-derived low-pass circuit.

IV. CHARACTERISTICS OF THE HIGH-PASS CIRCUITS

The high-pass circuits are shown in Fig. 4.1. The first two have longitudinal interaction gaps and the third one has transverse interaction gaps.

The equations for the characteristics are

$$\theta = -2\sin^{-1}\frac{m}{\sqrt{x^2-1+m^2}} \tag{4.1}$$

$$|y_{pn}| = \frac{2x}{|\theta+2n\pi|} \tag{4.2}$$

$$y_g = \frac{\sqrt{x^2-1}}{mx} \qquad (x^2-1+m^2) \tag{4.3}$$

$$Z_{O\pi} = \sqrt{\frac{L_2}{C_1}}\;\frac{x^2-1+m^2}{x\sqrt{x^2-1}} \tag{4.4}$$

$$Z_{OT} = \sqrt{\frac{L_2}{C_1}}\;\frac{\sqrt{x^2-1}}{x} \tag{4.5}$$

Fig. 14(a) and (c)

$$Z_{OT} = \sqrt{\frac{L_2}{C_1}}\;\frac{x\sqrt{x^2-1}}{x^2-1+m^2} \tag{4.6}$$

$$Z_{O\pi} = \sqrt{\frac{L_2}{C_1}}\;\frac{x}{\sqrt{x^2-1}} \tag{4.7}$$

Fig. 14(b)

$$K_{Ln} = \sqrt{\frac{L_2}{C_1}}\left(\frac{\sin\frac{\beta_n D}{2}}{\frac{\beta_n D}{2}}\right)^2 \frac{x^2-1+m^2}{x\sqrt{x^2-1}} \tag{4.8}$$

Fig. 14(a)

Sanitized Copy Approved for Release 2010/06/30 : CIA-RDP81-01043R000200070007-1

Sanitized Copy Approved for Release 2010/06/30 : CIA-RDP81-01043R000200070007-1

POOR COPY

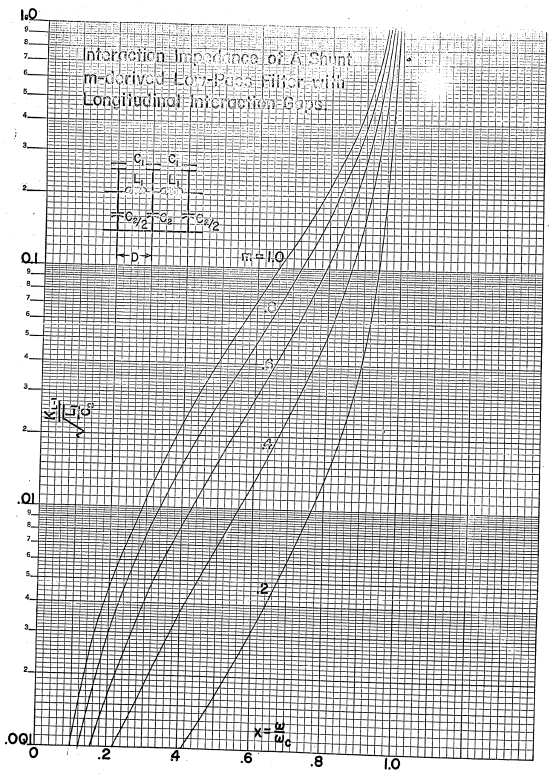

FIG. 3.12.--Longitudinal interaction impedance K_{L-1} of a shunt m-derived low-pass circuit.

IV. CHARACTERISTICS OF THE HIGH-PASS CIRCUITS

The high-pass circuits are shown in Fig. 4.1. The first two have longitudinal interaction gaps and the third one has transverse interaction gaps.

The equations for the characteristics are

$$\theta = -2\sin^{-1}\frac{m}{\sqrt{x^2-1+m^2}} \tag{4.1}$$

$$|y_{pn}| = \frac{2x}{|\theta+2n\pi|} \tag{4.2}$$

$$y_g = \frac{\sqrt{x^2-1}}{mx} \qquad (x^2-1+m^2) \tag{4.3}$$

$$\left.\begin{aligned} Z_{O\pi} &= \sqrt{\frac{L_2}{C_1}}\;\frac{x^2-1+m^2}{x\sqrt{x^2-1}} && (4.4)\\ Z_{OT} &= \sqrt{\frac{L_2}{C_1}}\;\frac{\sqrt{x^2-1}}{x} && (4.5)\end{aligned}\right\}\quad \text{Fig. 14(a) and (c)}$$

$$\left.\begin{aligned} Z_{OT} &= \sqrt{\frac{L_2}{C_1}}\;\frac{x\sqrt{x^2-1}}{x^2-1+m^2} && (4.6)\\ Z_{O\pi} &= \sqrt{\frac{L_2}{C_1}}\;\frac{x}{\sqrt{x^2-1}} && (4.7)\end{aligned}\right\}\quad \text{Fig. 14(b)}$$

$$K_{Ln} = \sqrt{\frac{L_2}{C_1}}\left(\frac{\sin\frac{\beta_n D}{2}}{\frac{\beta_n D}{2}}\right)^2\frac{x^2-1+m^2}{x\sqrt{x^2-1}} \quad \text{Fig. 14(a)} \tag{4.8}$$

Sanitized Copy Approved for Release 2010/06/30 : CIA-RDP81-01043R000200070007-1

Sanitized Copy Approved for Release 2010/06/30 : CIA-RDP81-01043R000200070007-1

(a)

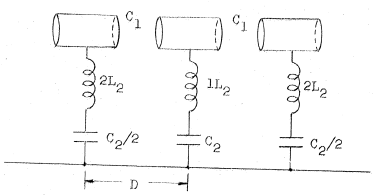

Series m-derived circuit with longitudinal interaction gaps.

(b)

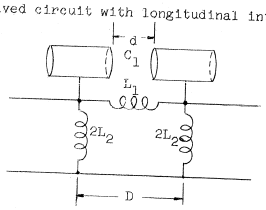

Shunt m-derived circuit with longitudinal interaction gaps.

(c)

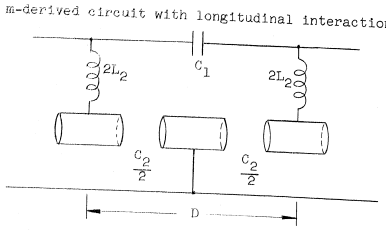

Series m-derived circuit with transverse interaction gaps.

FIG. 4.1.--High-pass circuits.

$$K_{Ln} = \sqrt{\frac{L_2}{C_1}} \left(\frac{\sin \frac{\beta_n D}{2}}{\frac{\beta_n D}{2}} \right)^2 \frac{x}{\sqrt{x^2-1}} \qquad \text{Fig. 14(b)} \qquad (4.9)$$

$$K_{Tn} = \sqrt{\frac{L_2}{C_1}} \left(\frac{\sin \frac{\beta_n D}{4}}{\frac{\beta_n D}{4}} \right)^2 \frac{x^2-1+m^2}{x\sqrt{x^2-1}} \qquad \text{Fig. 14(c)} \qquad (4.10)$$

These equations are plotted as curves in Figs. 4.2 to 4.12.

Sanitized Copy Approved for Release 2010/06/30 : CIA-RDP81-01043R000200070007-1

Sanitized Copy Approved for Release 2010/06/30 : CIA-RDP81-01043R000200070007-1

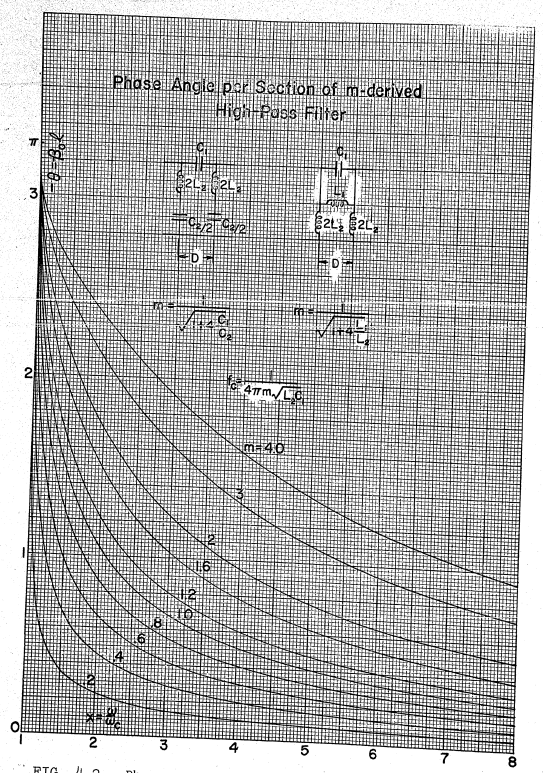

FIG. 4.2.--Phase angle per section of high-pass circuits.

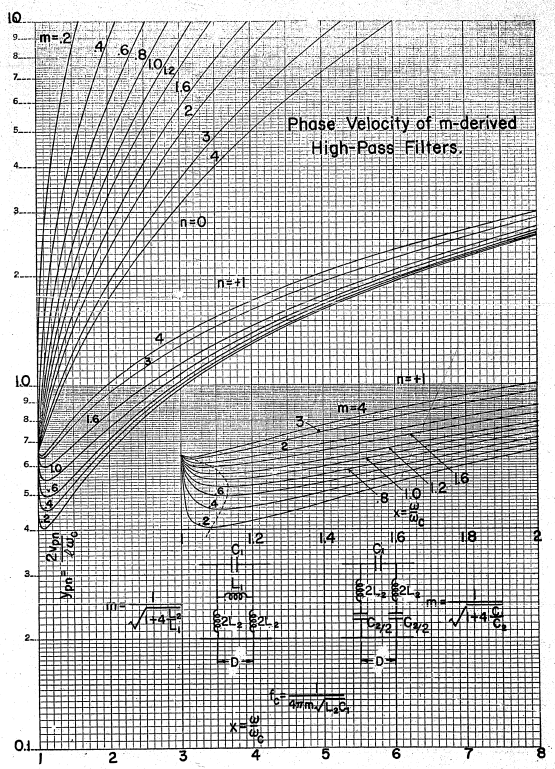

FIG. 4.3.--Phase velocity of high-pass circuits.

Sanitized Copy Approved for Release 2010/06/30 : CIA-RDP81-01043R000200070007-1

Sanitized Copy Approved for Release 2010/06/30 : CIA-RDP81-01043R000200070007-1

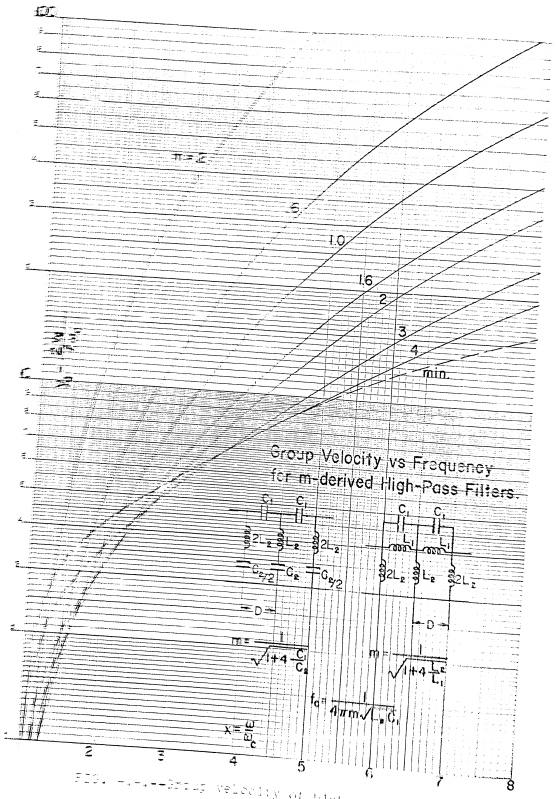

FIG. 4.4.--Group velocity of high-pass circuits.

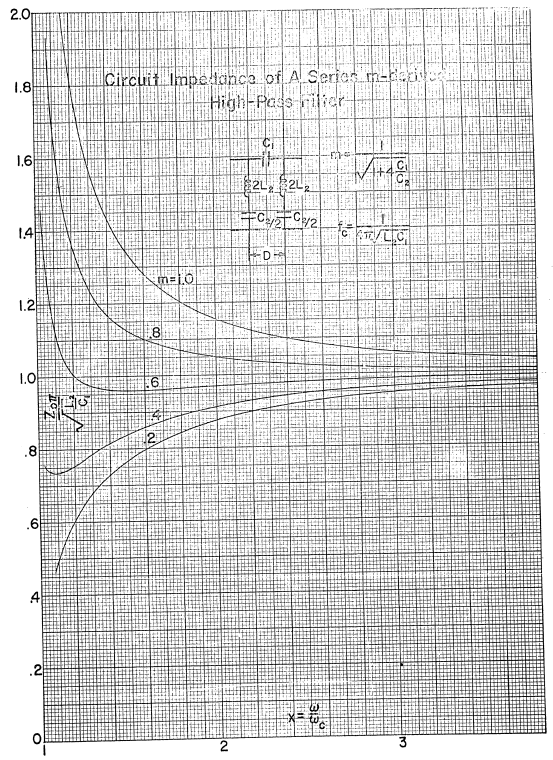

FIG. 4.5.--Circuit impedance of high-pass circuits of Pi section.

Sanitized Copy Approved for Release 2010/06/30 : CIA-RDP81-01043R000200070007-1

Sanitized Copy Approved for Release 2010/06/30 : CIA-RDP81-01043R000200070007-1

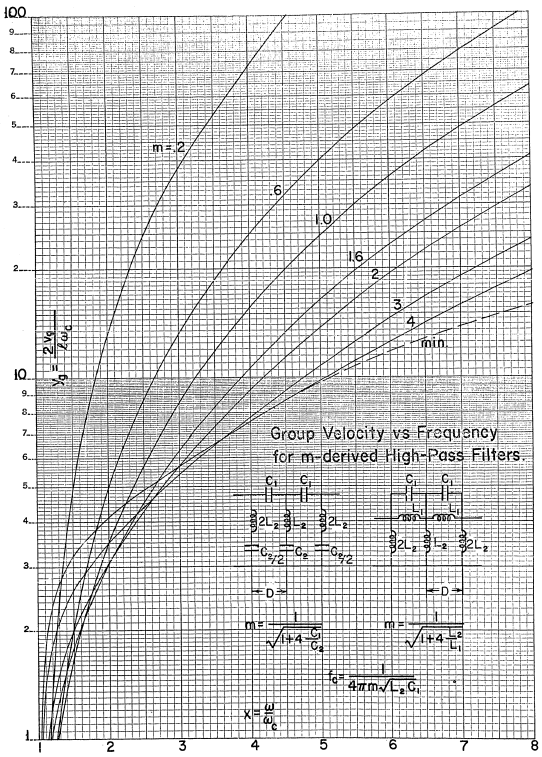

FIG. 4.4.--Group velocity of high-pass circuits.

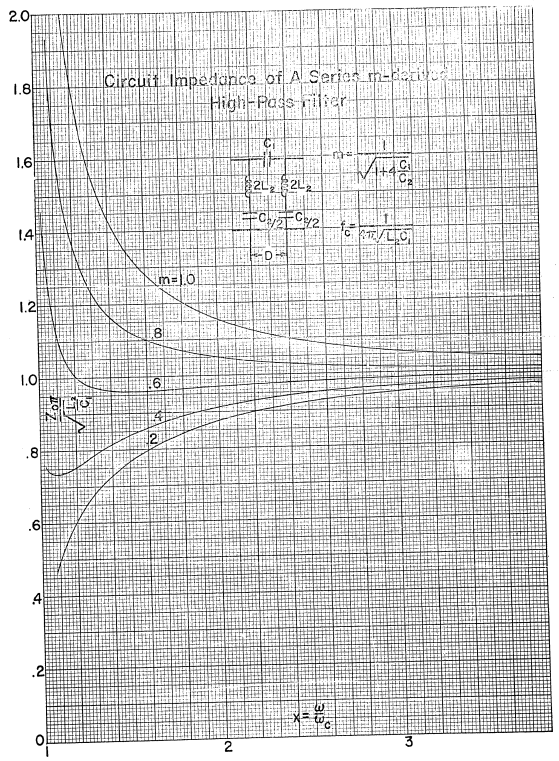

FIG. 4.5.--Circuit impedance of high-pass circuits of Pi section.

Sanitized Copy Approved for Release 2010/06/30 : CIA-RDP81-01043R000200070007-1

Sanitized Copy Approved for Release 2010/06/30 : CIA-RDP81-01043R000200070007-1

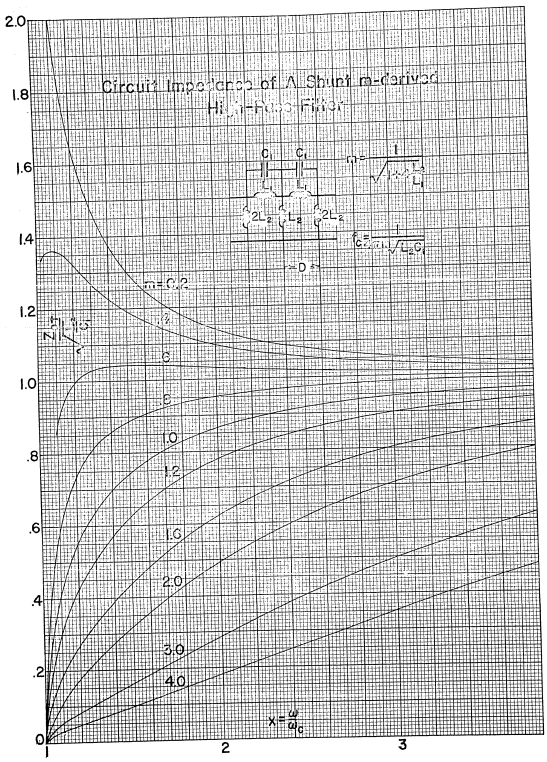

FIG. 4.6.--Circuit impedance of high-pass circuits of Tee section.

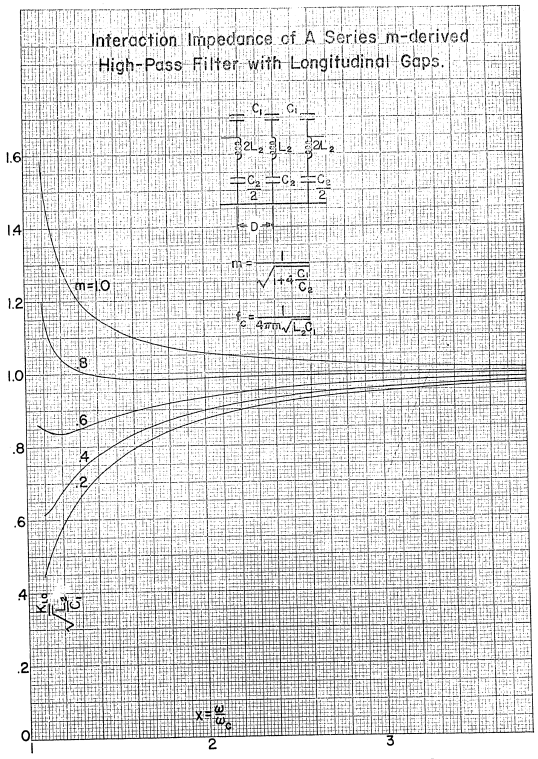

FIG. 4.7.--Longitudinal interaction impedance K_{LO} of a series m-derived high-pass circuit.

Sanitized Copy Approved for Release 2010/06/30 : CIA-RDP81-01043R000200070007-1

Sanitized Copy Approved for Release 2010/06/30 : CIA-RDP81-01043R000200070007-1

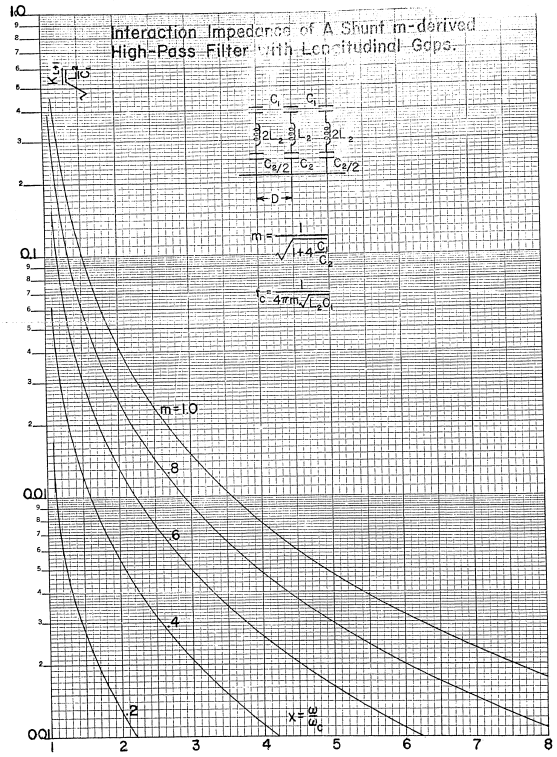

FIG. 4.8.--Longitudinal interaction impedance K_{L+1} of a series m-derived high-pass circuit.

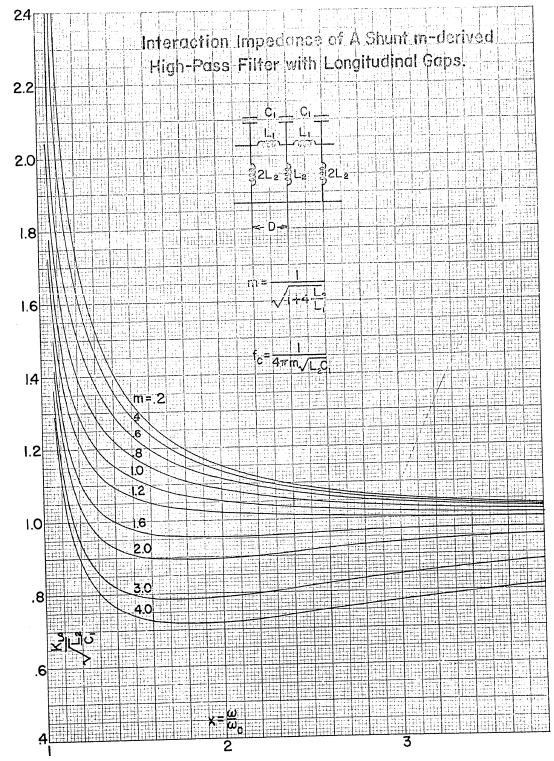

FIG. 4.9.--Longitudinal interaction impedance K_{LO} of a shunt m-derived high-pass circuit.

Sanitized Copy Approved for Release 2010/06/30 : CIA-RDP81-01043R000200070007-1

Sanitized Copy Approved for Release 2010/06/30 : CIA-RDP81-01043R000200070007-1

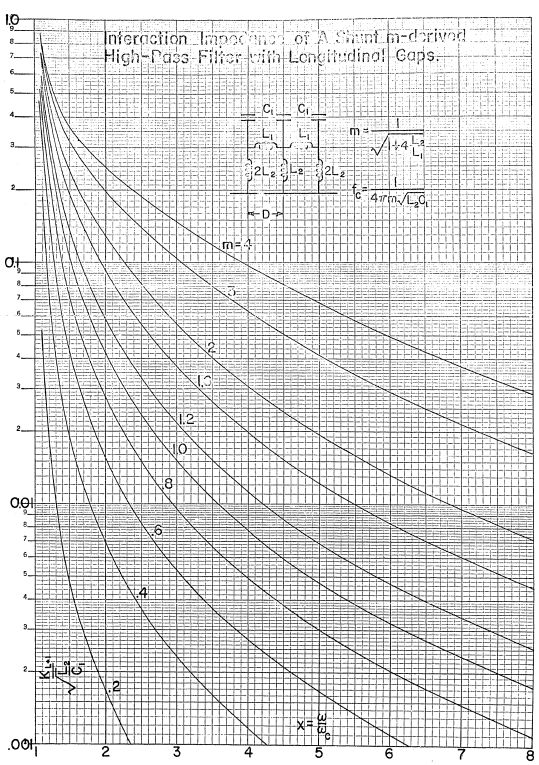

FIG. 4.10.--Longitudinal interaction impedance K_{L+1} of a shunt m-derived high-pass circuit.

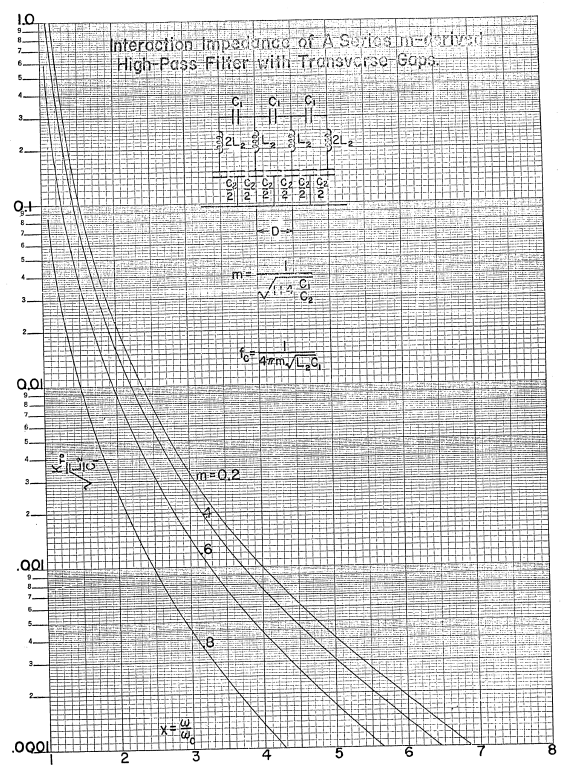

FIG. 4.11.--Transverse interaction impedance K_{TO} of a series m-derived high-pass circuit.

Sanitized Copy Approved for Release 2010/06/30 : CIA-RDP81-01043R000200070007-1

Sanitized Copy Approved for Release 2010/06/30 : CIA-RDP81-01043R000200070007-1

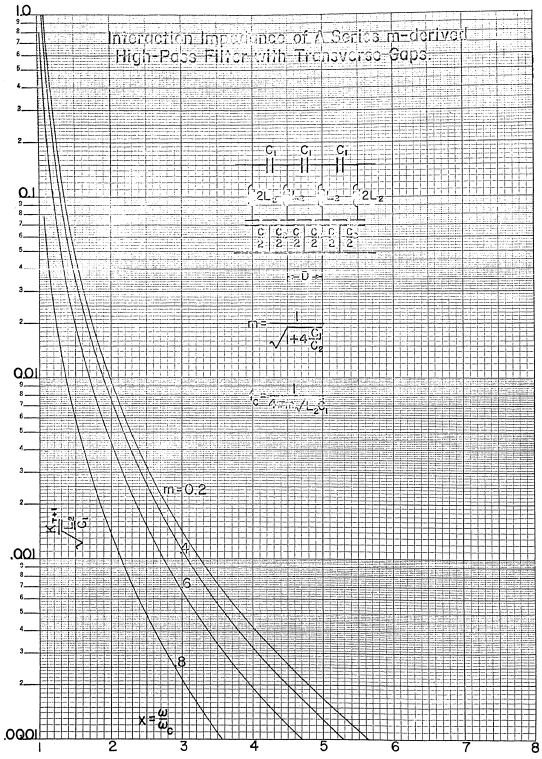

FIG. 4.12.--Transverse interaction impedance K_{T+1} of a series m-derived high-pass circuit.

V. CHARACTERISTICS OF THE THREE-ELEMENT INDUCTIVELY COUPLED BAND-PASS CIRCUIT

The inductively coupled band-pass circuit is shown in Fig. 5.1.

The equations for the characteristics are

$$\theta = \pm 2\sin^{-1}\sqrt{\frac{x^2-m_s^2}{1-m_s^2}} \tag{5.1}$$

$$y_{pn} = \frac{2x}{\theta+2n\pi} \tag{5.2}$$

$$y_g = \frac{\sqrt{1-x^2}\sqrt{x^2-m_s^2}}{x} \tag{5.3}$$

$$Z_{O\pi} = \sqrt{\frac{L_1}{C_2}}\;\frac{\sqrt{1-m_s^2}}{\sqrt{x^2-m_s^2}}\;\frac{x}{\sqrt{1-x^2}} \tag{5.4}$$

$$Z_{OT} = \sqrt{\frac{L_1}{C_2}}\;\frac{x\sqrt{x^2-1}}{\sqrt{m_s^2-x^2}\sqrt{1-m_s^2}} \tag{5.5}$$

$$K_{Tn} = \left(\frac{\sin\frac{\beta_n D}{4}}{\frac{\beta_n D}{4}}\right)^2 \frac{1}{4}\sqrt{\frac{L_1}{C_2}}\;\frac{\sqrt{1-m_s^2}}{\sqrt{x^2-m_s^2}}\;\frac{x}{\sqrt{1-x^2}} \tag{5.6}$$

The cutoff frequencies are given by $x_c = 1$ or $\omega_c = 1/m_s\sqrt{L_2C_2}$ and $x_1 = m_s$ where $m_s = 1/\sqrt{1+4L_2/L_1}$

For positive mutual coupling, i.e. when L_2 and L_1 are both greater than zero, the circuit is fundamentally a forward-wave circuit and the normalized pass-band is between m_s and 1.

Sanitized Copy Approved for Release 2010/06/30 : CIA-RDP81-01043R000200070007-1

Sanitized Copy Approved for Release 2010/06/30 : CIA-RDP81-01043R000200070007-1

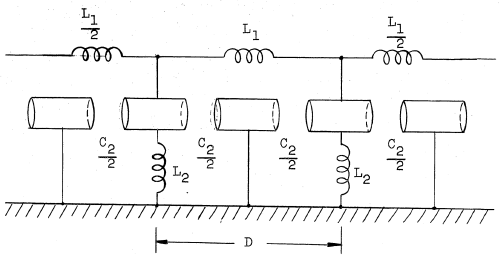

FIG. 5.1.--Three-element inductively coupled band-pass circuit.

When L_2 or L_1 is negative, the circuit is fundamentally a backward-wave circuit and the normalized pass-band is between 1 and m_s. For the fundamental forward-wave circuit, the positive sign is to be used in the θ expression and for the fundamental backward-wave circuit the negative sign is to be used in the θ expression. The negative-mutual-coupled circuit requires a center-tapped coil with the two halves wound in the same direction. The positive-mutual-coupled circuit on the other hand requires a center-tapped coil with the two halves wound in the opposite direction. A band-pass space-harmonic amplifier can be designed using the negative-mutual- coupled circuit with good bandwidth when the pass band is between about 1 to 1.60.

Equations (4.1) to (4.6) are plotted in Figs. 5.2 to 5.16. Cases for m_s = 1.5, 1.6 and 1.7 are also plotted on an enlarged scale. Curves include both the positive and the negative-mutual-coupling cases.

Sanitized Copy Approved for Release 2010/06/30 : CIA-RDP81-01043R000200070007-1

Sanitized Copy Approved for Release 2010/06/30 : CIA-RDP81-01043R000200070007-1

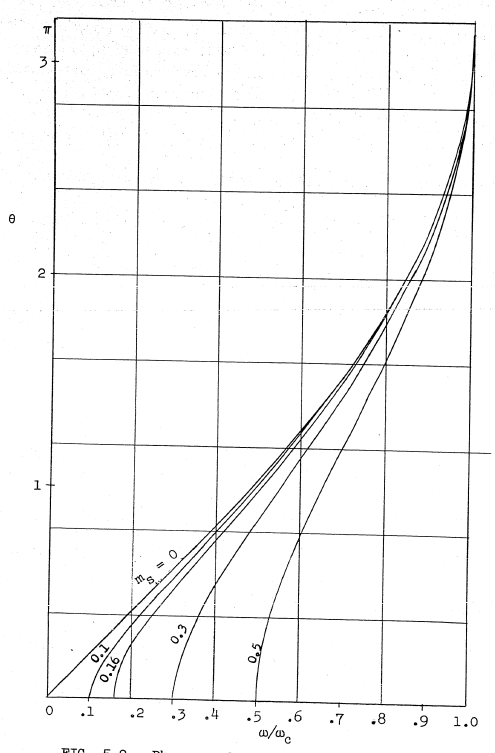

FIG. 5.2.--Phase angle per section of the positive mutual coupled three-element band-pass circuit.

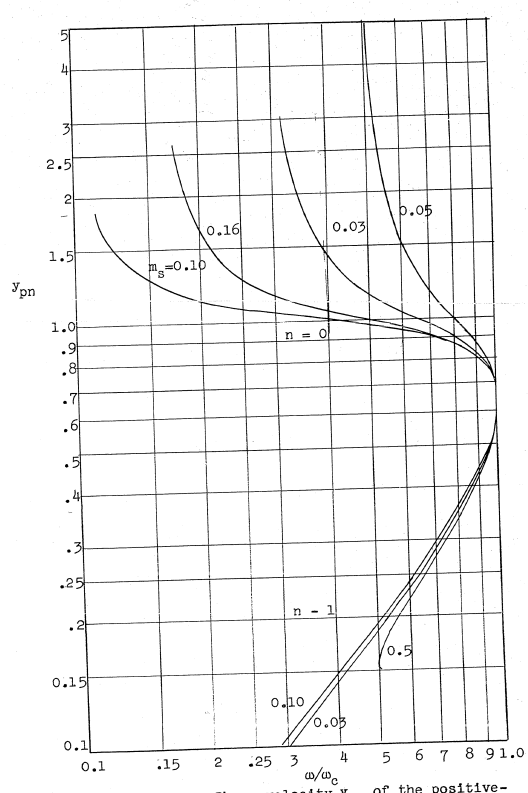

FIG. 5.3.--Phase velocity y_{pn} of the positive-mutual-coupled three-element band-pass circuit.

Sanitized Copy Approved for Release 2010/06/30 : CIA-RDP81-01043R000200070007-1

Sanitized Copy Approved for Release 2010/06/30 : CIA-RDP81-01043R000200070007-1

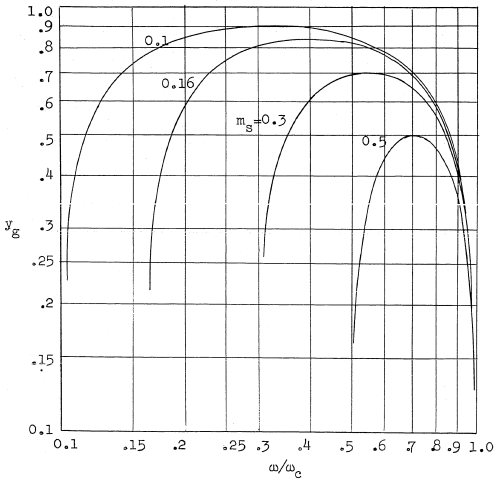

FIG. 5.4.--Group velocity y_g of the positive-mutual-coupled three-element band-pass circuit.

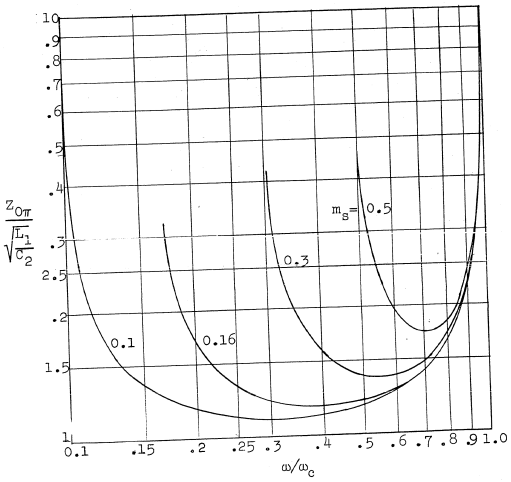

FIG. 5.5.--Circuit impedance $Z_{0\pi}$ of the positive-mutual-coupled three-element band-pass circuit of Pi section.

Sanitized Copy Approved for Release 2010/06/30 : CIA-RDP81-01043R000200070007-1

Sanitized Copy Approved for Release 2010/06/30 : CIA-RDP81-01043R000200070007-1

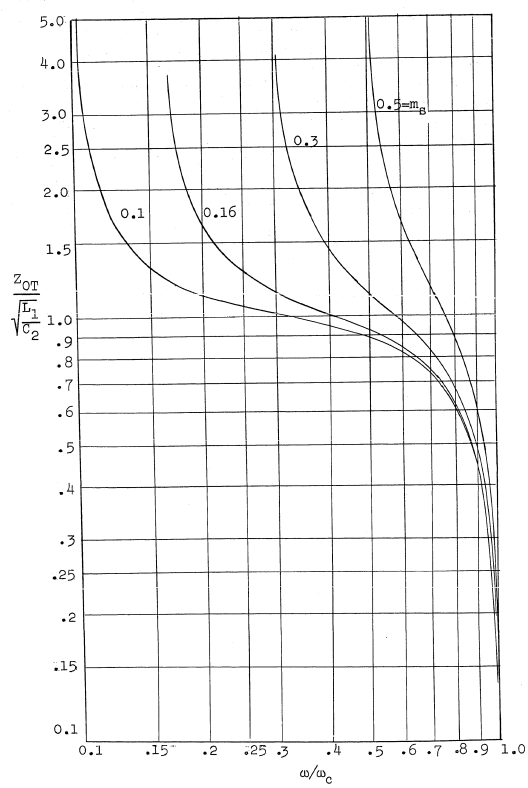

FIG. 5.6.--Circuit impedance Z_{OT} of the positive-mutual coupled three-element band-pass circuit of Tee section.

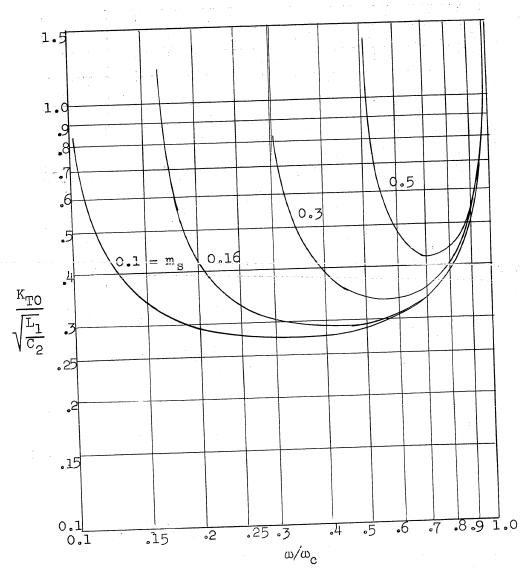

FIG. 5.7.--Transverse interaction impedance K_{TO} of the positive-mutual-coupled three-element band-pass circuit.

Sanitized Copy Approved for Release 2010/06/30 : CIA-RDP81-01043R000200070007-1

Sanitized Copy Approved for Release 2010/06/30 : CIA-RDP81-01043R000200070007-1

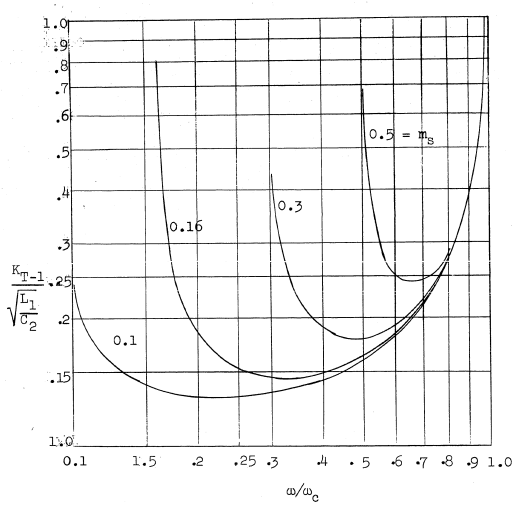

FIG. 5.8.--Transverse interaction impedance K_{T-1} of the positive-mutual-coupled three-element band-pass circuit.

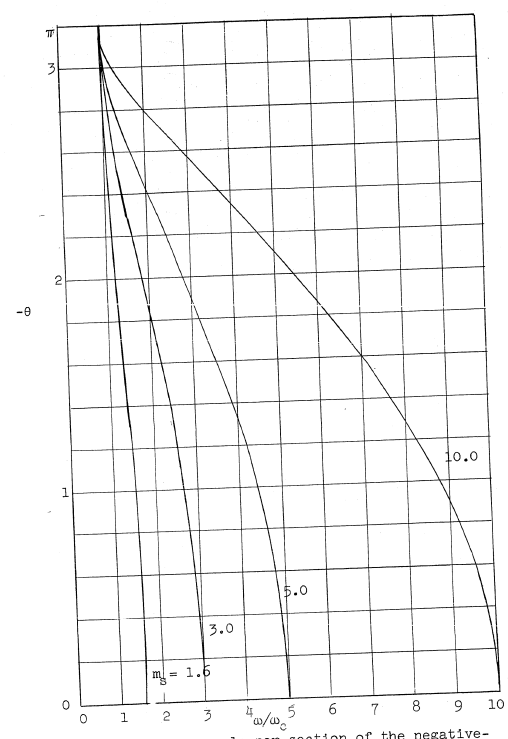

FIG. 5.9.--Phase angle per section of the negative-mutual-coupled three-element band-pass circuit.

Sanitized Copy Approved for Release 2010/06/30 : CIA-RDP81-01043R000200070007-1

Sanitized Copy Approved for Release 2010/06/30 : CIA-RDP81-01043R000200070007-1

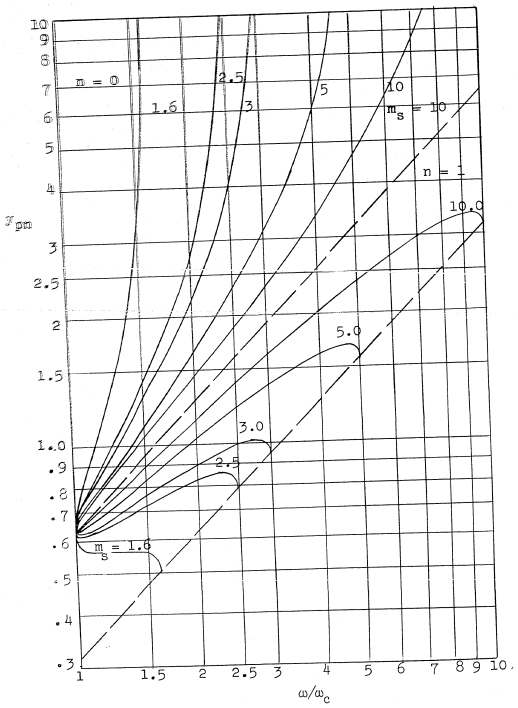

FIG. 5.10.--Phase velocity y_{pp} of the negative-mutual-coupled three-element band-pass circuit.

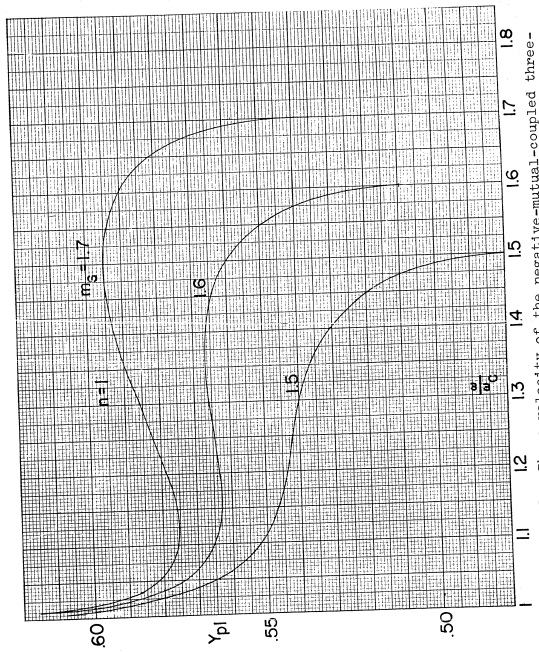

FIG. 5.11.--Phase velocity of the negative-mutual-coupled three-element band-pass circuit (enlarged scale).

Sanitized Copy Approved for Release 2010/06/30 : CIA-RDP81-01043R000200070007-1

Sanitized Copy Approved for Release 2010/06/30 : CIA-RDP81-01043R000200070007-1

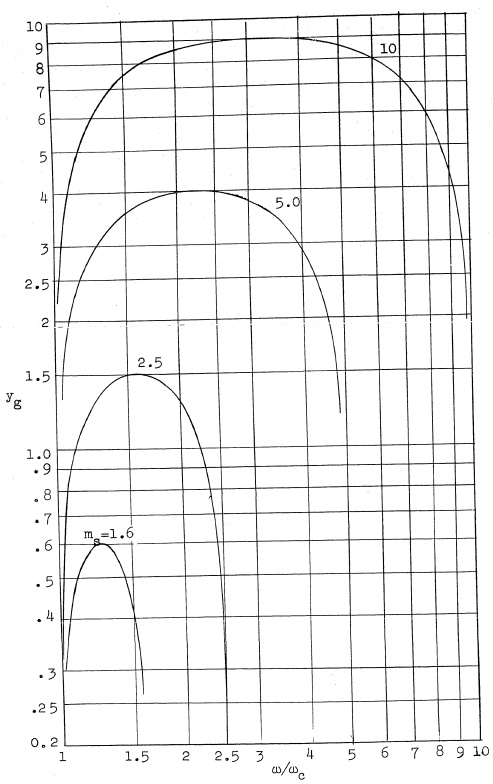

FIG. 5.12.--Group velocity y_g of the negative-mutual-coupled three-element band-pass circuit.

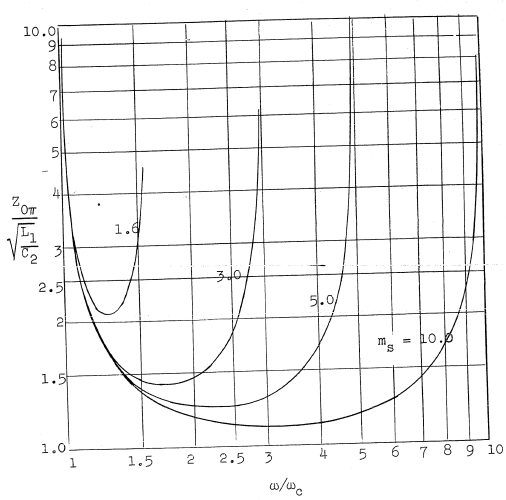

FIG. 5.13.--Circuit impedance $Z_{0\pi}$ of the negative-mutual-coupled three-element band-pass circuit of Pi section.

Sanitized Copy Approved for Release 2010/06/30 : CIA-RDP81-01043R000200070007-1

Sanitized Copy Approved for Release 2010/06/30 : CIA-RDP81-01043R000200070007-1

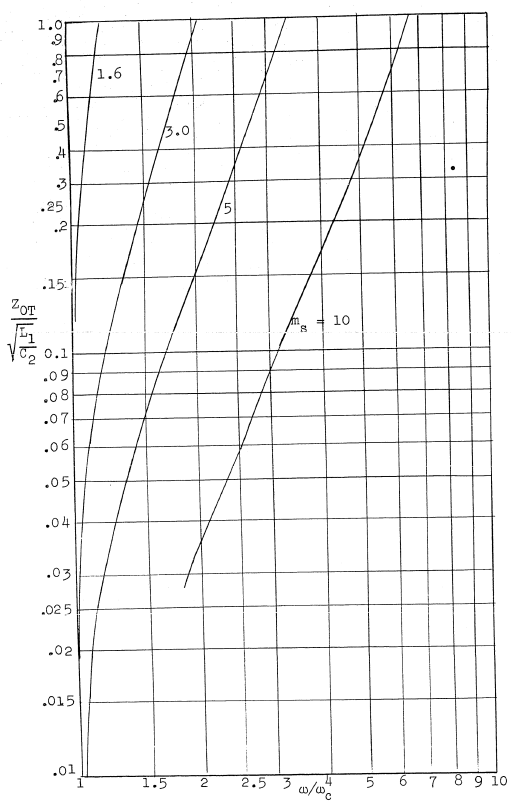

FIG. 5.14.--Circuit impedance Z_{OT} of the negative-mutual-coupled three-element band-pass circuit of Tee section.

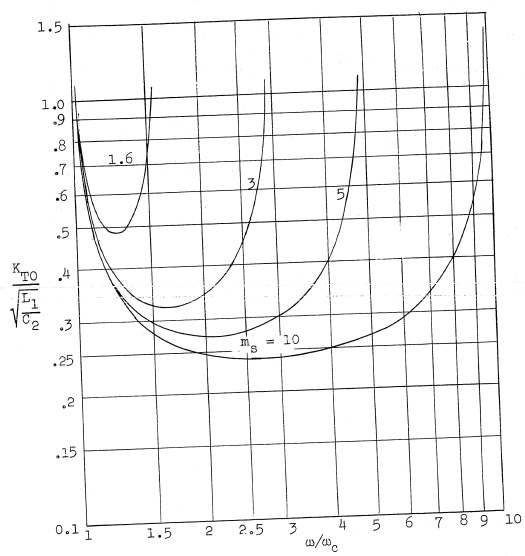

FIG. 5.15.--Transverse interaction impedance K_{TO} of the negative-mutual-coupled three-element band-pass circuit.

Sanitized Copy Approved for Release 2010/06/30 : CIA-RDP81-01043R000200070007-1

Sanitized Copy Approved for Release 2010/06/30 : CIA-RDP81-01043R000200070007-1

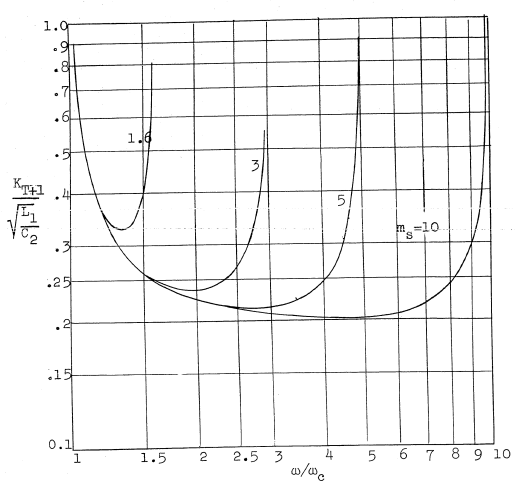

FIG. 5.16.--Transverse interaction impedance K_{T+1} of the negative-mutual-coupled three-element band-pass circuit.

VI. CHARACTERISTICS OF THE THREE-ELEMENT CAPACITIVELY COUPLED BAND-PASS CIRCUITS

The capacitively coupled band-pass circuits are shown in Figs. 6.1 (a) and (b).

The equations for the characteristics are

$$\theta = -2\sin^{-1}\sqrt{\frac{x^{-2}-m_r^2}{1-m_r^2}} \tag{6.1}$$

$$y_{pn} = \frac{2x}{|\theta+2n\pi|} \tag{6.2}$$

$$y_g = x^2\sqrt{x^2-1}\;\sqrt{x^{-2}-m_r^2} \tag{6.3}$$

$$Z_{O\pi} = \sqrt{\frac{L_2}{C_1}}\;\frac{\sqrt{1-m_r^2}}{x\sqrt{1-x^{-2}}\sqrt{x^{-2}-m_r^2}} \tag{6.4}$$

$$Z_{OT} = \sqrt{\frac{L_2}{C_1}}\;\frac{\sqrt{1-x^{-2}}}{\sqrt{1-m_r^2}\sqrt{x^{-2}-m_r^2}\;x} \tag{6.5}$$

$$K_{Ln} = \sqrt{\frac{L_2}{C_1}}\;\frac{\sqrt{1-m_r^2}}{x\sqrt{1-x^{-2}}\sqrt{x^{-2}-m_r^2}}\left(\frac{\sin\frac{\beta_n D}{2}}{\frac{\beta_n D}{2}}\right)^2 \tag{6.6}$$

$$K_{Tn} = \sqrt{\frac{L_2}{C_1}}\;\frac{\sqrt{1-m_r^2}}{x\sqrt{1-x^{-2}}\sqrt{x^{-2}-m_r^2}}\;\frac{1}{4}\left(\frac{\sin\frac{\beta_n D}{4}}{\frac{\beta_n D}{4}}\right)^2 \tag{6.7}$$

and $\omega_c = \frac{m_r}{\sqrt{L_2C_2}}$ where $m_r = x_1^{-1} = \frac{1}{\sqrt{1+\frac{4C_1}{C_2}}}$

Sanitized Copy Approved for Release 2010/06/30 : CIA-RDP81-01043R000200070007-1

Sanitized Copy Approved for Release 2010/06/30 : CIA-RDP81-01043R000200070007-1

(a)

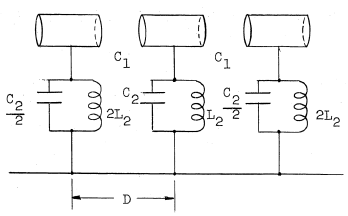

Longitudinal interaction structure

(b)

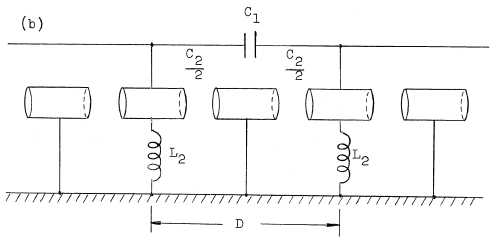

Transverse interaction structure

FIG. 6.1.--Three-element capacitively coupled band-pass circuits.

The capacitively coupled circuit is a backward-wave circuit. There are two possible locations for the interaction electrodes, i.e., at C_1 for the longitudinal type and at C_2 for the transverse type.

Equations (6.1) to (6.7) are plotted in Figs. 6.2 to 6.13.

Sanitized Copy Approved for Release 2010/06/30 : CIA-RDP81-01043R000200070007-1

Sanitized Copy Approved for Release 2010/06/30 : CIA-RDP81-01043R000200070007-1

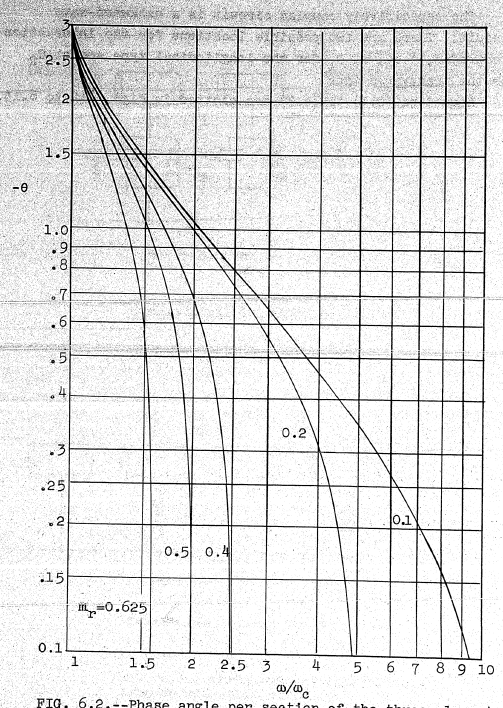

FIG. 6.2.--Phase angle per section of the three-element capacitively coupled band-pass circuit.

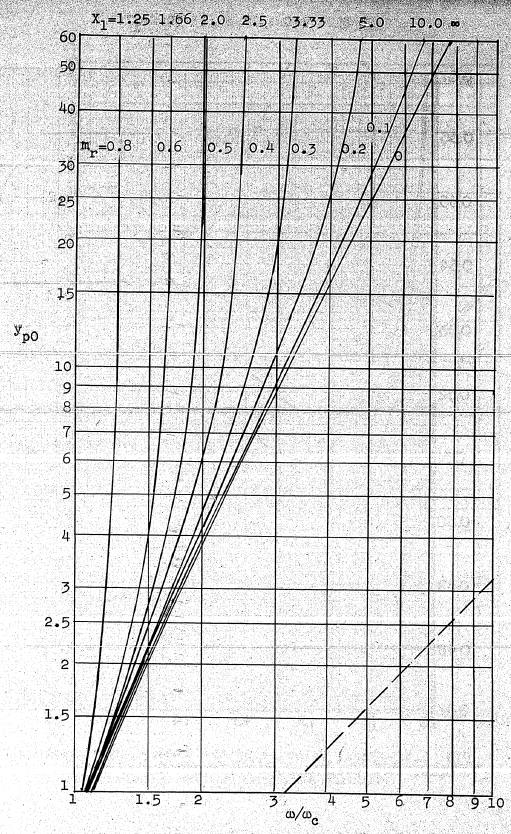

FIG. 6.3.--Phase velocity y_{p0} of the three-element capacitively coupled band-pass circuit.

Sanitized Copy Approved for Release 2010/06/30 : CIA-RDP81-01043R000200070007-1

Sanitized Copy Approved for Release 2010/06/30 : CIA-RDP81-01043R000200070007-1

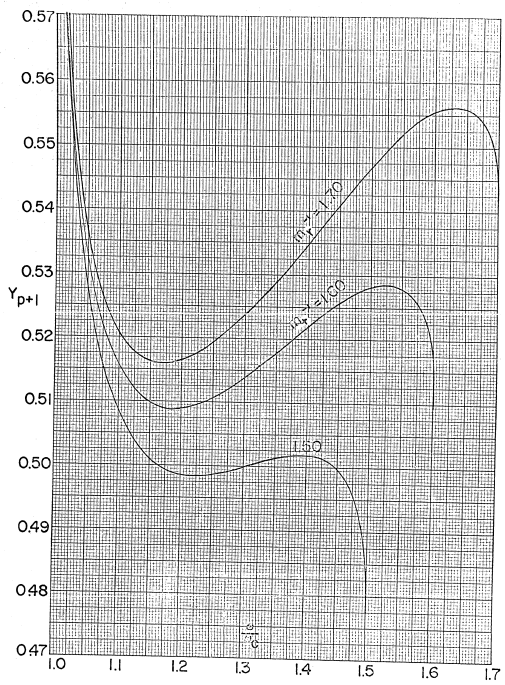

FIG. 6.4.--Phase velocity of the three-element capacitively coupled band-pass circuit (enlarged scale) y_{p+1}.

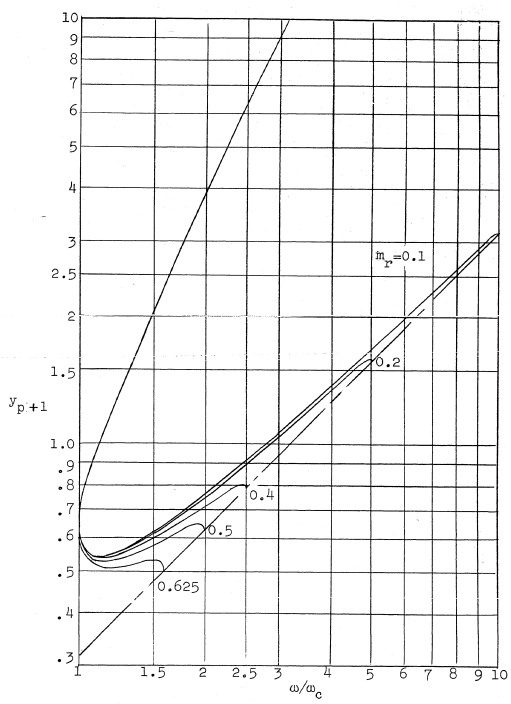

FIG. 6.5.--Phase velocity y_{p+1} of the three-element capacitively coupled band-pass circuit.

Sanitized Copy Approved for Release 2010/06/30 : CIA-RDP81-01043R000200070007-1

Sanitized Copy Approved for Release 2010/06/30 : CIA-RDP81-01043R000200070007-1

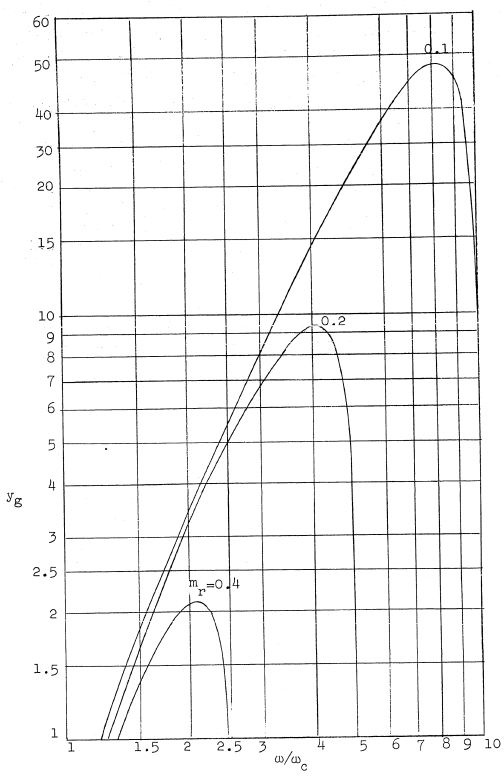

FIG. 6.6.--Group velocity y_g of the three-element capacitively coupled band-pass circuit.

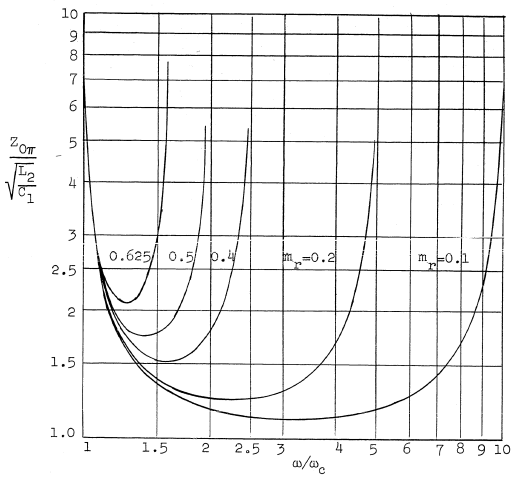

FIG. 6.7.--Circuit impedance $Z_{0\pi}$ of the three element capacitively coupled band-pass circuit of Pi section.

Sanitized Copy Approved for Release 2010/06/30 : CIA-RDP81-01043R000200070007-1

Sanitized Copy Approved for Release 2010/06/30 : CIA-RDP81-01043R000200070007-1

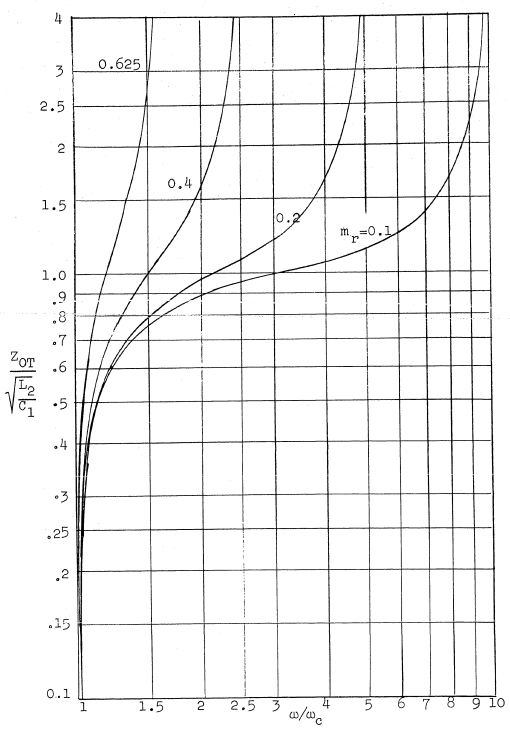

FIG. 6.8.--Circuit impedance Z_{OT} of the three-element capacitively coupled band-pass circuit of Tee section.

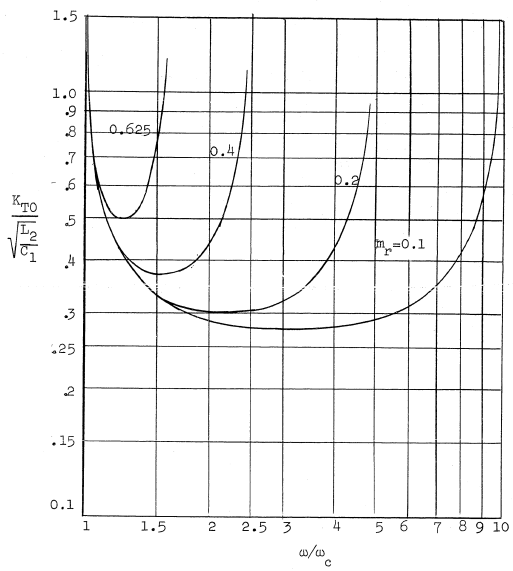

FIG. 6.9.--Transverse interaction impedance K_{TO} of the three-element capacitively-coupled band-pass circuit.

Sanitized Copy Approved for Release 2010/06/30 : CIA-RDP81-01043R000200070007-1

Sanitized Copy Approved for Release 2010/06/30 : CIA-RDP81-01043R000200070007-1

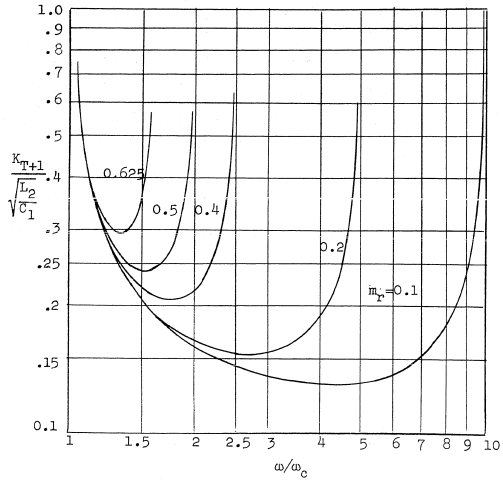

FIG. 6.10.--Transverse interaction impedance K_{T+1} of the three-element capacitively-coupled band-pass circuit.

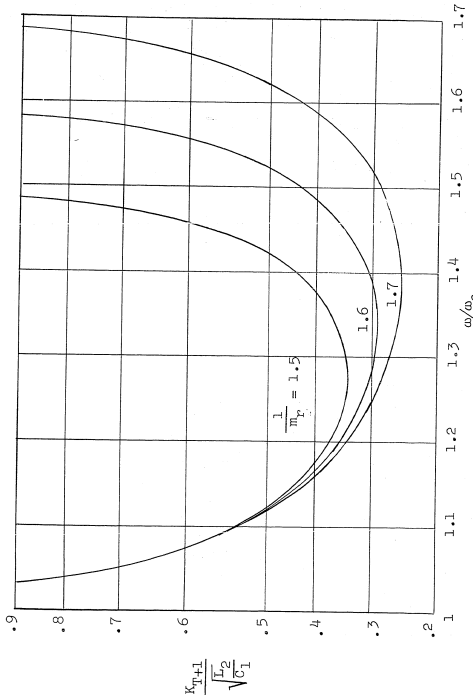

FIG. 6.11.--Transverse interaction impedance K_{T+1} of the three element capacitively-coupled band-pass circuit (enlarged scale).

Sanitized Copy Approved for Release 2010/06/30 : CIA-RDP81-01043R000200070007-1

Sanitized Copy Approved for Release 2010/06/30 : CIA-RDP81-01043R000200070007-1

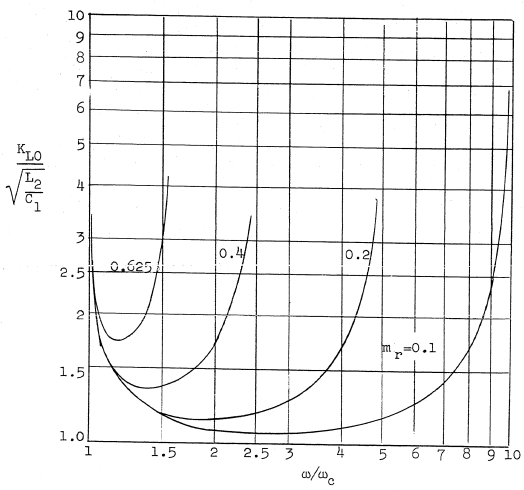

FIG. 6.12.--Longitudinal interaction impedance K_{LO} of the three-element capacitively-coupled band-pass circuit.

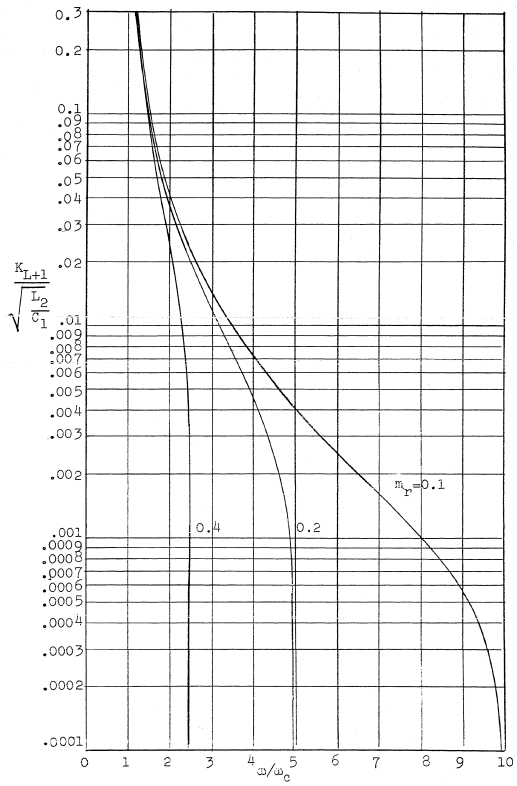

FIG. 6.13.--Longitudinal interaction impedance K_{L+1} of the three-element capacitively-coupled band-pass circuit.

Sanitized Copy Approved for Release 2010/06/30 : CIA-RDP81-01043R000200070007-1

Sanitized Copy Approved for Release 2010/06/30 : CIA-RDP81-01043R000200070007-1

VII. CHARACTERISTICS OF THE FOUR-ELEMENT BAND-PASS CIRCUIT

The four-element band-pass circuits are shown in Fig. 7.1. The equations for the characteristics are

$$\theta = \pm 2\sin^{-1}\sqrt{\frac{x^2-x_1^{\,2}}{(1-x_1^{\,2}) + r(1-x^2)}} \tag{7.1}$$

$$y_{pn} = \frac{2x}{|\theta+2n\pi|} \tag{7.2}$$

$$y_g = \frac{\sqrt{1-x^2}\,\sqrt{x^2-x_1^{\,2}}\left(1+r\,\dfrac{1-x^2}{1-x_1^{\,2}}\right)}{x\,\sqrt{1+r}} \tag{7.3}$$

$$Z_{O\pi} = \sqrt{\frac{L_2}{C_1}}\;\frac{\sqrt{r}\;x}{\sqrt{x^2-x_1^{\,2}}\,\sqrt{1+s}\,\sqrt{1-x^2}} \tag{7.4}$$

$$Z_{OT} = \sqrt{\frac{L_2}{C_1}}\,\sqrt{\frac{r}{s}}\;\frac{x}{x_1}\sqrt{\frac{(s+1)-(r+1)\dfrac{x^2}{x_1^{\,2}}}{s\left(\dfrac{x^2}{x_1^{\,2}}-1\right)\left(1-\dfrac{r}{s}\,\dfrac{x^2}{x_1^{\,2}}\right)}}^{\,2} \tag{7.5}$$

$$K_{Ln} = Z_{O\pi}\left(\frac{\sin\dfrac{\beta_n D}{2}}{\dfrac{\beta_n D}{2}}\right)^2 \tag{7.6}$$

$$K_{Tn} = Z_{O\pi}\;\frac{1}{4}\left(\frac{\sin\dfrac{\beta_n D}{4}}{\dfrac{\beta_n D}{4}}\right)^2 \tag{7.7}$$

$$\omega_c = \frac{1}{\sqrt{L_2 C_2}}\;\frac{\sqrt{1+s}}{\sqrt{1+r}}\;, \quad x_1 = \frac{m_s}{m_r} \tag{7.8}$$

(a)

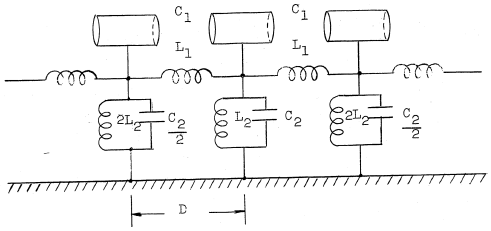

Longitudinal interaction structure.

(b)

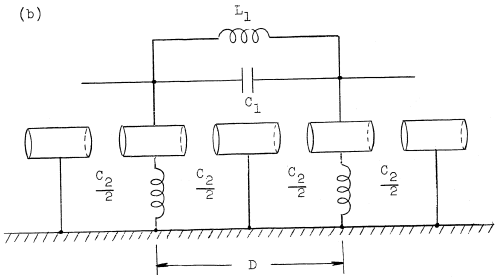

Transverse interaction structure.

FIG. 7.1.--Four-element band-pass circuits.

Sanitized Copy Approved for Release 2010/06/30 : CIA-RDP81-01043R000200070007-1

Sanitized Copy Approved for Release 2010/06/30 : CIA-RDP81-01043R000200070007-1

where

$$m_r = \frac{1}{\sqrt{1+r}} = \frac{1}{\sqrt{1+\frac{4C_1}{C_2}}}$$

$$m_s = \frac{1}{\sqrt{1+s}} = \frac{1}{\sqrt{1+\frac{4L_2}{L_1}}}$$

For the fundamental-backward-wave circuit, x_1 is greater than unity and the negative sign in the θ expression should be used. For the fundamental-forward-wave circuit, x_1 is less than unity and the positive sign in the θ expression should be used.

For the case of negative mutual coupling, L_1 is negative and L_2 is positive. The circuit is then fundamentally a backward-wave circuit. When L_1 and L_2 are both positive, i.e. for the case of positive mutual coupling, the circuit can fundamentally be a forward-wave or a backward-wave circuit depending on whether x_1 is less than unity or greater than unity.

Curves are presented in Figs. 7.2 to 7.91 for both the forward-wave and the backward-wave circuits.

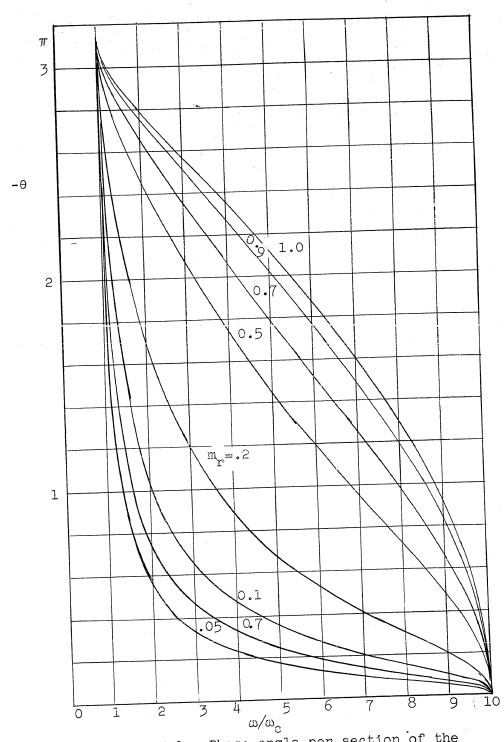

FIG. 7.2.--Phase angle per section of the four-element band-pass circuit, x_1=5.

Sanitized Copy Approved for Release 2010/06/30 : CIA-RDP81-01043R000200070007-1

Sanitized Copy Approved for Release 2010/06/30 : CIA-RDP81-01043R000200070007-1

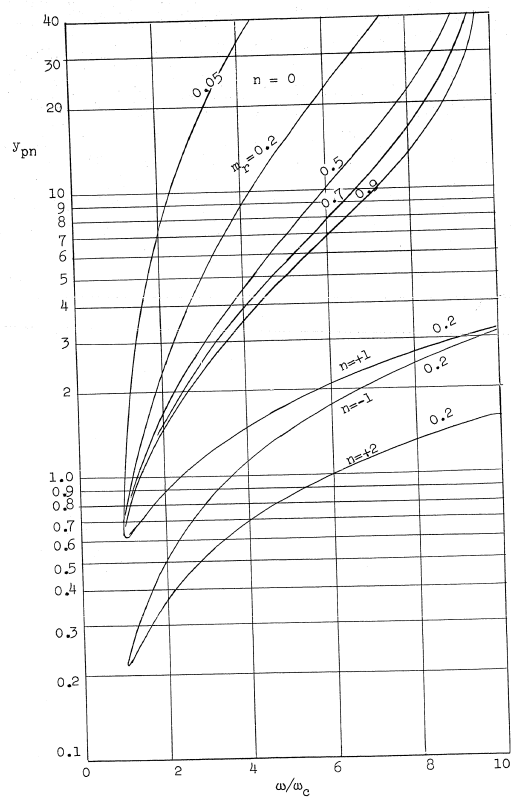

FIG. 7.3.--Phase velocity y_{pn} of the four-element band-pass circuit, x_1=10.

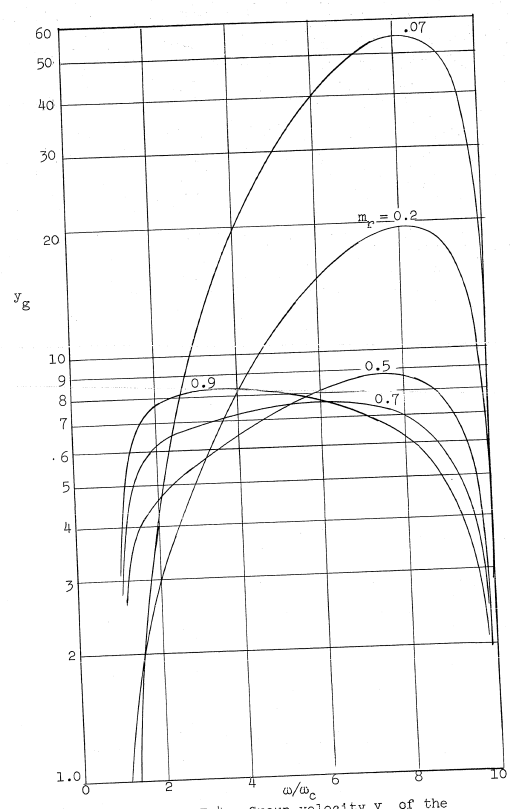

FIG. 7.4.--Group velocity y_g of the four-element band-pass circuit, x_1=10.

Sanitized Copy Approved for Release 2010/06/30 : CIA-RDP81-01043R000200070007-1

Sanitized Copy Approved for Release 2010/06/30 : CIA-RDP81-01043R000200070007-1

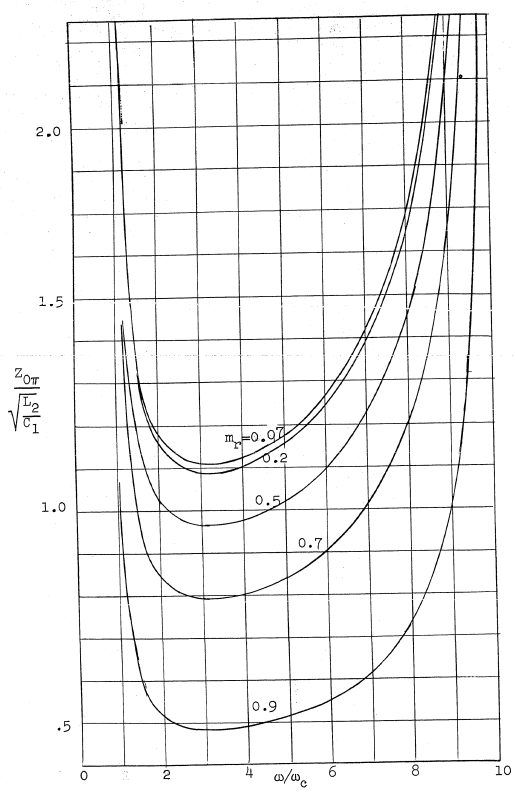

FIG. 7.5.--Circuit impedance $Z_{0\pi}$ of the four-element band-pass circuit of Pi section, x_1 = 10.

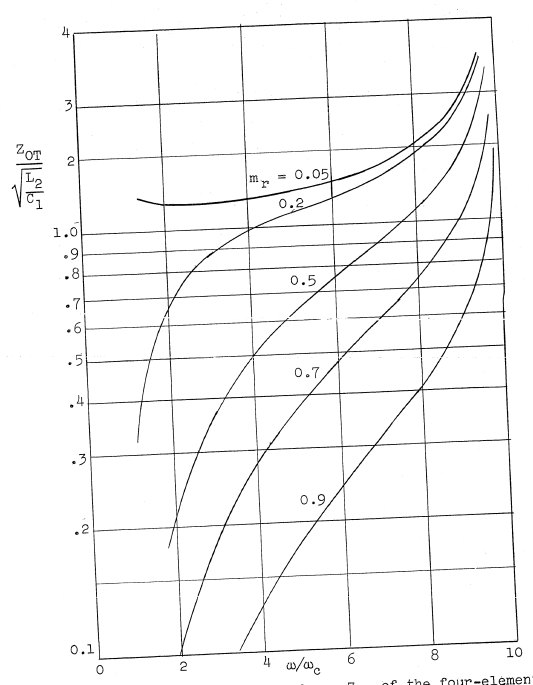

FIG. 7.6.--Circuit impedance Z_{0T} of the four-element band-pass circuit of Tee section, x_1 = 10.

Sanitized Copy Approved for Release 2010/06/30 : CIA-RDP81-01043R000200070007-1

Sanitized Copy Approved for Release 2010/06/30 : CIA-RDP81-01043R000200070007-1

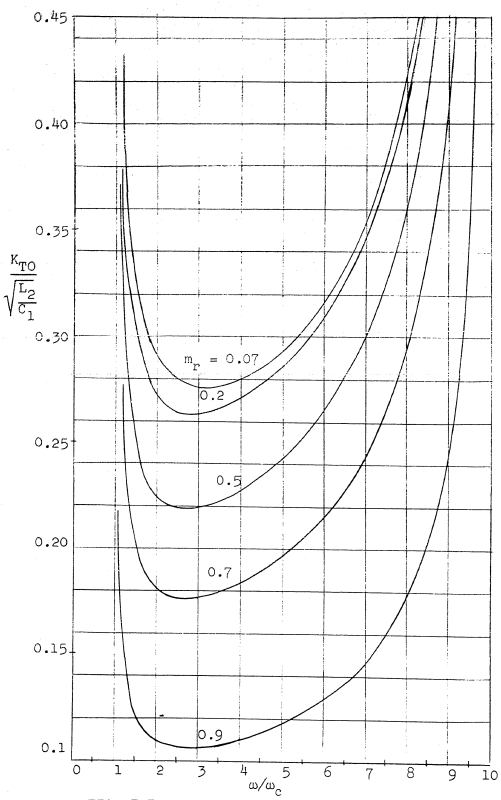

FIG. 7.7.--Transverse interaction impedance K_{TO} of the four-element band-pass circuit, $x_1 = 10$.

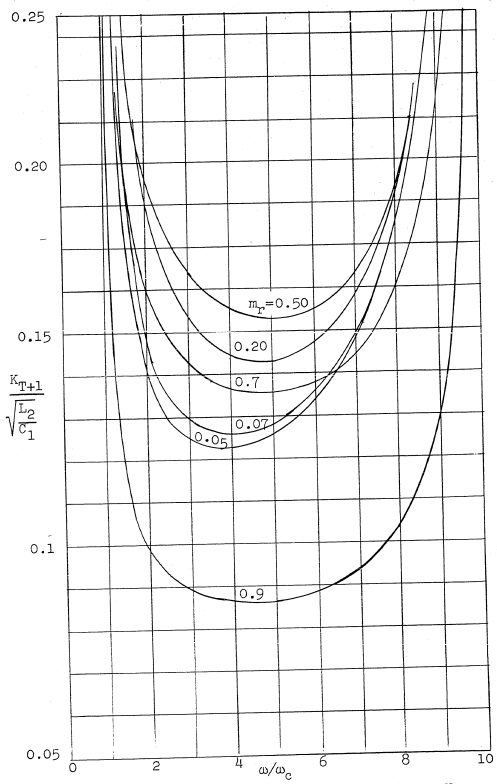

FIG. 7.8.--Transverse interaction impedance K_{T+1} of the four-element band-pass circuit, $x_1 = 10$.

Sanitized Copy Approved for Release 2010/06/30 : CIA-RDP81-01043R000200070007-1

Sanitized Copy Approved for Release 2010/06/30 : CIA-RDP81-01043R000200070007-1

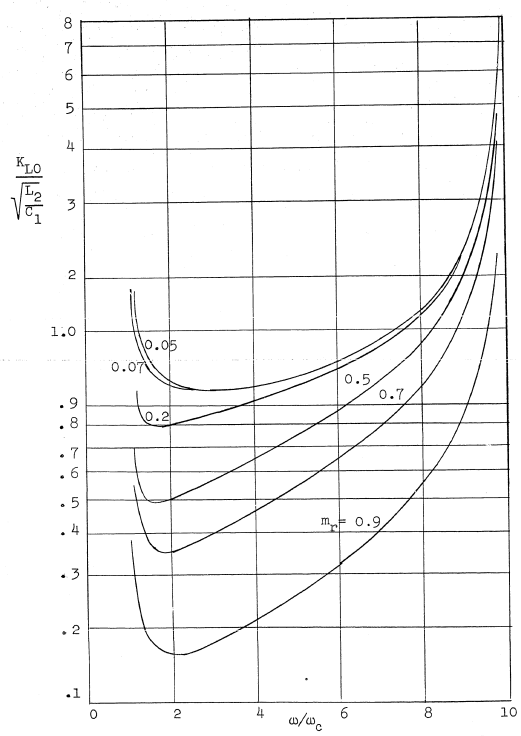

FIG. 7.9.--Longitudinal interaction impedance K_{LO} of the four-element band-pass circuit, x_1 = 10.

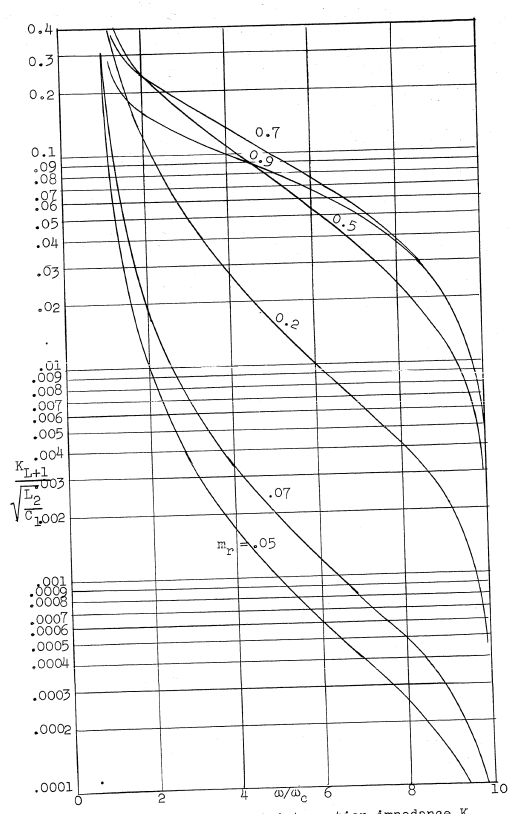

FIG. 7.10.--Longitudinal interaction impedance K_{L+1} of the four-element band-pass circuit, x_1 = 10.

Sanitized Copy Approved for Release 2010/06/30 : CIA-RDP81-01043R000200070007-1

Sanitized Copy Approved for Release 2010/06/30 : CIA-RDP81-01043R000200070007-1

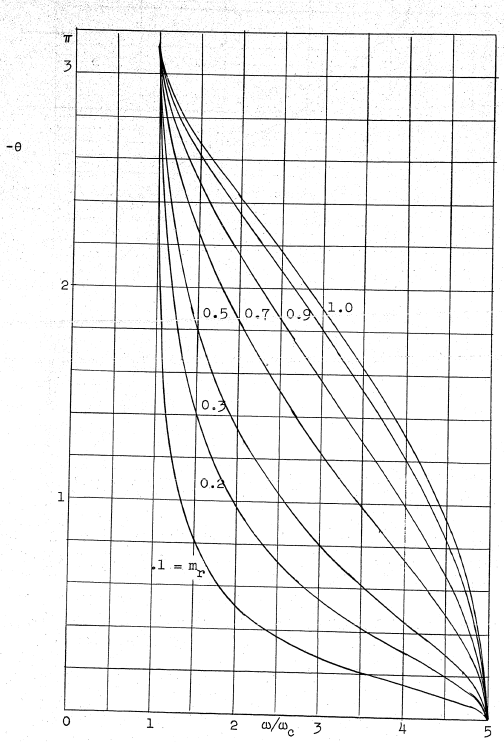

FIG. 7.11.--Phase angle per section of the four-element band-pass circuit, $x_1 = 5$.

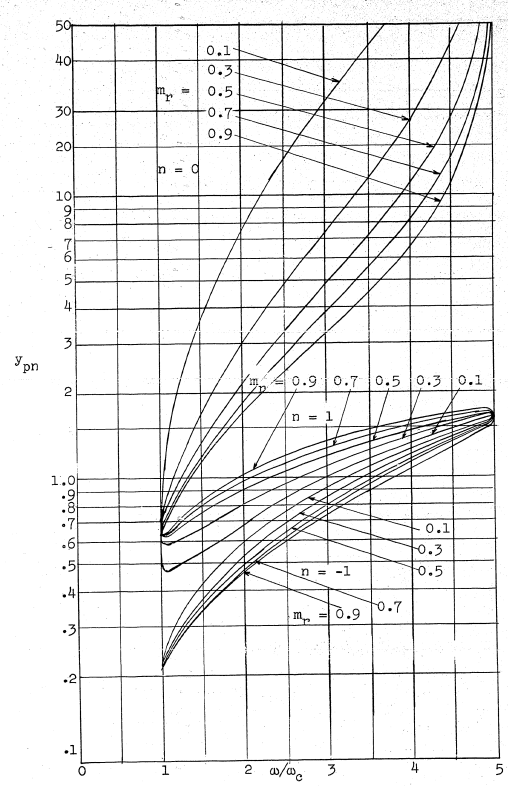

FIG. 7.12.--Phase velocity y_{pn} of the four-element band-pass circuit, $x_1 = 5$.

Sanitized Copy Approved for Release 2010/06/30 : CIA-RDP81-01043R000200070007-1

Sanitized Copy Approved for Release 2010/06/30 : CIA-RDP81-01043R000200070007-1

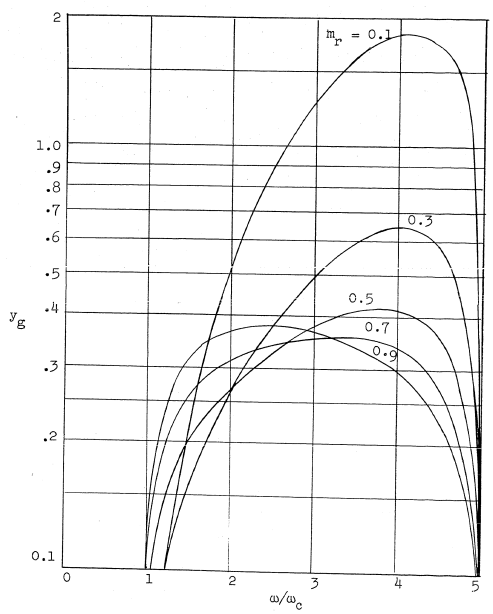

FIG. 7.13.--Group velocity y_g of the four-element band-pass circuit, x_1=5.

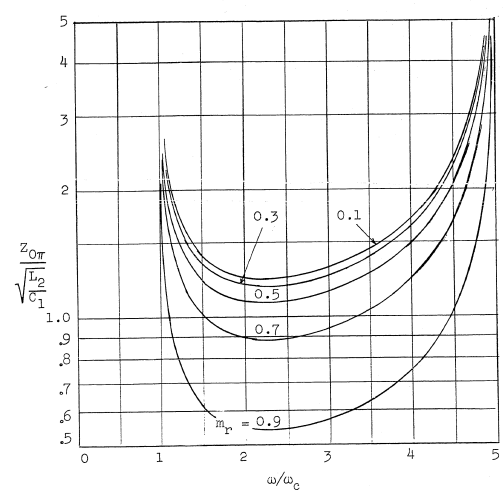

FIG. 7.14.--Circuit impedance $Z_{0\pi}$ of the four-element band-pass circuit of Pi section, x_1=5.

Sanitized Copy Approved for Release 2010/06/30 : CIA-RDP81-01043R000200070007-1

Sanitized Copy Approved for Release 2010/06/30 : CIA-RDP81-01043R000200070007-1

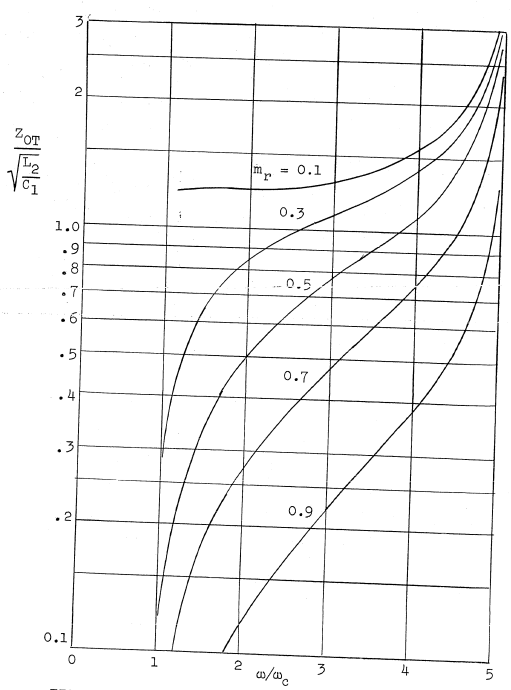

FIG. 7.15.--Circuit impedance Z_{OT} of the four-element band-pass circuit of Tee section, $x_1 = 5$.

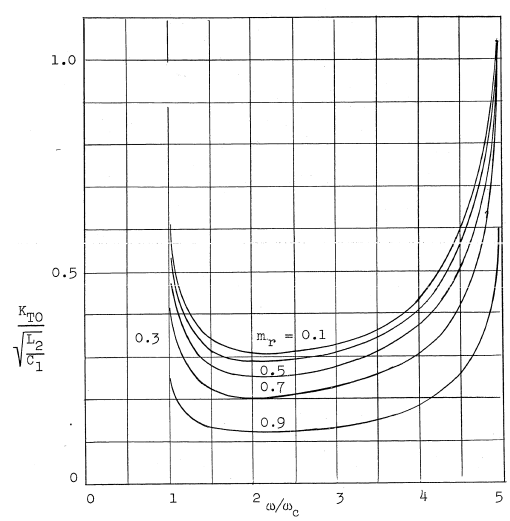

FIG. 7.16.--Transverse interaction impedance K_{TO} of the four-element band-pass circuit, $x_1 = 5$.

Sanitized Copy Approved for Release 2010/06/30 : CIA-RDP81-01043R000200070007-1

Sanitized Copy Approved for Release 2010/06/30 : CIA-RDP81-01043R000200070007-1

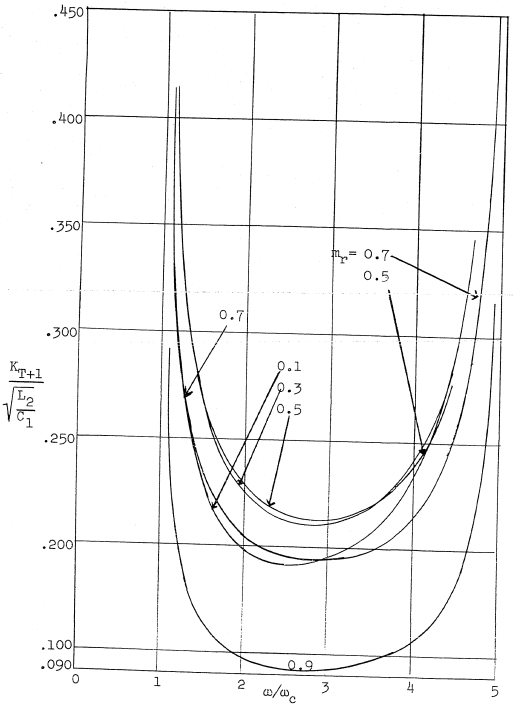

FIG. 7.17.--Transverse interaction impedance K_{T+1} of the four-element band-pass circuit, $x_1 = 5$.

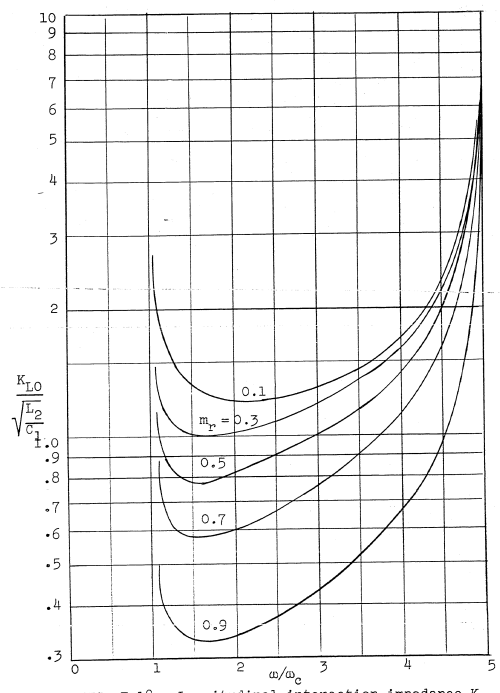

FIG. 7.18.--Longitudinal interaction impedance K_{LO} of the four-element band-pass circuit, $x_1 = 5$.

Sanitized Copy Approved for Release 2010/06/30 : CIA-RDP81-01043R000200070007-1

Sanitized Copy Approved for Release 2010/06/30 : CIA-RDP81-01043R000200070007-1

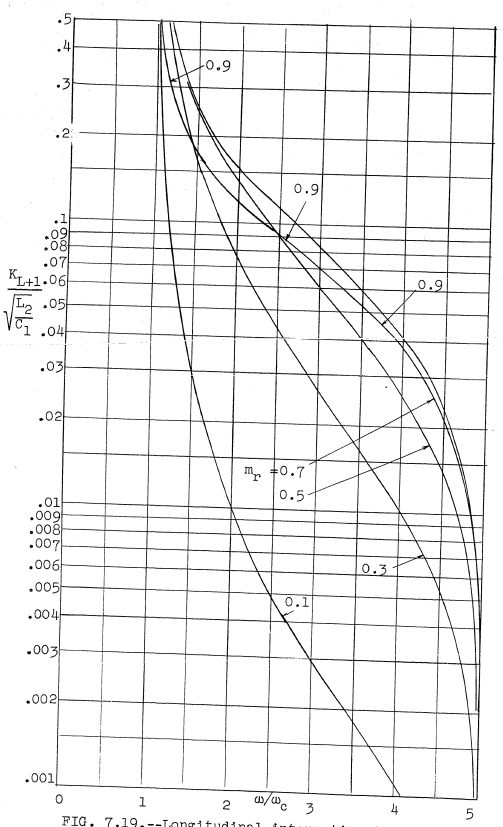

FIG. 7.19.--Longitudinal interaction impedance K_{L+1} of the four-element band-pass circuit, $x_1 = 5$.

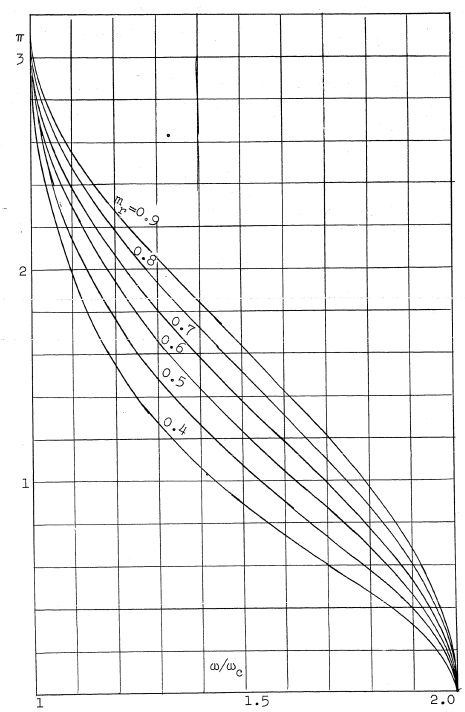

FIG. 7.20.--Phase angle per section of the four-element band-pass circuit, x_1=2.

Sanitized Copy Approved for Release 2010/06/30 : CIA-RDP81-01043R000200070007-1

Sanitized Copy Approved for Release 2010/06/30 : CIA-RDP81-01043R000200070007-1

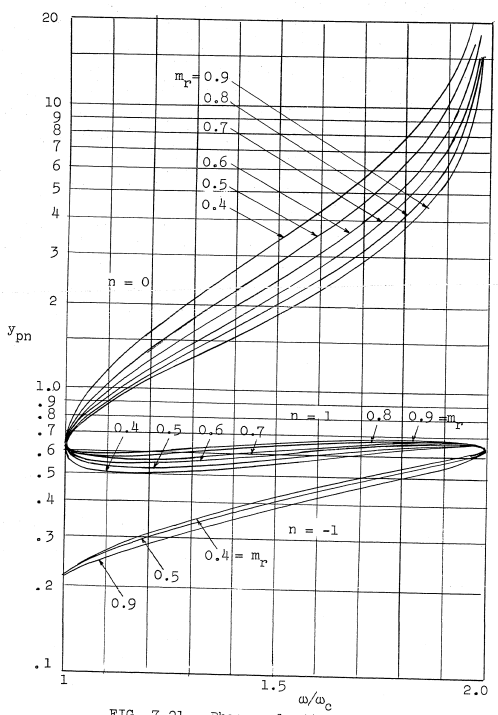

FIG. 7.21.--Phase velocity y_{pn} of the four-element band-pass circuit, x_1 = 2.

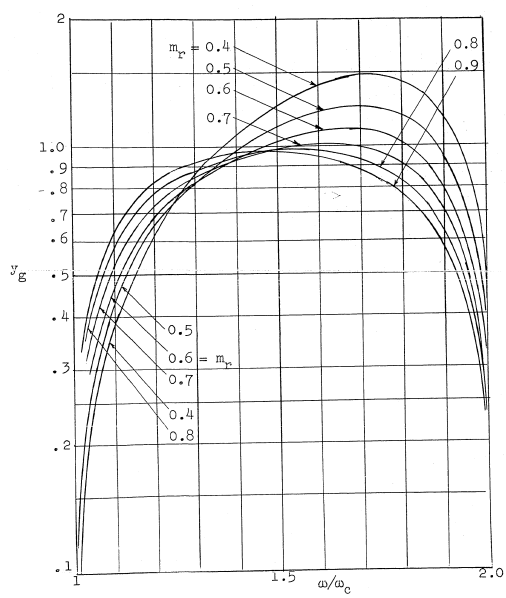

FIG. 7.22.--Group velocity y_g of the four-element band-pass circuit, x_1 = 2.

Sanitized Copy Approved for Release 2010/06/30 : CIA-RDP81-01043R000200070007-1

Sanitized Copy Approved for Release 2010/06/30 : CIA-RDP81-01043R000200070007-1

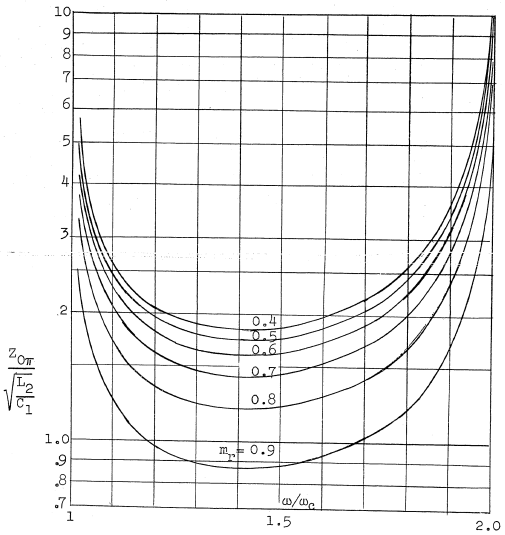

FIG. 7.23.--Circuit impedance $Z_{O\pi}$ of the four-element band-pass circuit of Pi section, $x_1 = 2$.

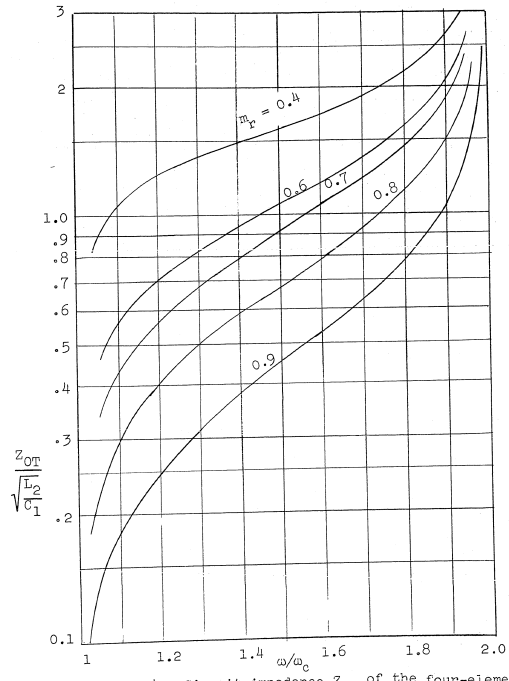

FIG. 7.24.--Circuit impedance Z_{OT} of the four-element band-pass circuit of Tee section, $x_1 = 2$.

Sanitized Copy Approved for Release 2010/06/30 : CIA-RDP81-01043R000200070007-1

Sanitized Copy Approved for Release 2010/06/30 : CIA-RDP81-01043R000200070007-1

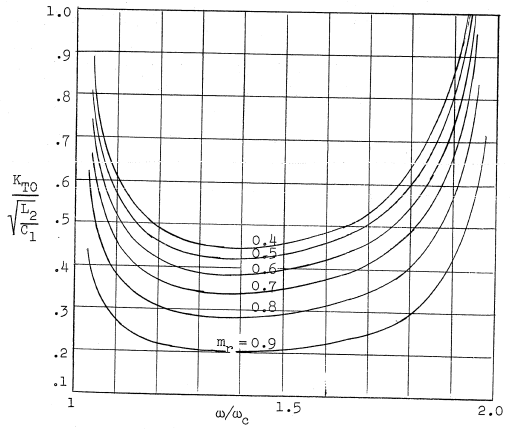

FIG. 7.25.--Transverse interaction impedance K_{TO} of the four-element band-pass circuit, $x_1 = 2$.

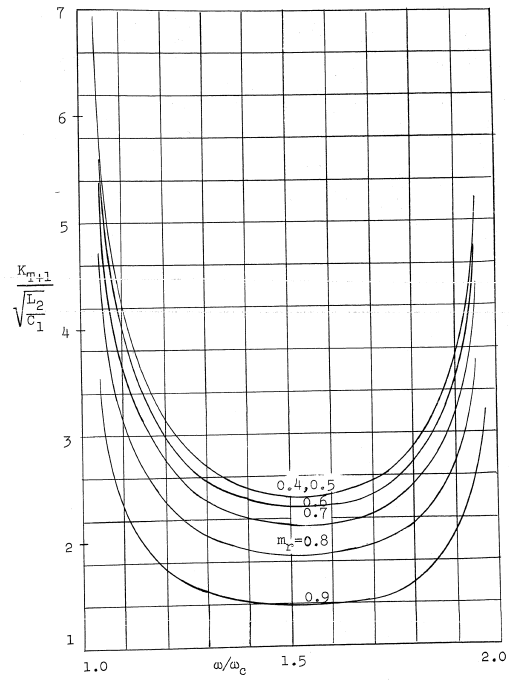

FIG. 7.26.--Transverse interaction impedance K_{T+1} of the four-element band-pass circuit, $x_1 = 2$.

Sanitized Copy Approved for Release 2010/06/30 : CIA-RDP81-01043R000200070007-1

Sanitized Copy Approved for Release 2010/06/30 : CIA-RDP81-01043R000200070007-1

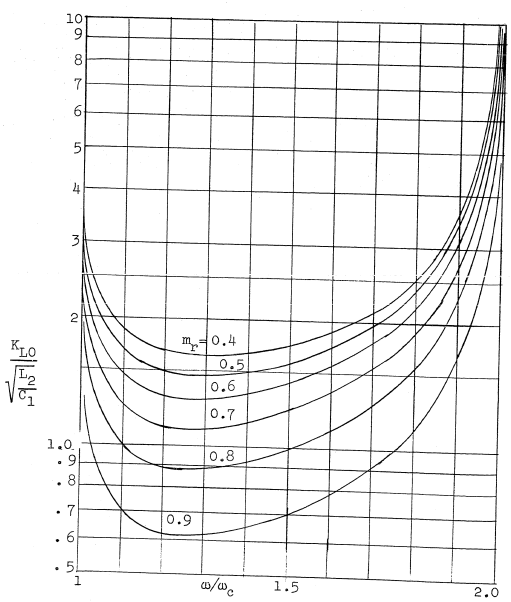

FIG. 7.27.--Longitudinal interaction impedance K_{LO} of the four-element band-pass circuit, $x_1=2$.

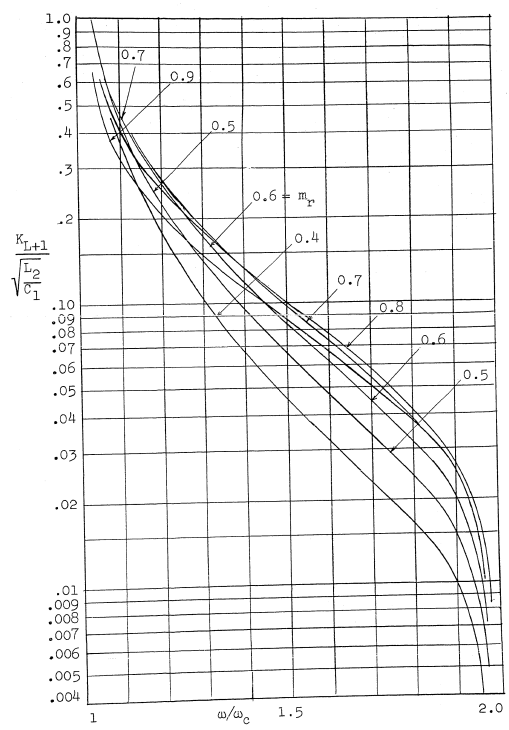

FIG. 7.28.--Longitudinal interaction impedance K_{L+1} of the four-element band-pass circuit, $x_1=2$.

Sanitized Copy Approved for Release 2010/06/30 : CIA-RDP81-01043R000200070007-1

Sanitized Copy Approved for Release 2010/06/30 : CIA-RDP81-01043R000200070007-1

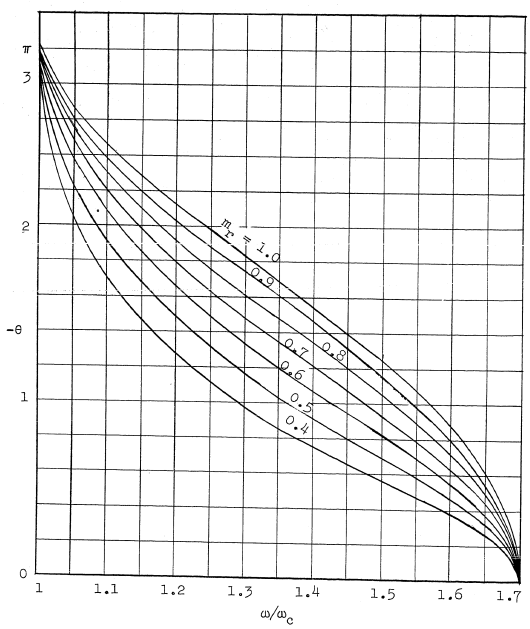

FIG. 7.29.--Phase angle per section of the four-element band-pass circuit, $x_1 = 1.70$.

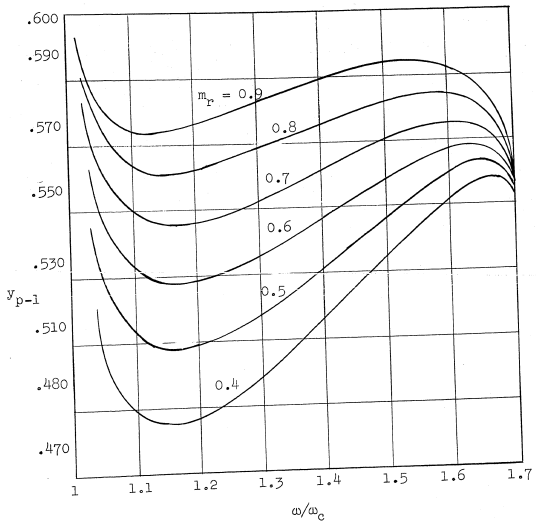

FIG. 7.30.--Phase velocity y_{p-1} of the four-element band-pass circuit, $x_1 = 1.70$.

Sanitized Copy Approved for Release 2010/06/30 : CIA-RDP81-01043R000200070007-1

Sanitized Copy Approved for Release 2010/06/30 : CIA-RDP81-01043R000200070007-1

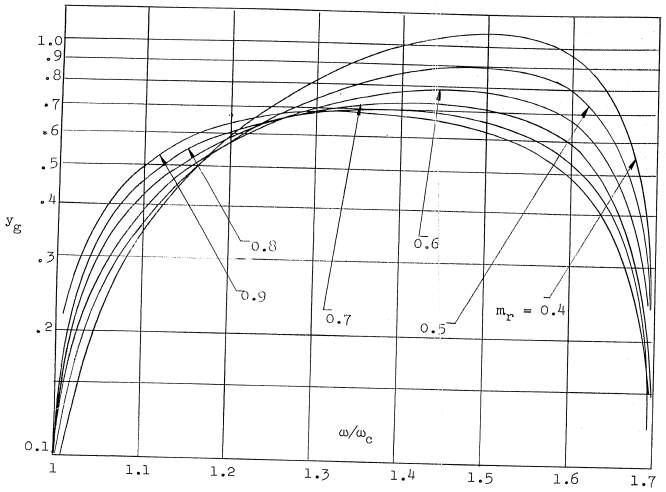

FIG. 7.31.--Group velocity y_g of the four-element band-pass circuit, x_1=1.70.

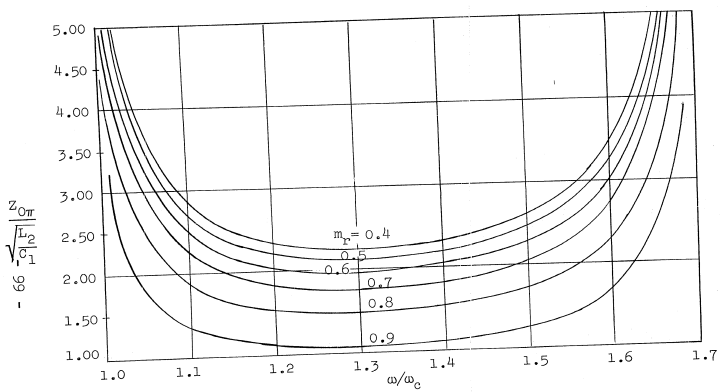

FIG. 7.32.--Circuit impedance $Z_{0\pi}$ of the four-element band-pass circuit of Pi section, x_1 = 1.70.

Sanitized Copy Approved for Release 2010/06/30 : CIA-RDP81-01043R000200070007-1

Sanitized Copy Approved for Release 2010/06/30 : CIA-RDP81-01043R000200070007-1

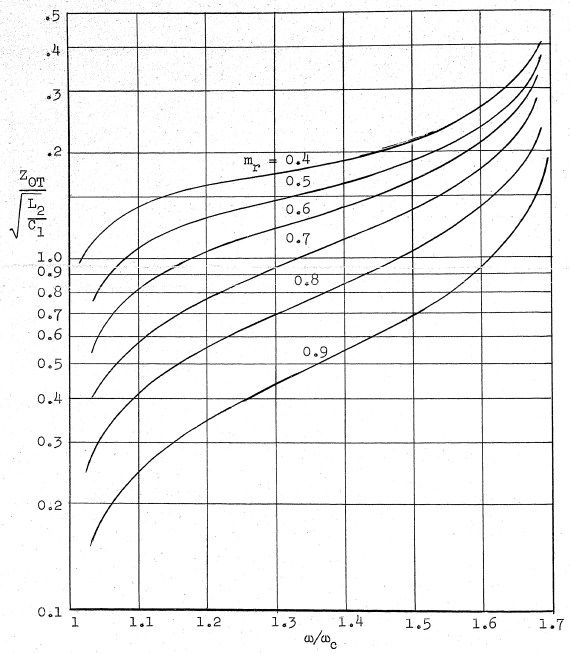

FIG. 7.33.--Circuit impedance Z_{OT} of the four-element band-pass circuit of Tee section, x_1=1.70.

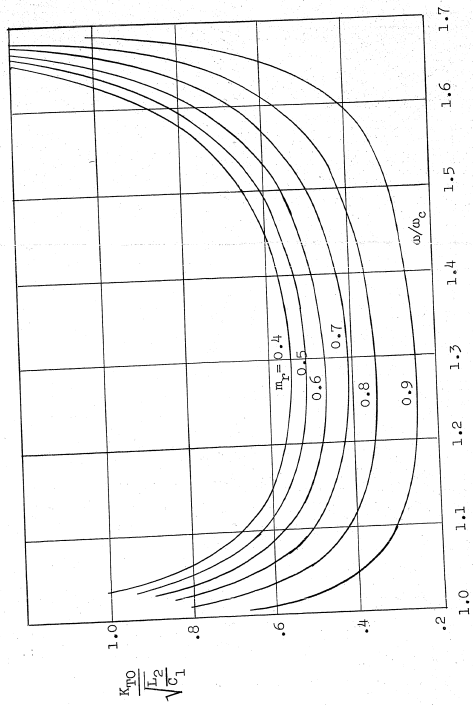

FIG. 7.34.--Transverse interaction impedance K_{TO} of the four-element band-pass circuit, x_1 = 1.70.

Sanitized Copy Approved for Release 2010/06/30 : CIA-RDP81-01043R000200070007-1

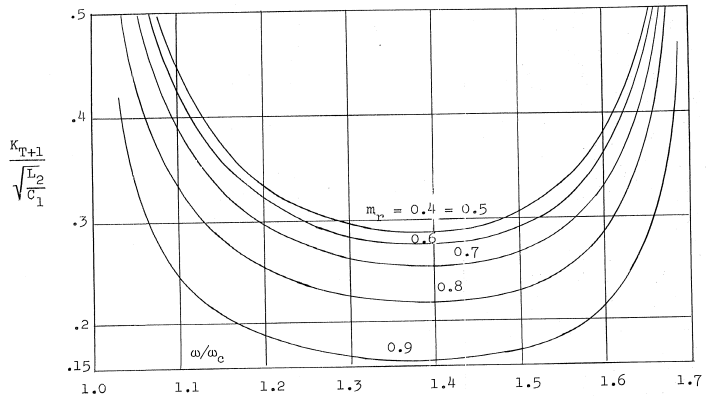

FIG. 7.35.--Transverse interaction impedance K_{T+1} of the four-element band-pass circuit, x_1 = 1.70.

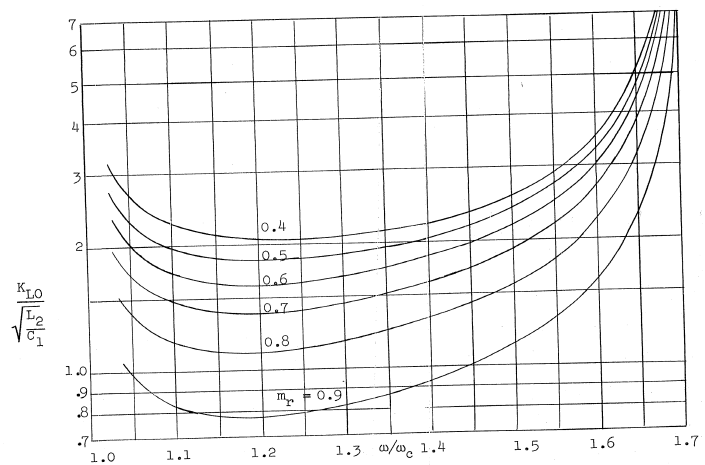

FIG. 7.36.--Longitudinal interaction impedance K_{LO} of the four-element band-pass circuit, x_1=1.70.

Sanitized Copy Approved for Release 2010/06/30 : CIA-RDP81-01043R000200070007-1
Sanitized Copy Approved for Release 2010/06/30 : CIA-RDP81-01043R000200070007-1

Sanitized Copy Approved for Release 2010/06/30 : CIA-RDP81-01043R000200070007-1

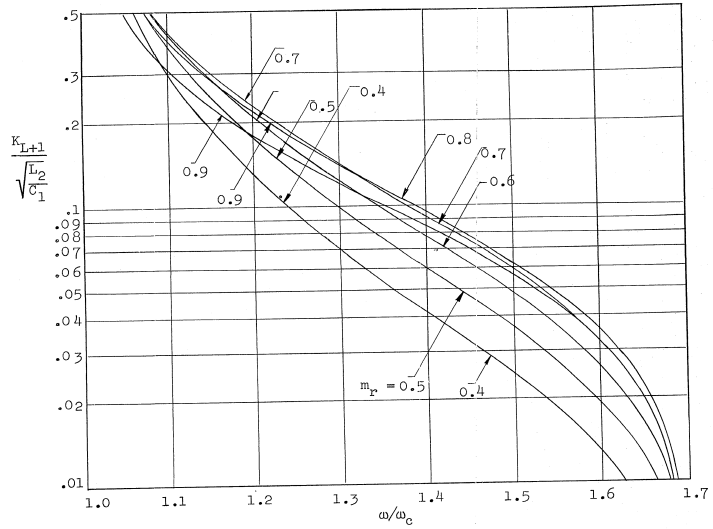

FIG. 7.37.--Longitudinal interaction impedance K_{L+1} of the four-element band-pass circuit, $x_1 = 1.70$.

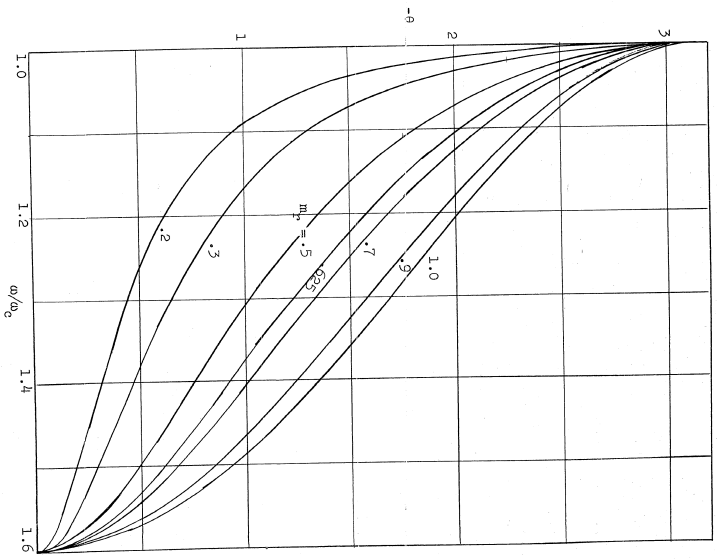

FIG. 7.38.--Phase angle per section of the four-element band-pass circuit, $x_1 = 1.6$.

Sanitized Copy Approved for Release 2010/06/30 : CIA-RDP81-01043R000200070007-1

Sanitized Copy Approved for Release 2010/06/30 : CIA-RDP81-01043R000200070007-1

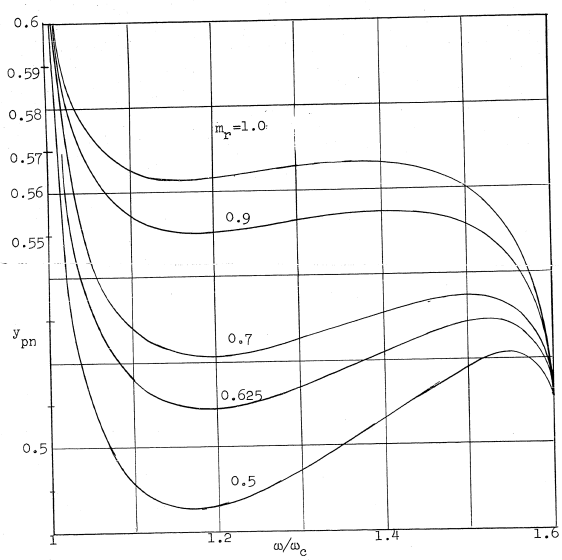

FIG. 7.39.--Phase velocity y_{pn} of the four-element band-pass circuit, x_1 = 1.6.

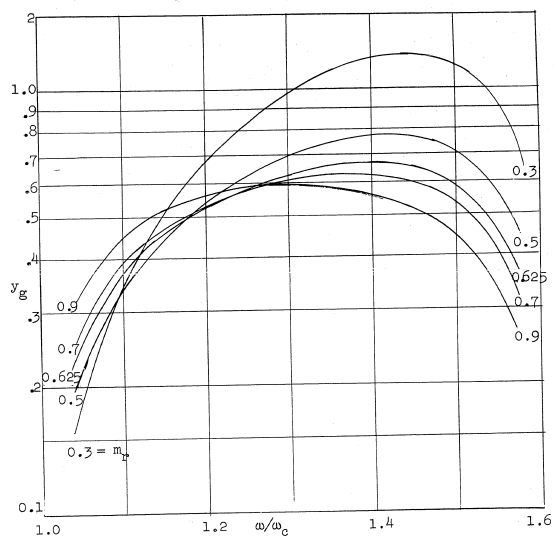

FIG. 7.40.--Group velocity y_g of the four-element band-pass circuit, x_1=1.6.

Sanitized Copy Approved for Release 2010/06/30 : CIA-RDP81-01043R000200070007-1

Sanitized Copy Approved for Release 2010/06/30 : CIA-RDP81-01043R000200070007-1

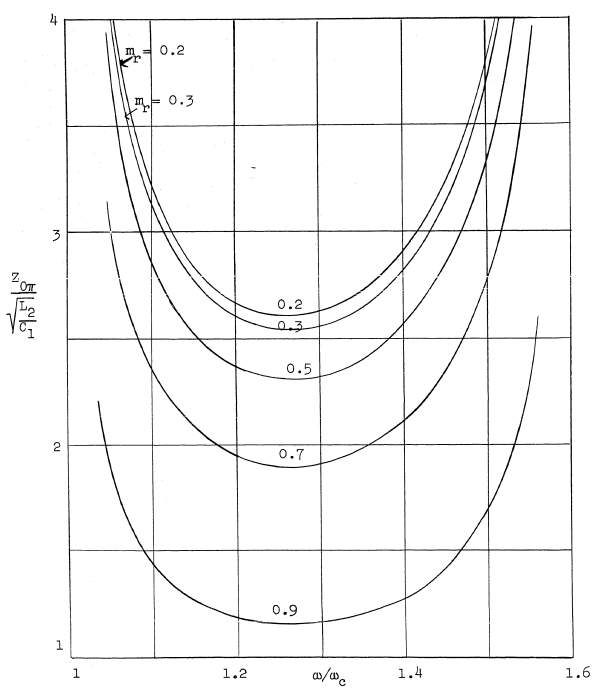

FIG. 7.41.--Circuit impedance $Z_{0\pi}$ of the four-element band-pass circuit of Pi section; $x_1 = 1.6$.

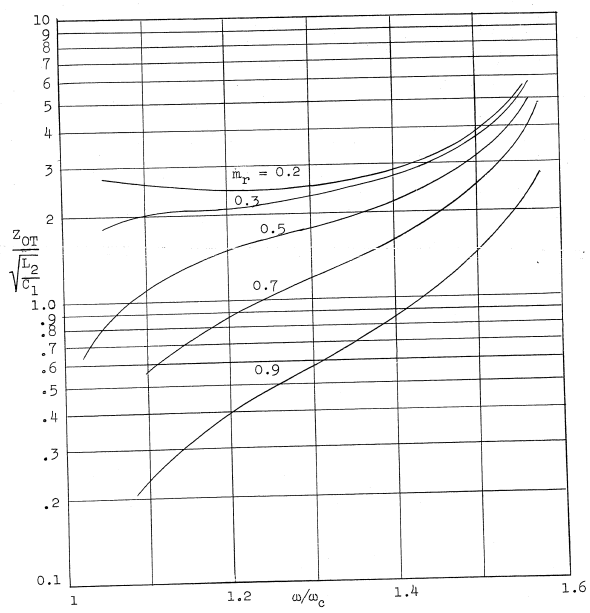

FIG. 7.42.--Circuit impedance Z_{0T} of the four-element band-pass circuit of Tee section; $x_1 = 1.6$.

Sanitized Copy Approved for Release 2010/06/30 : CIA-RDP81-01043R000200070007-1

Sanitized Copy Approved for Release 2010/06/30 : CIA-RDP81-01043R000200070007-1

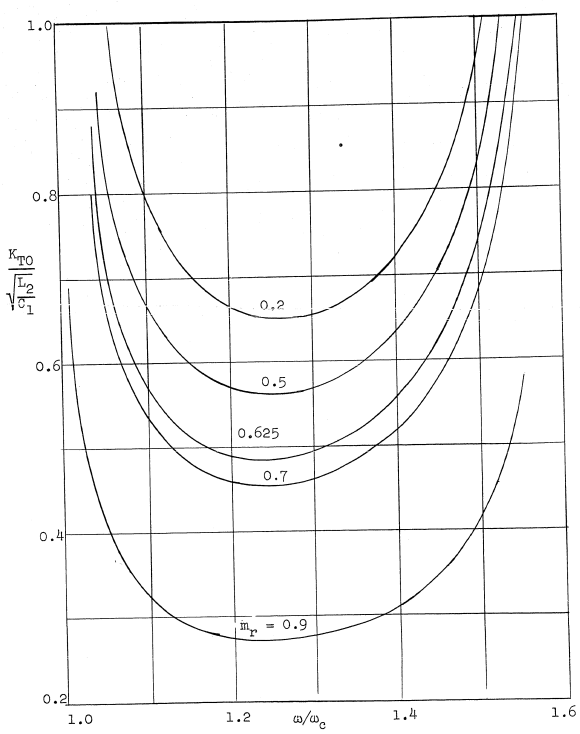

FIG. 7.43.--Transverse interaction impedance K_{TO} of the four-element band-pass circuit, x_1=1.6.

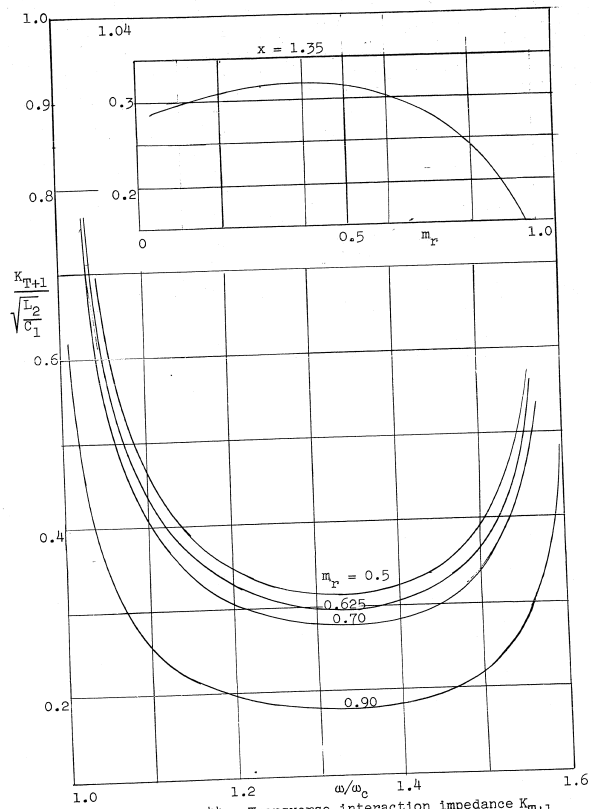

FIG. 7.44.--Transverse interaction impedance K_{T+1} of the four-element band-pass circuit, x_1=1.6.

Sanitized Copy Approved for Release 2010/06/30 : CIA-RDP81-01043R000200070007-1

Sanitized Copy Approved for Release 2010/06/30 : CIA-RDP81-01043R000200070007-1

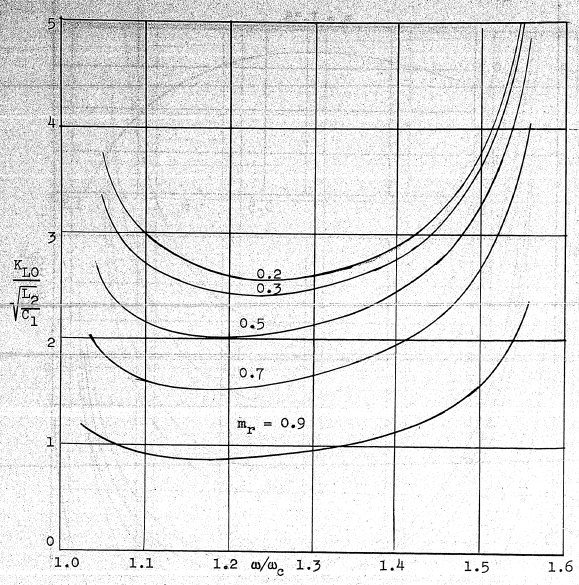

FIG. 7.45.--Longitudinal interaction impedance K_{LO} of the four-element band-pass circuit, x_1=1.6.

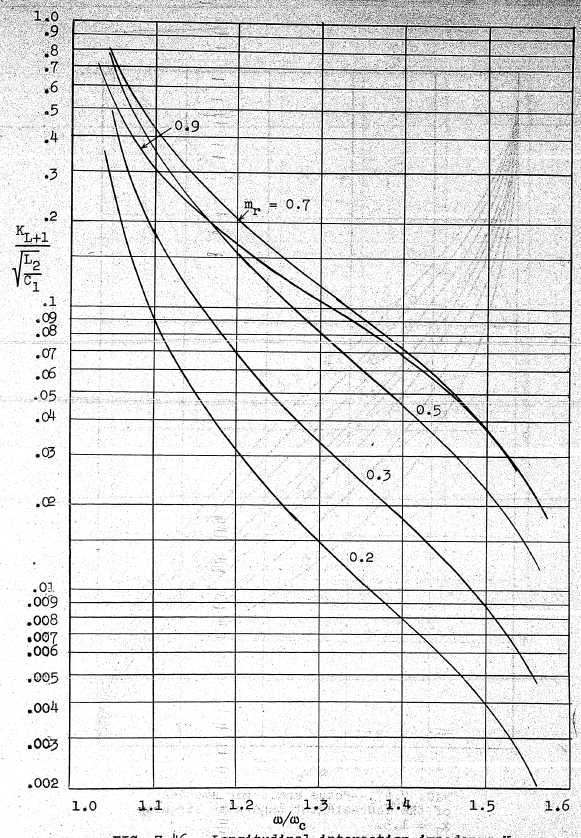

FIG. 7.46.--Longitudinal interaction impedance K_{L+1} of the four-element band-pass circuit, x_1 = 1.6.

Sanitized Copy Approved for Release 2010/06/30 : CIA-RDP81-01043R000200070007-1

Sanitized Copy Approved for Release 2010/06/30 : CIA-RDP81-01043R000200070007-1

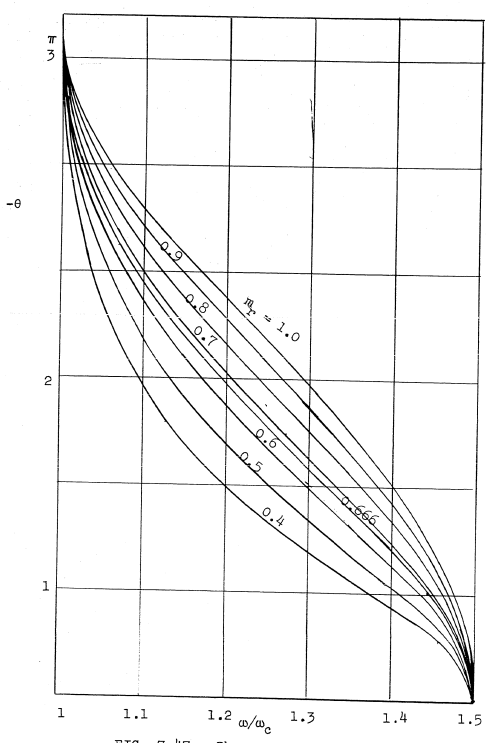

FIG. 7.47.--Phase angle per section of the four-element band-pass circuit, $x_1 = 1.5$.

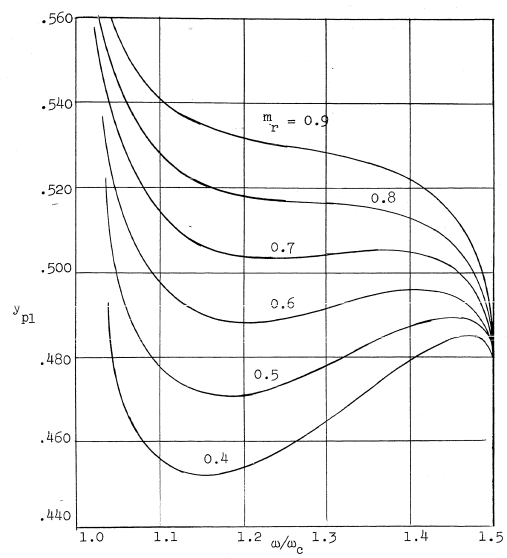

FIG. 7.48.--Phase velocity y_{pl} of the four-element band-pass circuit, $x_1 = 1.5$.

Sanitized Copy Approved for Release 2010/06/30 : CIA-RDP81-01043R000200070007-1

Sanitized Copy Approved for Release 2010/06/30 : CIA-RDP81-01043R000200070007-1

FIG. 7.49.--Group velocity y_g of the four-element band-pass circuit, x_1 = 1.5.

FIG. 7.50.--Circuit impedance $Z_{0\pi}$ of the four-element band-pass circuit of Pi section, x_1 = 1.5.

Sanitized Copy Approved for Release 2010/06/30 : CIA-RDP81-01043R000200070007-1

Sanitized Copy Approved for Release 2010/06/30 : CIA-RDP81-01043R000200070007-1

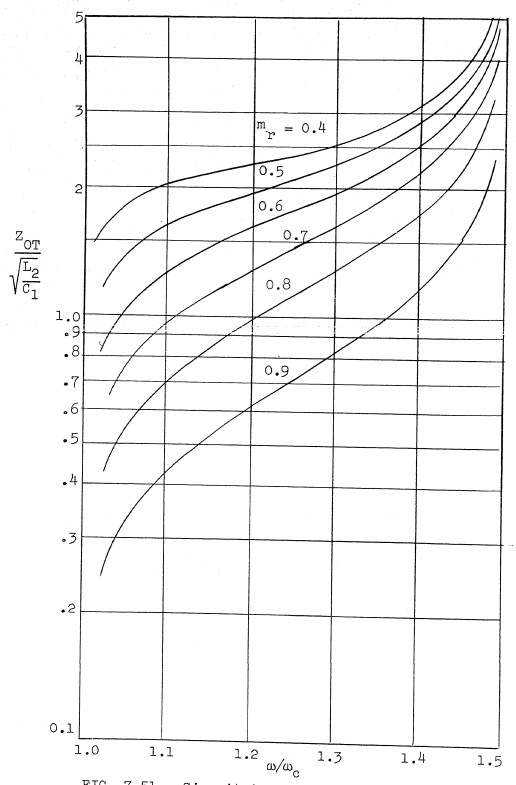

FIG. 7.51.--Circuit impedance Z_{OT} of the four-element band-pass circuit of Tee section, $x_1 = 1.5$.

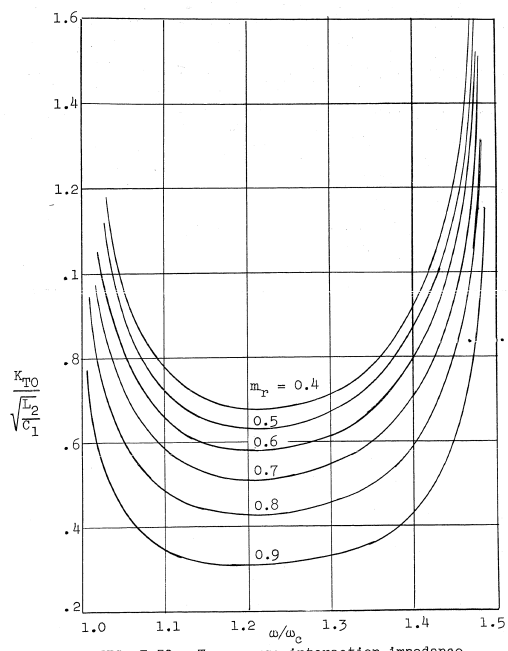

FIG. 7.52.--Transverse interaction impedance K_{TO} of the four-element band-pass circuit, $x_1 = 1.5$.

Sanitized Copy Approved for Release 2010/06/30 : CIA-RDP81-01043R000200070007-1

Sanitized Copy Approved for Release 2010/06/30 : CIA-RDP81-01043R000200070007-1

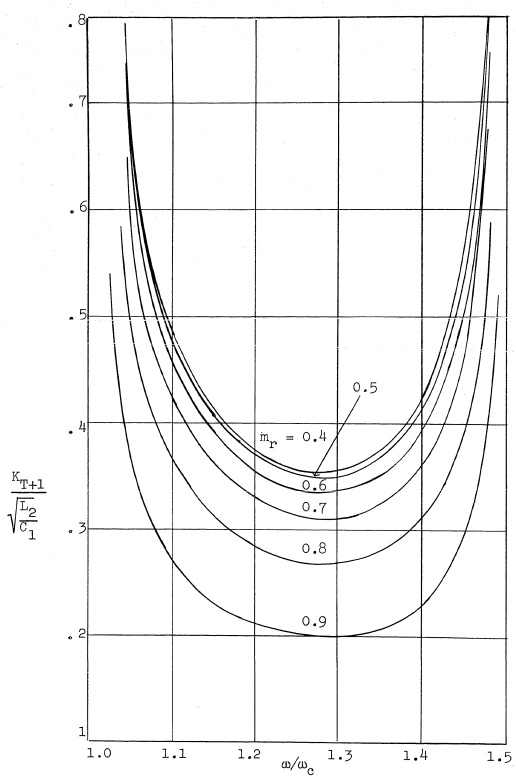

FIG. 7.53.--Transverse interaction impedance K_{T+1} of the four-element band-pass circuit, $x_1 = 1.5$.

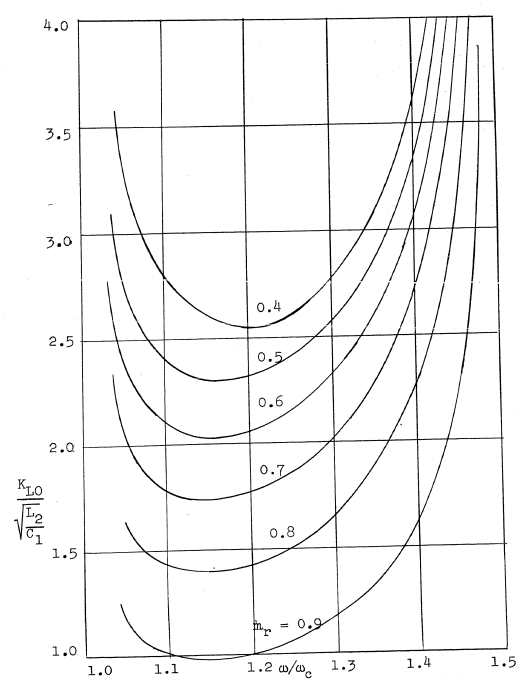

FIG. 7.54.--Longitudinal interaction impedance K_{LO} of the four-element band-pass circuit, $x_1 = 1.5$.

Sanitized Copy Approved for Release 2010/06/30 : CIA-RDP81-01043R000200070007-1

Sanitized Copy Approved for Release 2010/06/30 : CIA-RDP81-01043R000200070007-1

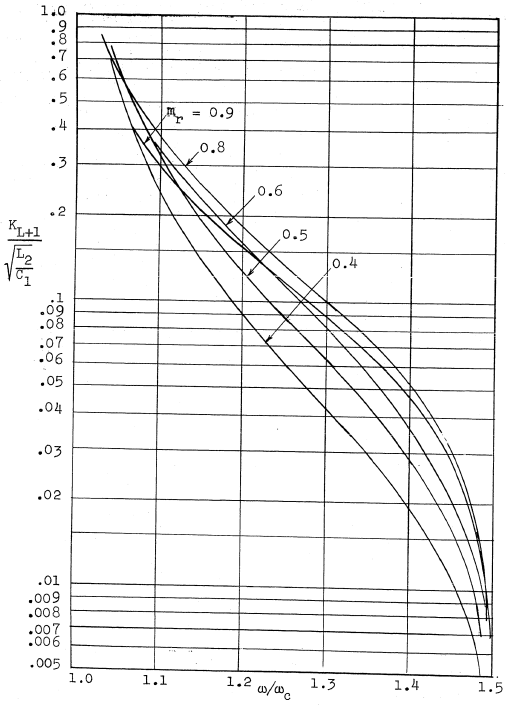

FIG. 7.55.--Longitudinal interaction impedance K_{L+1} of the four-element band-pass circuit, $x_1 = 1.5$.

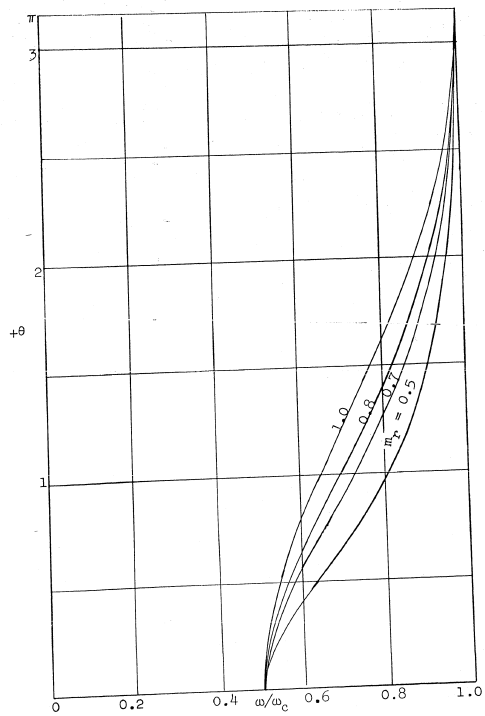

FIG. 7.56.--Phase angle per section of the four-element band-pass circuit, $x_1 = 0.5$.

Sanitized Copy Approved for Release 2010/06/30 : CIA-RDP81-01043R000200070007-1

Sanitized Copy Approved for Release 2010/06/30 : CIA-RDP81-01043R000200070007-1

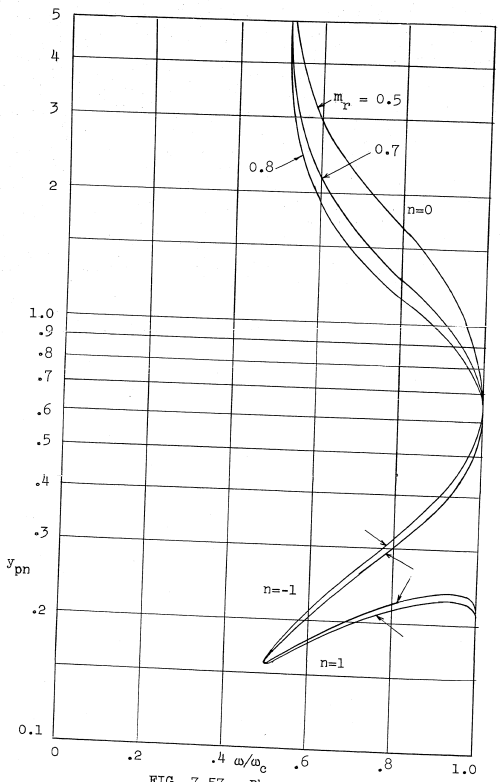

FIG. 7.57.--Phase velocity y_{pn} of the four-element band-pass circuit, x_1 = 0.5.

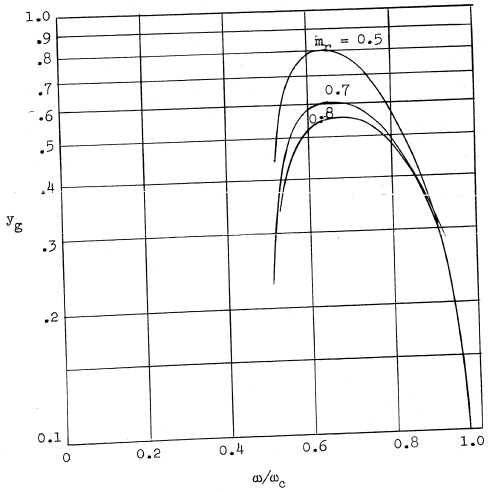

FIG. 7.58.--Group velocity y_g of the four-element band-pass circuit x_1=0.5.

Sanitized Copy Approved for Release 2010/06/30 : CIA-RDP81-01043R000200070007-1

Sanitized Copy Approved for Release 2010/06/30 : CIA-RDP81-01043R000200070007-1

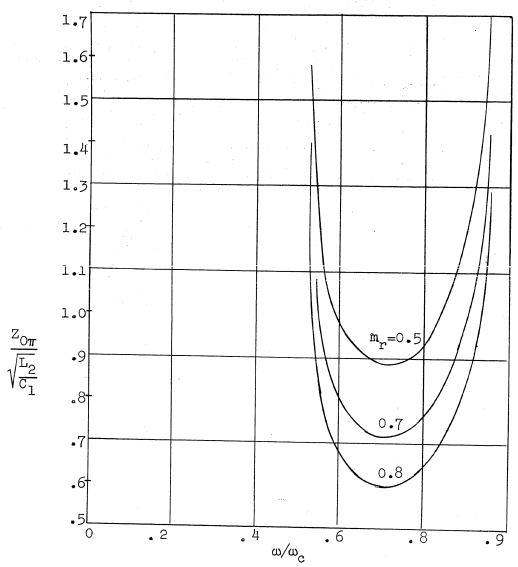

FIG. 7.59.--Circuit impedance Z_{OT} of the four-element band-pass circuit of Pi section, x_1 = 0.5.

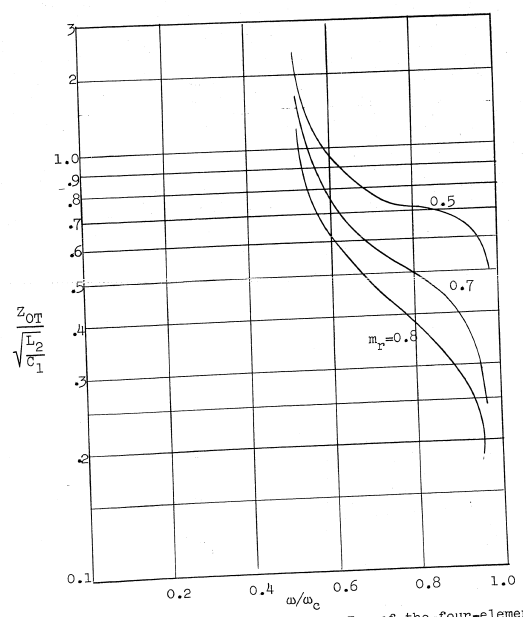

FIG. 7.60.--Circuit impedance Z_{OT} of the four-element band-pass circuit of Tee section, x_1 = 0.5.

Sanitized Copy Approved for Release 2010/06/30 : CIA-RDP81-01043R000200070007-1

Sanitized Copy Approved for Release 2010/06/30 : CIA-RDP81-01043R000200070007-1

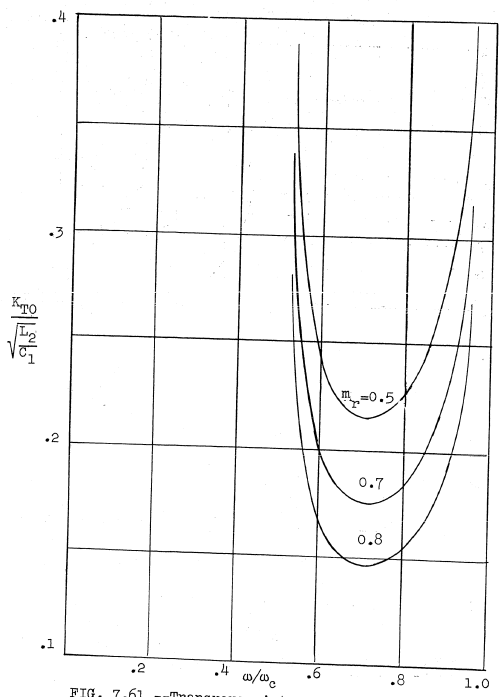

FIG. 7.61.--Transverse interaction impedance K_{TO} of the four-element band-pass circuit, x_1=0.5.

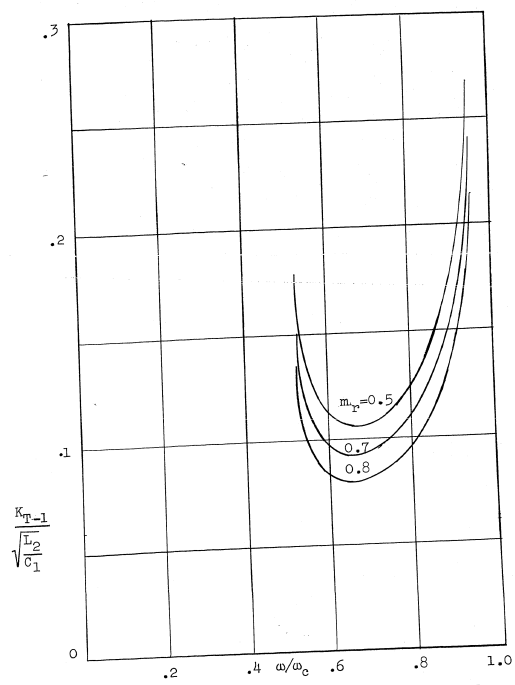

FIG. 7.62.--Transverse interaction impedance K_{T+1} of the four-element band-pass circuit, x_1 = 0.5.

Sanitized Copy Approved for Release 2010/06/30 : CIA-RDP81-01043R000200070007-1

Sanitized Copy Approved for Release 2010/06/30 : CIA-RDP81-01043R000200070007-1

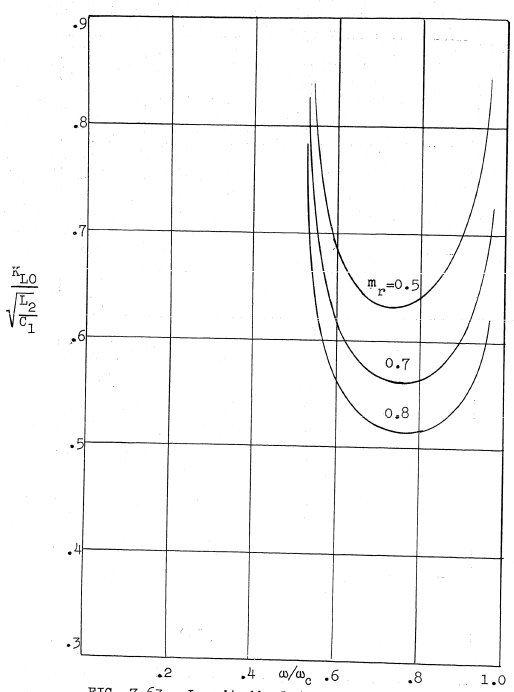

FIG. 7.63.--Longitudinal interaction impedance K_{LO} of the four-element band-pass circuit, x_1=0.5.

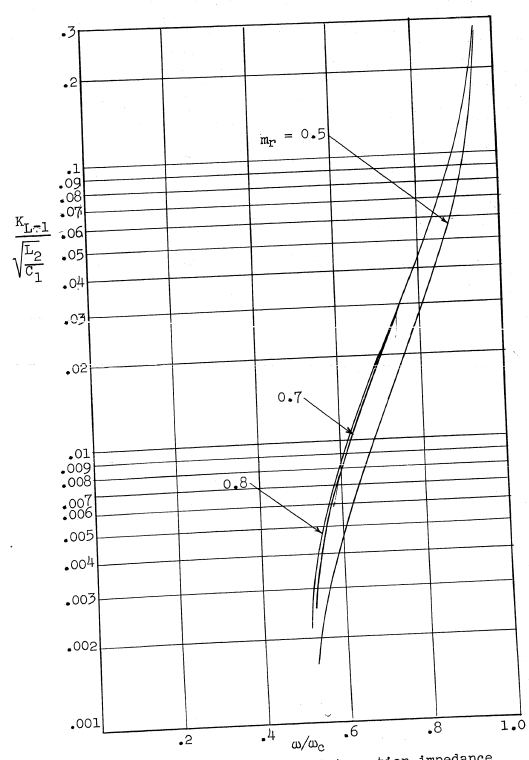

FIG. 7.64.--Longitudinal interaction impedance K_{L-1} of the four-element band-pass circuit, x_1=0.5.

Sanitized Copy Approved for Release 2010/06/30 : CIA-RDP81-01043R000200070007-1

Sanitized Copy Approved for Release 2010/06/30 : CIA-RDP81-01043R000200070007-1

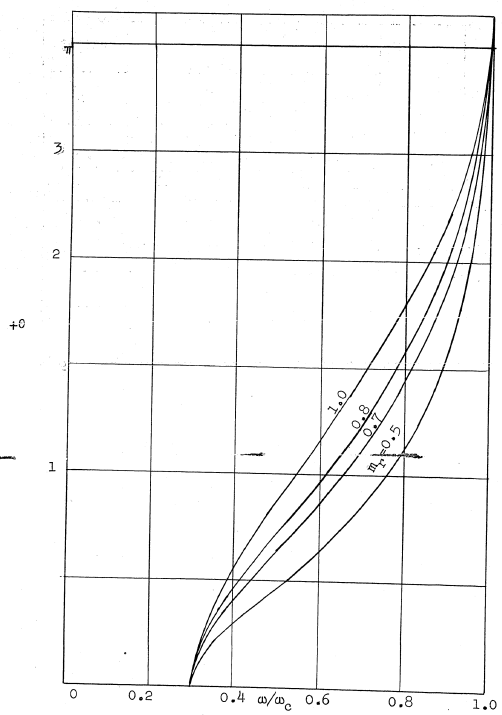

FIG. 7.65.--Phase angle per section of the four-element band-pass circuit, x_1 = 0.3.

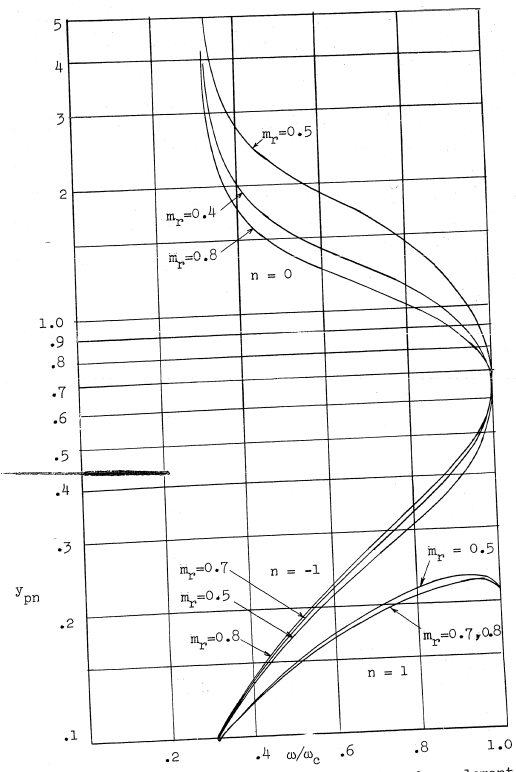

FIG. 7.66.--Phase velocity y_{pn} of the four-element band-pass circuit, x_1 = 0.3.

Sanitized Copy Approved for Release 2010/06/30 : CIA-RDP81-01043R000200070007-1

Sanitized Copy Approved for Release 2010/06/30 : CIA-RDP81-01043R000200070007-1

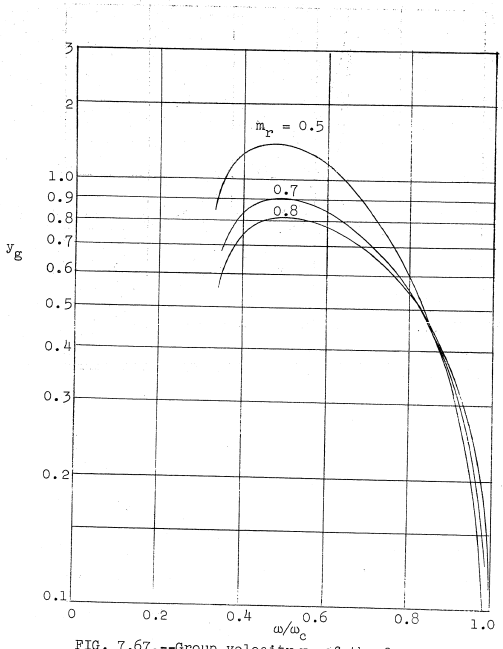

FIG. 7.67.--Group velocity y_g of the four-element band-pass circuit, x_1 = 0.3.

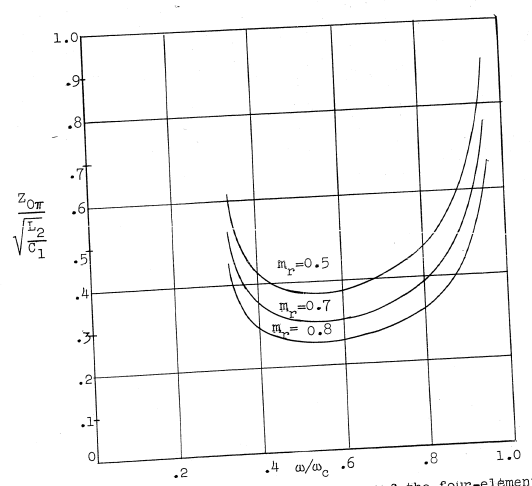

FIG. 7.68.--Circuit impedance $Z_{0\pi}$ of the four-element band-pass circuit of Pi section, x_1 = 0.3.

Sanitized Copy Approved for Release 2010/06/30 : CIA-RDP81-01043R000200070007-1

Sanitized Copy Approved for Release 2010/06/30 : CIA-RDP81-01043R000200070007-1

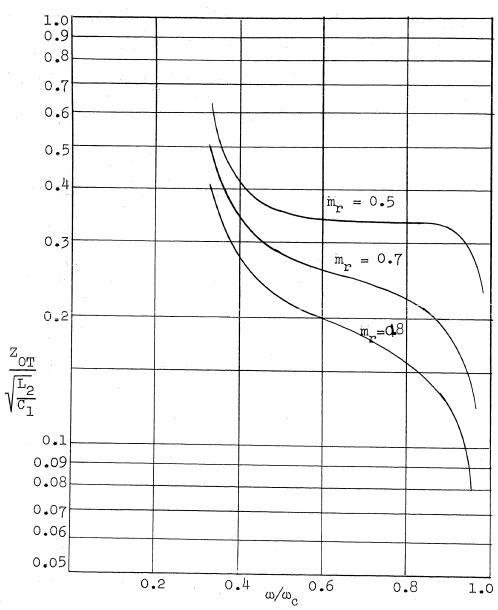

FIG. 7.69.--Circuit impedance Z_{OT} of the four-element band-pass circuit of Tee section, x_1 = 0.3.

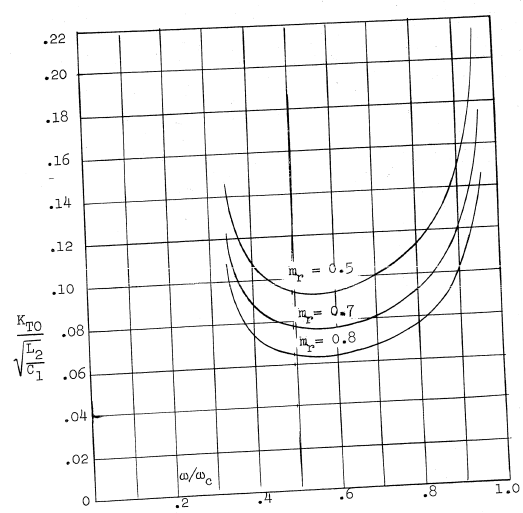

FIG. 7.70.--Transverse interaction impedance K_{TO} of the four-element band-pass circuit, x_1 = 0.3.

Sanitized Copy Approved for Release 2010/06/30 : CIA-RDP81-01043R000200070007-1

Sanitized Copy Approved for Release 2010/06/30 : CIA-RDP81-01043R000200070007-1

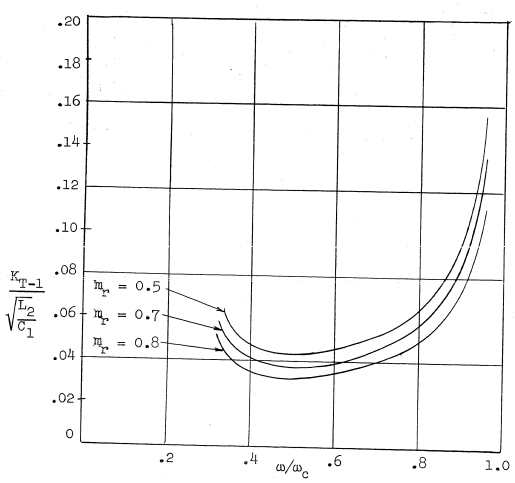

FIG. 7.71.--Transverse interaction impedance K_{T-1} of the four-element band-pass circuit, x_1 = 0.3.

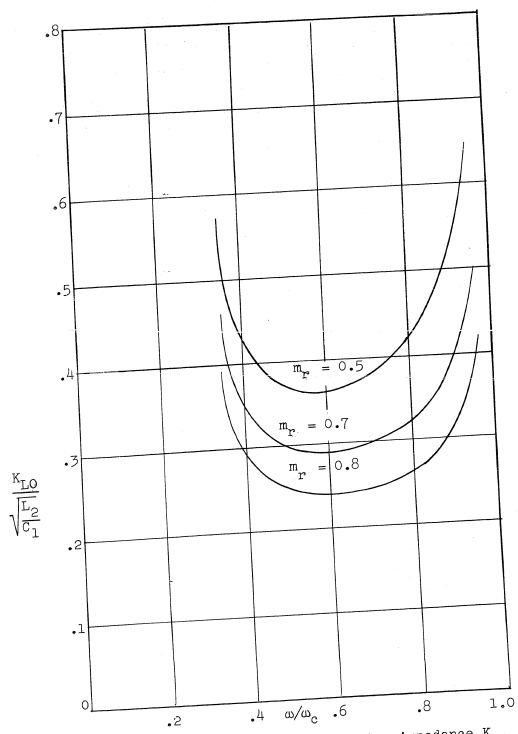

FIG. 7.72.--Longitudinal interaction impedance K_{LO} of the four-element band-pass circuit, x_1 = 0.3.

Sanitized Copy Approved for Release 2010/06/30 : CIA-RDP81-01043R000200070007-1

Sanitized Copy Approved for Release 2010/06/30 : CIA-RDP81-01043R000200070007-1

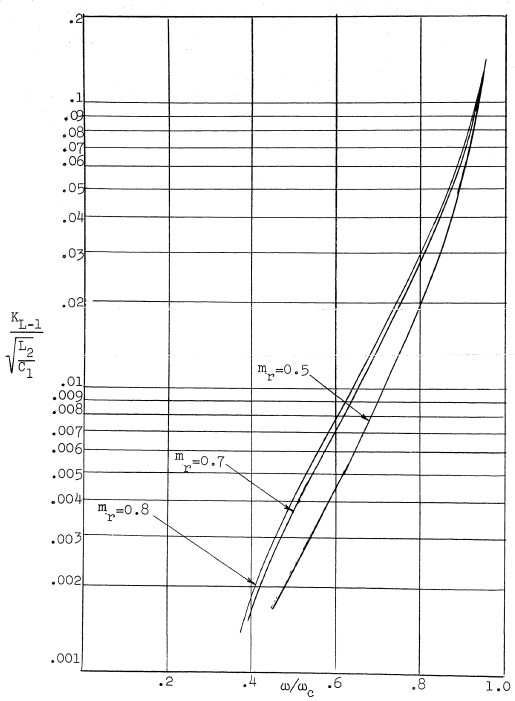

FIG. 7.73.--Longitudinal interaction impedance K_{L-1} of the four-element band-pass circuit $x_1 = 0.3$.

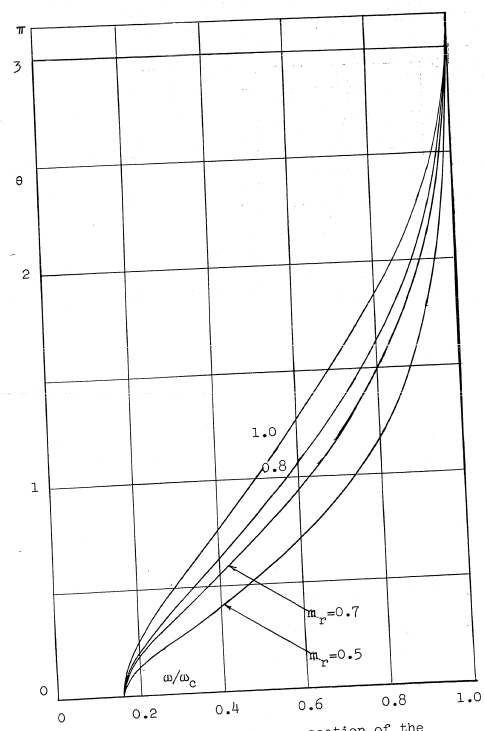

FIG. 7.74.--Phase angle per section of the four-element band-pass circuit, $x_1 = 0.16$.

Sanitized Copy Approved for Release 2010/06/30 : CIA-RDP81-01043R000200070007-1

Sanitized Copy Approved for Release 2010/06/30 : CIA-RDP81-01043R000200070007-1

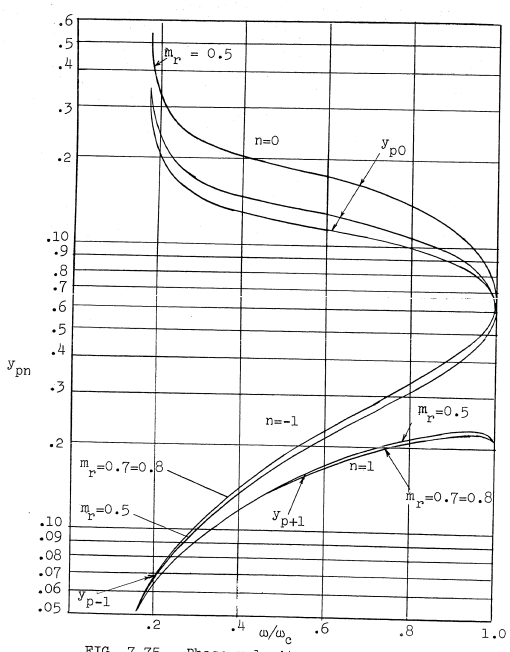

FIG. 7.75.--Phase velocity y_{pn} of the four-element band-pass circuit, x_1 = 0.16.

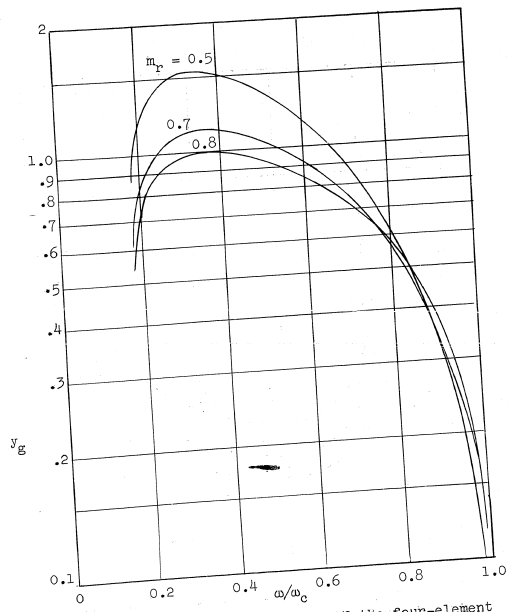

FIG. 7.76.--Group velocity y_g of the four-element band-pass circuit, x_1 = 0.16.

Sanitized Copy Approved for Release 2010/06/30 : CIA-RDP81-01043R000200070007-1

Sanitized Copy Approved for Release 2010/06/30 : CIA-RDP81-01043R000200070007-1

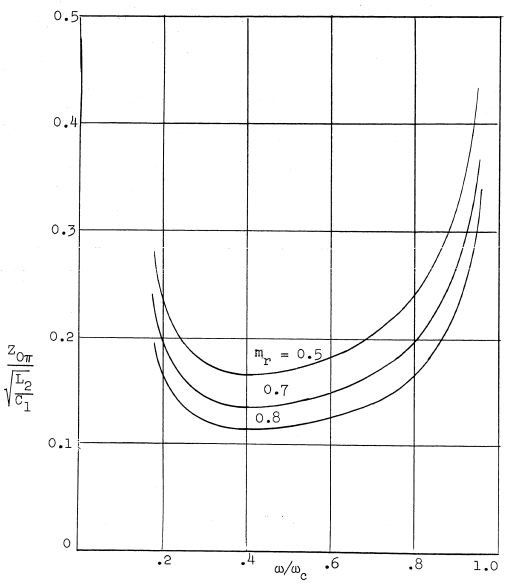

FIG. 7.77.--Circuit impedance $Z_{O\pi}$ of the four-element band-pass circuit of Pi section, x_1 = 0.16.

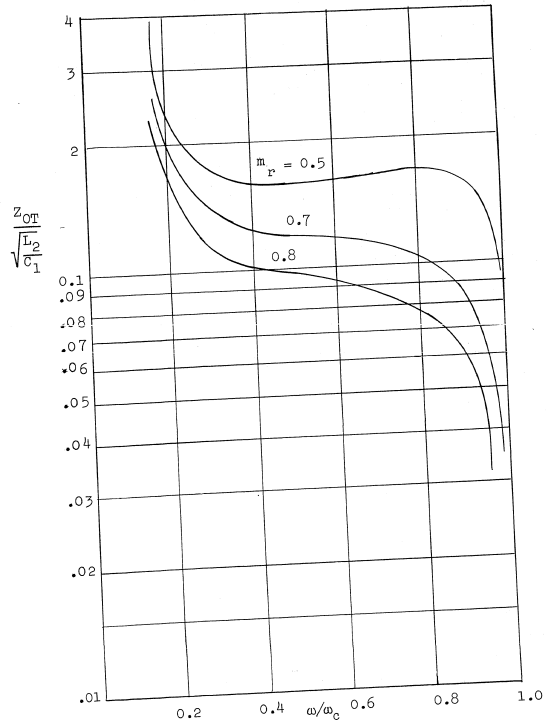

FIG. 7.78.--Circuit impedance Z_{OT} of the four-element band-pass circuit of Tee section x_1 = 0.16.

Sanitized Copy Approved for Release 2010/06/30 : CIA-RDP81-01043R000200070007-1

Sanitized Copy Approved for Release 2010/06/30 : CIA-RDP81-01043R000200070007-1

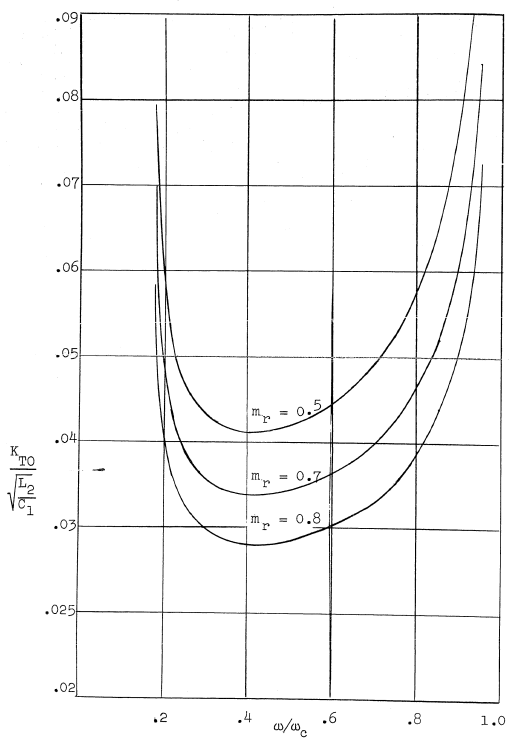

FIG. 7.79.--Transverse interaction impedance K_{TO} of the four-element band-pass circuit, x_1=0.16.

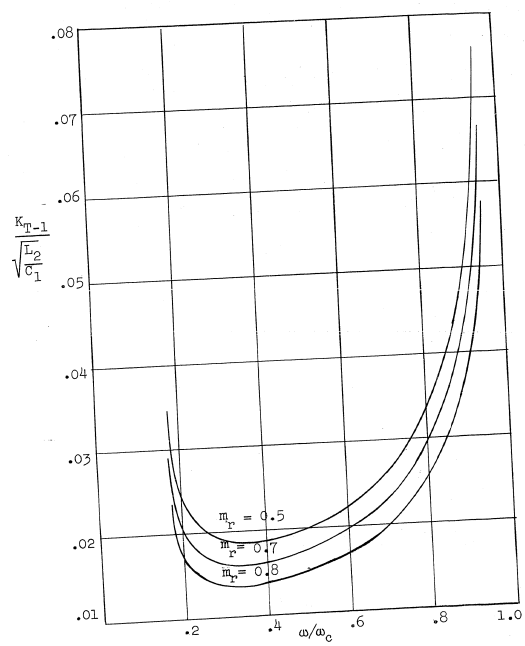

FIG. 7.80.--Transverse interaction impedance K_{T-1} of the four-element band-pass circuit, x_1 = 0.16.

Sanitized Copy Approved for Release 2010/06/30 : CIA-RDP81-01043R000200070007-1

Sanitized Copy Approved for Release 2010/06/30 : CIA-RDP81-01043R000200070007-1

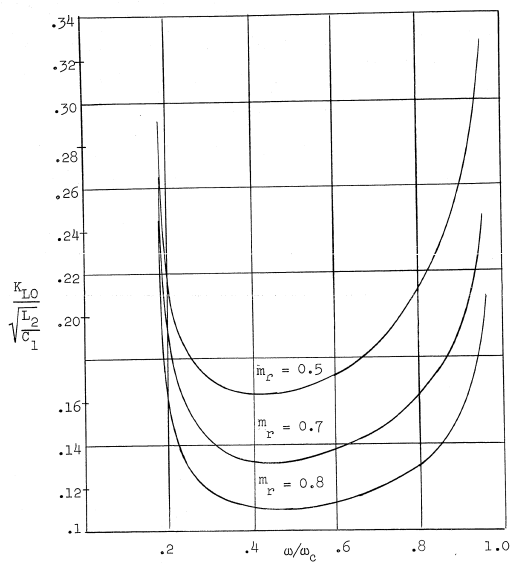

FIG. 7.81.--Longitudinal interaction impedance K_{LO} of the four-element band-pass circuit, $x_1 = 0.16$.

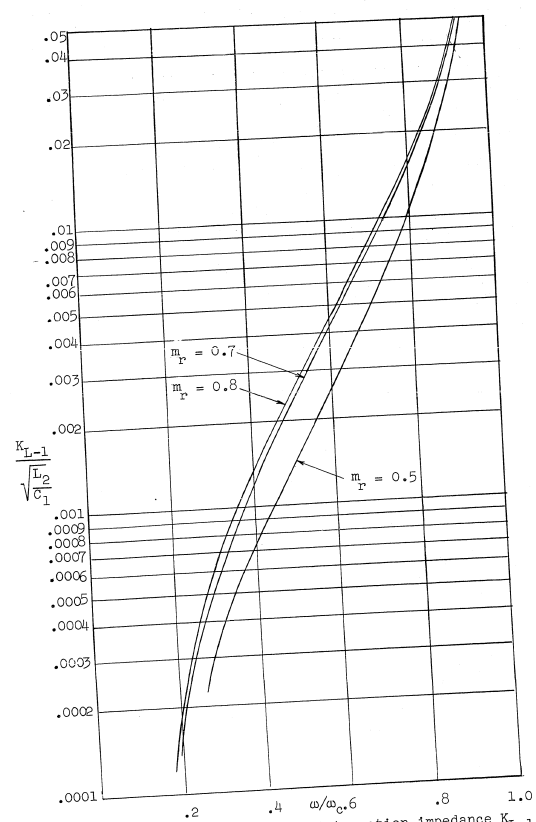

FIG. 7.82.--Longitudinal interaction impedance K_{L-1} of the four-element band-pass circuit, $x_1 = 0.16$.

Sanitized Copy Approved for Release 2010/06/30 : CIA-RDP81-01043R000200070007-1

Sanitized Copy Approved for Release 2010/06/30 : CIA-RDP81-01043R000200070007-1

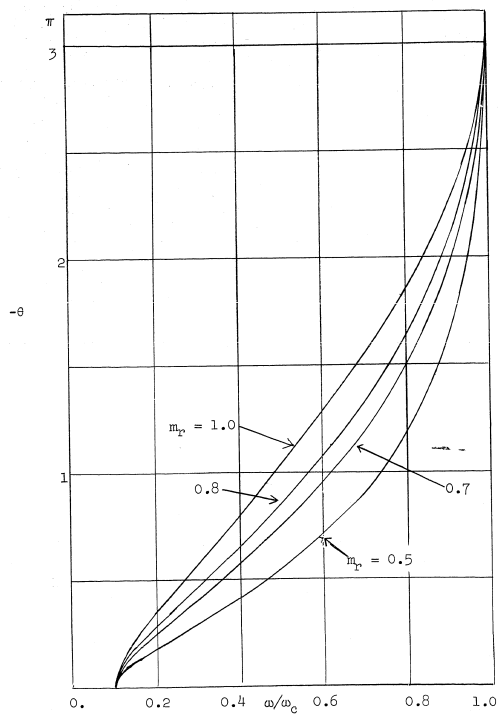

FIG. 7.83.--Phase angle per section of the four-element band-pass circuit, x_1 = 0.100.

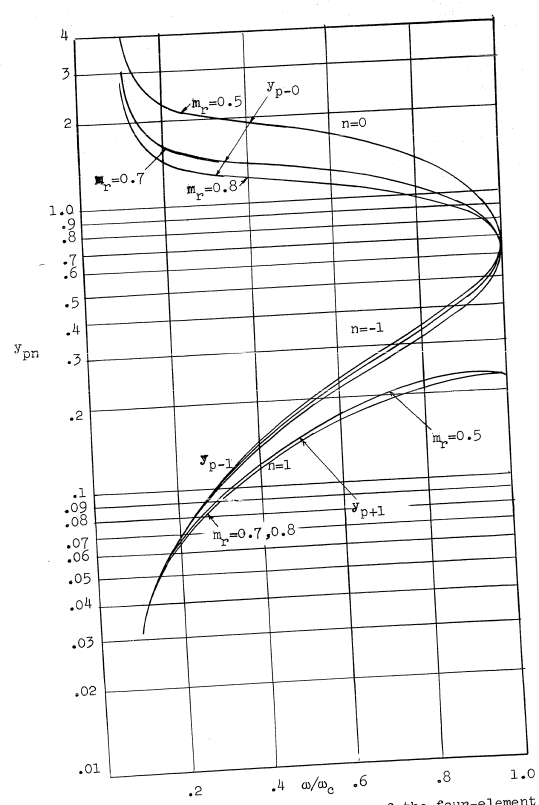

FIG. 7.84.--Phase velocity y_{pn} of the four-element band-pass circuit, x_1 = 0.100.

Sanitized Copy Approved for Release 2010/06/30 : CIA-RDP81-01043R000200070007-1

Sanitized Copy Approved for Release 2010/06/30 : CIA-RDP81-01043R000200070007-1

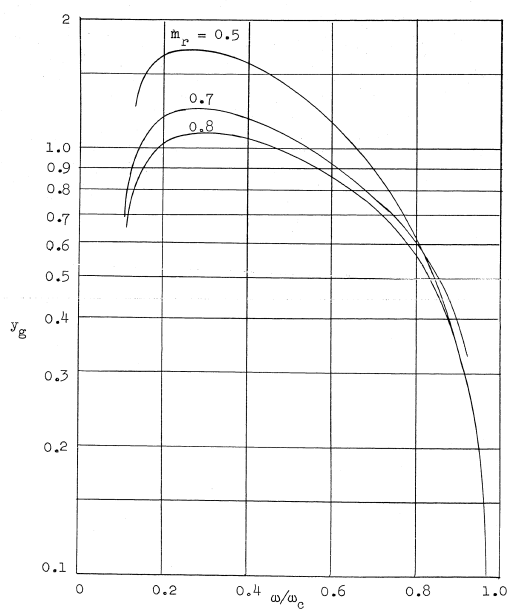

FIG. 7.85.--Group velocity y_g of the four-element band-pass circuit, x_1 = 0.100.

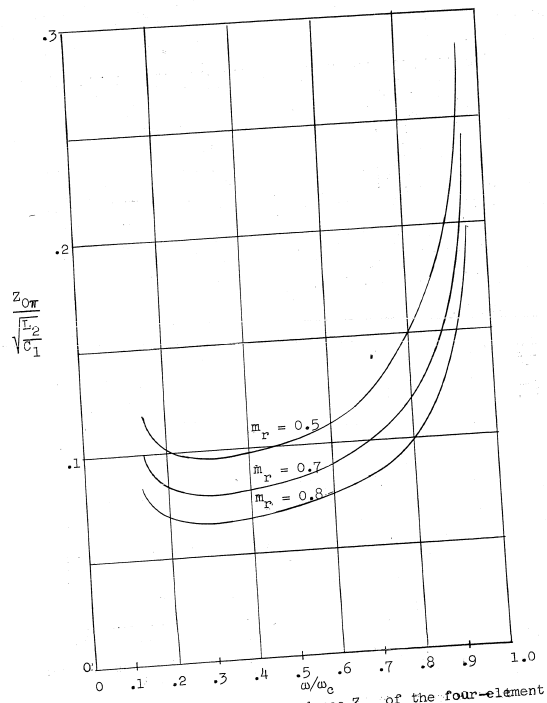

FIG. 7.86.--Circuit impedance $Z_{0\pi}$ of the four-element band-pass circuit of Pi section, x_1 = 0.100.

Sanitized Copy Approved for Release 2010/06/30 : CIA-RDP81-01043R000200070007-1

Sanitized Copy Approved for Release 2010/06/30 : CIA-RDP81-01043R000200070007-1

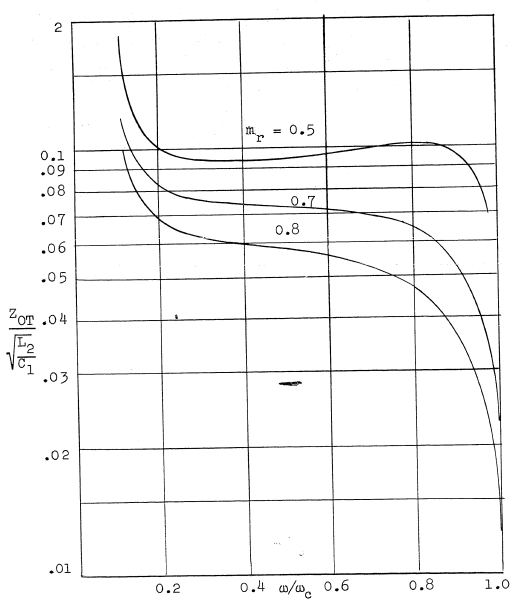

FIG. 7.87.--Circuit impedance Z_{OT} of the four-element band-pass circuit of Tee section $x_1 = 0.100$.

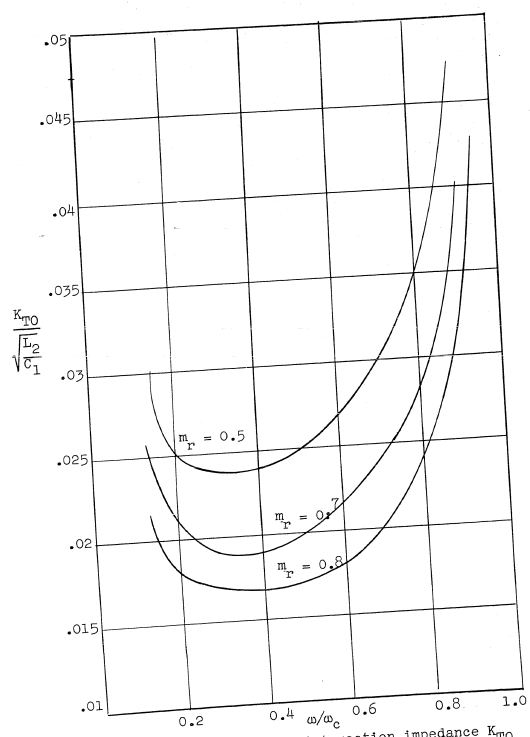

FIG. 7.88.--Transverse interaction impedance K_{TO} of the four-element band-pass circuit, $x_1 = 0.100$.

Sanitized Copy Approved for Release 2010/06/30 : CIA-RDP81-01043R000200070007-1

Sanitized Copy Approved for Release 2010/06/30 : CIA-RDP81-01043R000200070007-1

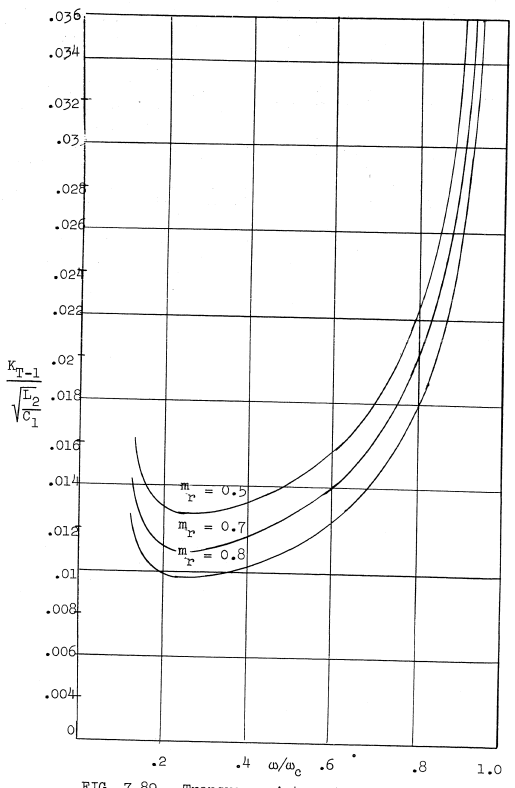

FIG. 7.89.--Transverse interaction impedance K_{T-1} of the four-element band-pass circuit, $x_1 = 0.100$.

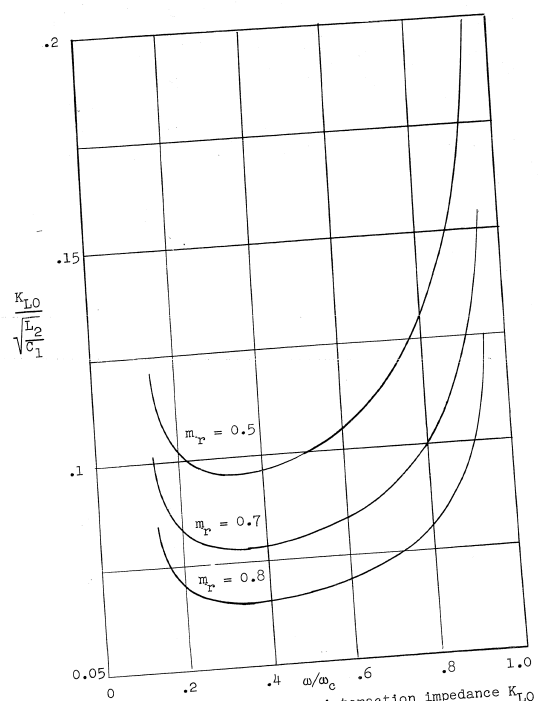

FIG. 7.90.--Longitudinal interaction impedance K_{LO} of the band-pass circuit, $x_1 = 0.100$.

Sanitized Copy Approved for Release 2010/06/30 : CIA-RDP81-01043R000200070007-1

Sanitized Copy Approved for Release 2010/06/30 : CIA-RDP81-01043R000200070007-1

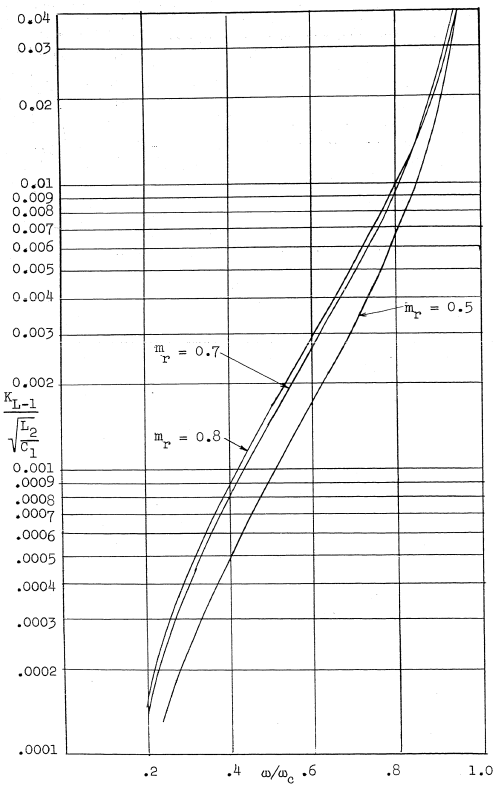

FIG. 7.91.--Longitudinal interaction impedance K_{L-1} of the four-element band-pass circuit, x_1=0.001.

REFERENCES

1. C. T. Sah, "Analysis for external-circuit traveling-wave tubes," T.R. No. 1, Nonr 225 (24), Stanford Electronics Laboratories, Stanford University, California.

Sanitized Copy Approved for Release 2010/06/30 : CIA-RDP81-01043R000200070007-1

Sanitized Copy Approved for Release 2010/06/30 : CIA-RDP81-01043R000200070007-1

DISTRIBUTION LIST

Technical Reports (Tubes) - NSonr 251(07)

cc	Addressee
	Chief of Naval Research Department of the Navy Washington 25, D. C. Attn: Code 427
2	
	Commanding Officer Office of Naval Research Branch Office 1000 Geary Street San Francisco 9, California
1	
	Commanding Officer Office of Naval Research Branch Office 1030 E. Green Street Pasadena, California
1	
	Commanding Officer Office of Naval Research Branch Office John Crerar Library Building 86 E. Randolph Street Chicago 1, Illinois
1	
	Commanding Officer Office of Naval Research Branch Office 346 Broadway New York 13, New York
1	
	Officer in Charge Office of Naval Research Navy 100, Fleet Post Office New York, New York
3	
	Director Naval Research Laboratory Washington 25, D. C. Attn: Code 2000
6	
1	Attn: Code 2040
1	Attn: Code 2100
1	Attn: Code 2430
1	Attn: Code 2000
1	Attn: Code 5200
1	Attn: Code 5270
1	Attn: Code 5260A
	Chief, Bureau of Ships Navy Department Washington 25, D. C. Attn: Code 840
1	
1	Attn: Code 816
1	Attn: Code 820
1	Attn: Code 840
	Chief, Bureau of Aeronautics Navy Department Washington 25, D. C. Attn: Code EL 4
1	
1	Attn: Code EL 43
1	Attn: Code EL 43
	Chief, Bureau of Ordnance Navy Department Washington 25, D. C. Attn: Code Re 9
1	
1	Attn: Code Re 9
	Chief of Naval Operations Navy Department Washington 25, D. C. Attn: Code Op 30
1	
1	Attn: Code Op 55
1	Attn: Code Op 51C
	Director Naval Ordnance Laboratory White Oak, Maryland
1	
	Director Naval Electronics Laboratory San Deigo 52, California
1	
	U. S. Naval Post Graduate School Monterey, California
1	
	Commander U. S. Air Missile Test Center Point Mugu, California Attn: Code 366
1	
	U. S. Naval Proving Ground Dahlgren, Virginia
1	
	Commander U. S. Naval Air Development Center Johnsville, Pennsylvania
1	
	Commanding Officer New York Naval Shipyard Material Laboratory Library Naval Base Brooklyn, New York
1	
	Naval Ordnance Laboratory Corona, California Attn: Ralph R. Lee, Chief, Missile Development Div.
1	
	Scientific Research Section Research Branch, Plans Division Office of Naval Research, Chief of Staff, G4 Headquarters, Army Washington 25, D. C.
1	
	Chief, S and T Division Office of the Chief Signal Officer Washington 25, D. C. Attn: SIGWO
1	
	Chief, F and D Division Office of the Chief Signal Officer Department of the Army Washington 25, D. C. Attn: SIGWO-5
1	
	Office of the Chief of Engineers Department of the Army Washington 25, D. C.
1	
	Office of the Chief of Ordnance Department of the Army Washington 25, D. C. Attn: ORDTU
2	
	Director Signal Corps Engineering Laboratories Evans Signal Laboratory Supply and Maintenance Section Building No. 42 Belmar, New Jersey Attn: Countermeasures Branch
28	
	Commanding Officer Eng. Research and Development Lab. Ft. Belvoir, Virginia
1	

cc	Addressee
	Commanding Officer Frankford Arsenal Bridesburg, Philadelphia, Pennsylvania
1	
	Ballistic Research Laboratory Aberdeen Proving Ground, Maryland Attn: D. W. Delaney
2	
	Commanding General Wright Air Development Center Wright-Patterson Air Force Base, Ohio
1	Attn: WCRRD-2
4	Attn: WCLGL
1	Attn: WCLRS-5
1	Attn: WCRP
1	Attn: WCRRM
1	Attn: WCRRE
	Chief of Staff United States Air Force Washington 25, D. C. Attn: AFDRD-SC-3
2	
	Commanding General Rome Air Development Center Griffiss Air Force Base Rome, New York Attn: RCRW
2	
	Commanding General Air Force Cambridge Research Center Air Research and Development Command L. G. Hanscom Field Bedford, Massachusetts Attn: CRHOUT-2, Electronics
8	
	Commander Patrick Air Force Base Cocoa, Florida
1	
	Chief, European Office Air Research and Development Command c/o Eg. USAFE APO 633, c/o Postmaster New York, New York
1	
	Air Force Special Weapons Center Kirtland Air Force Base Albuquerque, New Mexico Attn: SWOI
2	
	Director Air University Library Maxwell Air Force Base, Alabama Attn: CR 5602
1	
	Commanding General Air Research and Development Command Post Office Box 1395 Baltimore 3, Maryland Attn: RDTDRM
1	Attn: RDTDAM
1	Attn: RDTDEN
1	Attn: DRDPM
	U. S. Coast Guard 1300 E. Street, NW Washington 25, D. C. Attn: ESD
1	
	Assistant Secretary of Defense (Research and Development) Research and Development Board Department of Defense Washington 25, D. C. Attn: Technical Library
1	
	Secretary, Committee on Electronics Office of the Assistant Secretary of Defense (Research and Development) Department of Defense Washington 25, D. C.
1	
	Advisory Group on Electron Tubes 346 Broadway, 8th Floor East New York 13, New York Attn: Miss Ruth McDonald, Chief Technical Reference Section
1	
	Armed Services Technical Information Agency Document Service Center Knott Building Dayton 2, Ohio Attn: DSC-SA
10	
	Office of Technical Services Department of Commerce Washington 25, D. C.
1	
	Commanding Officer Signal Corps Laboratories Coronet Hill and Van Ness St., NW Washington 25, D. C. Attn: Division 14, Librarian Attn: CMOFL-52.1
1	
2	
	Library Boulder Laboratories National Bureau of Standards Boulder, Colorado
1	
	Chief, West Coast Office Signal Corps Engineering Labs 75 S. Grand Ave., Bldg. 6 Pasadena, California
1	
	Polytechnic Institute of Brooklyn Microwave Research Institute 55 Johnson Street Brooklyn 1, New York Attn: Prof. E. Weber
1	
	California Institute of Technology Department of Electrical Engineering Pasadena, California Attn: Prof. L. M. Field
1	
	University of California Electrical Engineering Department Berkeley 4, California Attn: Prof. J. R. Whinnery
1	
	University of Colorado Department of Electrical Engineering Boulder, Colorado Attn: Prof. W. H. Worcester
1	
	University of Florida Department of Electrical Engineering Gainesville, Florida
1	
	Georgia Institute of Technology Atlanta, Georgia Attn: Miss J. Bentley Crossland, Librarian
1	

cc	Addressee
	Harvard University Technical Reports Collection Room 303A, Pierce Hall Cambridge 38, Massachusetts Attn: M. E. Cox, Librarian
2	
	University of Illinois Electrical Engineering Department (Tube Section) Champaign, Illinois
1	
	University of Illinois Control Systems Laboratories Urbana, Illinois Attn: Prof. P. Sebe and M. E. Morberg
1	
	University of Illinois Department of Physics Urbana, Illinois Attn: Dr. John Bardeen
1	
	Johns Hopkins University Radiation Laboratory 1315 St. Paul Street Baltimore 2, Maryland Attn: Dr. D. D. King
1	
	Linfield Research Institute McMinnville, Oregon Attn: Dr. W. P. Dyke, Director
1	
	Loyola University Department of Physics New Orleans 18, Louisiana Attn: Dr. Paul B. Picker
1	
	Massachusetts Institute of Technology Cambridge 39, Massachusetts Research Laboratory of Electronics Lincoln Laboratory
1	
1	
	New York University University Heights College of Engineering New York 53, New York Attn: L. S. Schwartz Research Division
1	
	Ohio State University Department of Electrical Engineering Columbus 10, Ohio Attn: Prof. E. M. Boone
1	
	Princeton University Department of Electrical Engineering Princeton, New Jersey
1	
	Purdue University Research Library Lafayette, Indiana Attn: E. J. Gorthuys
1	
	Stanford Research Institute Stanford, California Attn: Technical Library
1	
	University of Washington Department of Electrical Engineering Seattle 5, Washington Attn: A. E. Harrison
1	
	Yale University New Haven, Connecticut Sloane Physics Laboratory Department of Electrical Engineering Durham Laboratory
1	
1	
	Director Electronics Defense Group Engineering Research Institute University of Michigan Ann Arbor, Michigan
1	
	Electron Tube Laboratory 3996 East Engineering Bldg. University of Michigan Ann Arbor, Michigan
1	
	Engineering Research Institute 351 East Engineering Building University of Michigan Ann Arbor, Michigan Attn: Joseph S. Howe, Research Associate
1	
	University of Michigan Electronic Research Center Engineering Research Institute Ypsilanti, Michigan Attn: Dr. H. Goode
1	
	Commanding Officer Signal Corps Electronics Research Unit 990Nth TV (Sylvania) P. O. Box 205 Mountain View, California
1	
	Airborne Instrument Laboratory 160 Old Country Road Mineola, L. I., New York Attn: Mr. John Gyer
1	
	Bell Telephone Laboratories Murray Hill Laboratory Murray Hill, New Jersey Attn: Technical Library
1	
	CBS Laboratories 135 Madison Avenue New York 22, New York
1	
	Columbia Radiation Laboratory 538 West 120th Street New York 27, New York
1	
	Cornell Aeronautical Labs. Inc. Cornell Research Foundation Buffalo 21, New York
2	
	Federal Telecommunications Labs.,Inc. 500 Washington Avenue Nutley, New Jersey Attn: Librarian
1	
	Attn: L. K. Wing via Inspector of Naval Material Naval Inspector, Reserve Shipyard Bldg. 77, Fort Hamers Newark 5, New Jersey
1	
	Gilfillan Bros. 1815 Venice Boulevard Los Angeles, California Attn: Countermeasures Laboratory
1	

cc	Addressee
	Electron Tube Division of the Research Laboratory General Electric Co. The Knolls Schenectady, New York Attn: E. D. Macarthur
1	
	General Electric Advanced Electronics Center Ithaca, New York Attn: D. R. Brown via J. E. Brown, Security Agent
1	
	General Electric Company Research Laboratory P. O. Box 1088 Schenectady, New York Attn: Alice V. Nell, Librarian
1	
	General Electric Microwave Laboratory at Stanford Stanford Industrial Park Palo Alto, California Attn: Technical Library
1	
	General Electric Co. General Engineering Laboratory Bldg. 37, Room 453 Schenectady, New York Attn: D. S. Pelser
1	
	Hewlett-Packard Company 275 Page Mill Road Palo Alto, California
1	
	Hughes Aircraft Co. Research and Development Culver City, California Attn: Mr. Jack T. Milek
1	
	Lenkurt Electric Co. San Carlos, California
1	
	The Marconi Corp. 25 West 45th Street New York 1, New York Attn: M. Simpson
1	
	Minneapolis-Honeywell Regulator Co. Aeronautical Division 2753 Fourth Avenue South Minneapolis 8, Minnesota
1	
	National Union Radio Co. Kinnelland Road Scotch Plains, New Jersey Attn: Dr. A. M. Skellet
1	
	Philco Corporation Lansdale Division Philadelphia, Pennsylvania Attn: W. S. Bradley
1	
	Philco Corporation 22nd and Lehigh Avenue Philadelphia 32, Pa. Attn: F. A. Sherman, Tech. Editor Tech. Rep. Div. Bull.
1	
	Radio Corporation of America RCA Victor Division Harrison, New Jersey Attn: Microwave Tube Development Section
1	
	RCA Laboratories Princeton, New Jersey Attn: E. W. Herold and Harwell Johnson
1	
	The Rand Corporation 1700 Main Street Santa Monica, California Attn: Margaret Anderson,LtLibrarian
1	
	Raytheon Corporation Waltham, Massachusetts Attn: M. P. Argento Attn: W. Welsh
1	
1	
	Sperry Gyroscope Company Engineering Library Mail Station C-32 Great Neck, L. I., New York
1	
	Sperry Gyroscope Co. Great Neck, L. I., New York Attn: E. L. Wallace Attn: Technical Library
1	
1	
	Sylvania Electric Products, Inc. 63-55 New Hardman Island, New York New Gardens, Long Island Attn: Microwave Tube Section Product Development Labs.
1	
	Sylvania Electric Products, Inc. Physics Labs. Sylvania Park Point Boulevard Seaford, L. I., New York Attn: D. Lazare, Security Officer
1	
	Sylvania Electric Products, Inc. 500 Ern Street Mountain View, California Attn: Technical Library
1	
	Tektronix, Inc. P. O. Box 500 Portland 7, Oregon
1	
	Texas Instruments, Inc. 6000 Lemmon Avenue Dallas 9, Texas
1	
	Varian Associates 611 Hansen Way Palo Alto, California Attn: Technical Library
1	
	Stanford University Stanford, California
95	

Sanitized Copy Approved for Release 2010/06/30 : CIA-RDP81-01043R000200070007-1